DISS. ETH NO. 21758

The Companion Mass Function across the Stellar and Substellar Regime

A thesis submitted to attain the degree of

DOCTOR OF SCIENCES of ETH ZURICH

(Dr. sc. ETH Zurich)

presented by

Maddalena Maria Reggiani

Dottore Magistrale in Fisica, Università degli Studi di Milano

born on Sep 15th, 1984

citizen of Italy

accepted on the recommendation of

Prof. Dr. Michael R. Meyer, examiner
Dr. Gael Chauvin, co-examiner

2014

Cover illustration:

Artist's Impression of a planet-forming disk.

(Adapted from an illustration by: ESO)

ACKNOWLEDGMENTS

I would like to thank my supervisor, Professor Michael R. Meyer, for his help, guidance and excellent scientific insight that helped me progressing through my PhD. His passion has been truly inspiring and his support with my family changes and needs inestimable. I would also like to thank him for allowing me to make the most of a number of opportunities that I have been offered during my PhD including numerous conferences, schools and research collaborations.

I would like to thank the Star and Planet Formation group, as well as the rest of the Institute of Astronomy at ETH Zürich, for inspiring discussions, for the immense support and priceless advice that they have given me with regards to my PhD and my future career, and their precious friendship in these four years.

I would also like to thank my co-examiner, Dr. Gael Chauvin, and the NaCo-LP collaboration for the many things I learned through this project, and Dr. Dimitri Mawet, Dr. Julien Girard and Dr. Oliver Absil for their support with the observations at the VLT.

In addition, I would like to thank my parents, Laura and Remo, for instilling me the curiosity about reality, and my brother and sister, Samuele and Cecilia, and all my friends, for having always been there when I needed.

Finally, many many thanks to my husband, Matteo, and my little boy, Pietro, for the patience in the last few months of intense writing and their continuous love.

Zurich, January 2014 Maddalena Reggiani

CONTENTS

LIST OF FIGURES

LIST OF TABLES

ABSTRACT

Since the 18th century, it has been recognized that pairs of stars on the sky can be bound due to mutual gravitational interaction: such systems are called "stellar binaries". Today we know that, unlike the Sun, roughly half of the stars in the Milky Way belong to binary systems with two or more components. Since the mid-90s, both "brown dwarfs" (BDs), objects that are too small to fuse hydrogen, and extrasolar planets have been discovered as companions to stars. The observed statistics of known planets indicate that they are common and diverse in terms of properties with respect to Solar System planets. A deeper understanding of the properties of multiple systems and of the frequency of planets around stars may help in determining in which environment the Sun formed and how common a Solar System like our own could be.

The dynamics of a double system can be explained by the two body problem of classical dynamics. The two components move on an elliptical orbit that can be described by 5 orbital parameters: the eccentricity, the inclination, the semi-major axis, and the two masses, M_1 and M_2. The mass-ratio is defined as $q = M_2/M_1$ and the distribution of q values is the Companion Mass Ratio Distribution (CMRD). Over the years, many observational techniques have been developed to detect compan-

ions (stars, BDs, and planets) to stars. Speckle and long baseline optical interferometry, radial velocity (RV), and adaptive optics (AO) are the most commonly used today to discover stellar binaries. Concerning substellar companions, gravitational microlensing, astrometric shifts and orbital timing methods are also adopted. Thanks to these techniques, the frequency and the orbital parameter distributions of stellar companions have been widely studied and compared to theories of stellar and planetary formation.

The main mechanisms that have been proposed for the formation of stellar binaries are the tidal capture of two unbound objects, the fragmentation of a collapsing molecular cloud core, and disk fragmentation due to density perturbations. BD companions are expected to form through the same processes as stellar companions, whereas for gas giant planets the most plausible formation theory is core accretion. As the different mechanisms overlap in the substellar-mass regime, the study of the CMRD across the stellar-substellar boundary can help in placing some constraints on star and giant planet formation theories.

By taking advantage of the existing multiplicity studies for M-dwarfs, solar-type and intermediate-mass primaries in the field and in young clusters and associations, we test through Monte Carlo simulations the hypothesis that the CMRD is consistent with random pairing from the stellar Initial Mass Function (IMF), as predicted by the tidal capture scenario. We find that for all the analyzed samples but Chamaeleon I, we can reject this hypothesis. This naturally suggests that tidal capture cannot be considered as the principal way of forming binary systems. The CMRDs in the field and in young star forming regions appear to be consistent with each other and independent of separation in the range covered by the observations. Larger and different samples are needed to understand which star formation events contribute most to the field population. Combining the CMRDs of M and G primaries in the field over the common range of mass-ratios, we find that the maximum likelihood fit follows a power law $dN/dq \propto q^{\alpha}$, with $\alpha = 0.25 \pm 0.29$.

Assuming that the field CMRD can be extrapolated into the BD regime, we create a model for the substellar Companion Mass Function (CMF) that consists of the superposition of the stellar CMRD down to

a few Jupiter masses and the planet mass distribution, measured with RV. To test this simple model, we develop a MonteCarlo simulation tool to predict the outcome of a given survey, depending on the shape of the orbital parameter distributions. We compare the results of simulations assuming the combined CMF of planets and BDs with those of directing imaging surveys searching for substellar companions around Sun-like stars. We find that observations are consistent with the proposed CMF, as long as a sufficiently small outer truncation radius ($\leq$80 AU) is introduced for the planet separation distribution. This mass distribution has a minimum between 10 and 40 $M_{Jupiter}$, in agreement with radial velocity measurements, and allows us to determine what is the probability for a substellar companion as a function of mass to have formed in a planet- or BD-like process. Future observations will enable us to determine the shape of the substellar CMF and the location of the minimum as a function of primary mass.

Another way of constraining initial conditions for planet formation theories would be to study planets in their birth environment. Through VLT/NACO L'-band high-contrast imaging observations of HD 169142, we detect a source located $\sim$ 23 AU north of the host star, right within the inner cavity of the transition disk. Although a smaller object would be more consistent with the observed cavity width, the observations are consistent with it being both a 35-80 $M_{Jupiter}$ object at the age of the star, according to the evolutionary models, and a lower-mass protoplanet still accreting gas in the cavity. If confirmed, HD 169142 b would represent one of the first and best laboratories to test both brown dwarf/planet formation and evolution theories. Furthermore, we place constraints on a second object forming in the annular gap ($\sim$50 AU) of HD 169142 that could be still surrounded by a circumplanetary disk, as suggested by millimeter observations. If the second companion is also confirmed, HD 169142 would be forming a planetary system that may enable us to explore sequential planet formation and planet evolution in the future.

RIASSUNTO

Fin dal XVIII secolo, è stato riconosciuto che coppie di stelle in cielo possono essere legate da attrazione gravitazionale. Tali sistemi stellari sono chiamati "stelle binarie". Oggi si sa che, diversamente dal nostro Sole, circa la metà delle stelle nella Via Lattea appartengono a sistemi binari con due o più componenti. A metà degli anni '90, sia nane brune, corpi celesti che sono troppo poco massivi per bruciare idrogeno, sia pianeti extra-solari sono stati scoperti come compagni di alcune stelle. Le statistiche dei pianeti che sono stati trovati indicano che tali oggetti sono comuni e molto vari in termini di proprietà rispetto ai pianeti del nostro Sistema Solare. Una conoscenza approfondita di queste proprietà, e della frequenza di pianeti attorno ad altre stelle, può essere utile per determinare in quale ambiente si sia formato il Sole e quanto comuni siano i sistemi solari come il nostro.

Il moto di un sistema doppio può essere spiegato dal problema dei due corpi della dinamica classica. Le due componenti, infatti, si muovono su un'orbita ellittica che è descritta da 5 parametri orbitali: l'eccentricità, l'inclinazione, il semi-asse maggiore e le due masse, M_1 e M_2 della stella primaria (più massiva) e secondaria, rispettivamente. Il rapporto fra le

masse è definito come $q = M_2/M_1$ e la sua distribuzione e' chiamata CMRD (da "Companion Mass Ratio Distribution"). Negli corso degli anni, sono state sviluppate molte tecniche per la rivelazione di compagne (stelle, nane brune o pianeti extrasolari) di stelle. Interferometria, misure di velocità radiali e ottica adattiva sono fra le più utilizzate oggi. Per quanto riguarda le compagne di tipo sub-stellare, vengono utilizzati anche il micro-lensing gravitazionale e misure di astrometria e di variazione temporale di parametri orbitali. Grazie a tutti questi metodi, la frequenza e la distribuzione dei parametri orbitali sono state ampiamente studiate e confrontate con le più recenti teorie per la formazione di stelle e pianeti.

I meccanismi principali che sono stati proposti per la formazione delle binarie sono la cattura, la fragmentazione del nucleo di una nube molecolare che collassa e la fragmentazione di un disco protostellare a causa di perturbazioni di densità. Generalmente si pensa che anche le nane brune, come compagne di stelle, si formino con gli stessi meccanismi delle compagne stellari. Per i pianeti, invece, il processo più accreditato è l'accrescimento di solidi nei dischi protostellari. Dal momento che i diversi meccanismi si sovrappongono nel regime di masse substellare, lo studio della distribuzione di masse delle compagne al limite stellare-substellare può aiutare a definire le teorie di formazione stellare e planetaria.

Sfruttando gli studi già esistenti sulle binarie per stelle di tipo M, G e A nel piano della galassia e in alcuni giovani ammassi stellari e associazioni di stelle, abbiamo testato con una serie di simulazioni Monte Carlo l'ipotesi che la CMRD sia in accordo con l'accoppiamento casuale di masse all'interno della distribuzione di masse per stelle singole (consciuta anche come "IMF", da Initial Mass Function). Tale connessione fra la CMRD e la IMF è suggerita dal meccanismo di cattura, menzionato in precedenza. Abbiamo riscontrato che e' possibile escludere questa ipotesi per tutti i campioni analizzati, fatta eccezione per Camaleonte I. Pertanto la cattura non può essere il meccanismo preponderante per la formazione di sistemi stellari. La CMRD sembra essere la stessa sia nel piano della galassia che nelle giovani regioni di formazione stellare e non sembra dipendere dalla distribuzione di semi-assi maggiori delle

binarie. Campioni più numerosi e con proprieta' differenti sono necessari per poter determinare quale evento di formazione stellare contribuisce in maggiormente alla popolazione del piano della galassia. La combinazione delle CMRD per i diversi campioni segue una legge di potenza del tipo $dN/dq \propto q^{\alpha}$, con $\alpha = 0.25 \pm 0.29$.

Se assumiamo che la CMRD per il disco della galassia possa essere estrapolata nel regime di masse delle nane brune, e' possibile creare un modello per la distribuzione substellare di masse delle compagne che consiste nella sovrapposizione della CMRD stellare e della distribuzione di masse dei pianeti (misurata con il metodo delle le velocità radiali). Per testare questo semplice modello, abbiamo sviluppato una serie di simulazioni Monte Carlo che predicono il risultato di una campagna di osservazioni per la scoperta di pianeti o nane brune, sulla base delle distribuzioni dei parametri orbitali. Grazie a queste simulazioni possiamo confrontare le previsioni del nostro modello con i risultati delle più recenti osservazioni. Tali osservazioni sono in buon accordo con la distribuzione substellare di masse delle compagne che abbiamo proposto, purchè venga introdotto un troncamento nella distribuzione di semi-assi maggiori per i pianeti ($\leq$80 unità astronomiche). Questa distribuzione di masse presenta un minimo fra le 10 e le 40 masse di Giove, cosi' come è stato rivelato anche da misure di velocità radiali. Inoltre, essa permette di determinare quale è la probabilità che una compagna substellare si sia formata con meccanismo di tipo stellare o planetario. Osservazioni future consentiranno di misurare con precisione la distribuzione di masse delle compagne e l'esatta posizione del minimo in funzione della massa della stella primaria.

Un modo alternativo per poter definire le condizioni iniziali per le teorie di formazioni planetaria e' quello di studiare i pianeti nel loro ambiente nativo. Attraverso osservazioni in banda L' della stella HD 169142, abbiamo scoperto una sorgente a 23 unità astromiche a nord della stella. Tale emissione sembra provenire direttamente da un oggetto nella cavità del disco di transizione di HD 169142. Sebbene un corpo di massa inferiore sia in maggior accordo con la dimensione delle cavità, l'emissione in banda L' è consistente sia con una nana bruna di 35-80 masse di giove, sia con un proto-pianeta in formazione e che sta ancora

accrescendo gas dalla cavità. Se HD 169142 b venisse confermato da nuove osservazioni, esso rappresenterebbe un laboratorio ideale per lo studio delle teorie di formazione di pianeti e nane brune. Inoltre, con le osservazioni attuali siamo in grado di porre alcuni limiti sulla presenza di un secondo pianeta in formazione nel disco, come e' stato suggerito da misure nel millimetrico. Qualora anche questo secondo corpo venisse confermato, HD 169142 starebbe formando un sistema planetario, che potrebbe permetterci di studiare la formazione sequenziale di pianeti e la loro evoluzione.

CHAPTER 1

INTRODUCTION

THE PATTERN IS SO LARGE THAT WITHIN
THE LITTLE FRAME OF EARTHLY EXPERIENCE
THERE APPEARS PIECES OF IT BETWEEN WHICH
WE CAN SEE NO CONNECTION,
AND OTHER PIECES BETWEEN WHICH
WE CAN SEE NO CONNECTION,
AND OTHER PIECES BETWEEN WHICH WE CAN.

C.S. Lewis, *Perelandra*

Humanity has always wondered about the origin of the Sun and our Solar System, and the existence of other worlds in the Universe. Much progress has been made in answering these questions, since the first attempts of characterizing the individual bodies of the Solar System with telescopic observations (Galileo Galilei, 1600). Space and ground based missions have discovered more than one thousand million stars in the Milky way, some of them in the vicinity of the Sun, populating the so-called "Galactic field", some grouped into clusters or associations.

Unlike the Sun, roughly half of these stars did not form as isolated objects, but in systems with two or more components. Understanding multiple system formation is therefore a key element to understand how stars form in general. In the mid-90s, astronomers also started detecting, both in isolation and as companions to nearby stars, objects that are too small to fuse hydrogen in their cores, but large enough to undergo a short deuterium-burning phase. These objects, also known as brown dwarfs (hereafter BDs) cover the mass range between a few Jupiter masses up to 0.08 $M_{\odot}$. In the same years, the discovery of the first exoplanets gave birth to a completely new field of astronomy. As of today, more than 1000 planets have been detected with different techniques. With the advent of a new generation of extremely large telescopes, we hope to boost our knowledge of planet populations and planet formation. A better understanding of the properties of binary systems and of the occurrence of planets around stars may help in determining in which environment the Sun formed and how common a solar system like our own could be.

This thesis represents an attempt at bridging the gap between stars, BDs and planets. By providing a solid statistical framework to compare observations with theoretical models, we can place some constraints on theories of star and planet formation. In the following sections we will describe in more detail the nature of stellar companions (Section 1.1), the observational techniques that have been developed for detecting them (Section 1.2), the observed statistics (Section 1.3) and the formation mechanisms that have been proposed (Section 1.4).

1.1 Companions to Stars: The Two Body Problem

Since ancient times people have attempted to group stars according to their spatial distribution on the sky. The vicinity of two (optical dou-

ble) or more stars on the sky however does not necessarily imply that they are physically close or bound together. This proximity could easily represent a chance alignment along the line of sight. In some cases, though, couples or multiple stellar systems can be bound due to mutual gravitational interaction. As first suggested by John Michell (1767) and later confirmed by Sir William Herschel, there is a wide category of objects, initially defined "binary sidereal systems" and now known as binary stars, consisting of a pair of stars orbiting each other. In order to determine whether an optical double is indeed a true binary, repeated observations of the system over several years are required. The first paper with a few confirmed binaries was published by Herschel in 1803 and gave origin to the astronomy of "visual binaries". At the beginning of the 20^{th} century more than 100 orbits had already been calculated from observations and collected in the classic work by Aitken "*The Binary Stars*" [Aitken, 1935].

Nowadays, we know that binaries are as common as single stars and, beside the aforementioned visual binaries (VBs), there are other categories of binary systems, divided by the observational methods used to detect them. In general, we classify stellar binaries into three main groups: visual binaries, spectroscopic binaries (SBs), and eclipsing binaries. Binary stars that are visually resolved are called visual binaries. The presence of a companion could also generate a change in the spectral lines of a star, due to Doppler shift, as the two components orbit each other. Systems detected through spectroscopic observations are called spectroscopic binaries. Finally, if a binary happens to orbit in a plane along our line of sight, its components will eclipse and transit each other. Such objects are detected by their changes in brightness during eclipses and are therefore called eclipsing binaries.

If a stellar companion is too small to fuse hydrogen, it is instead called "Brown Dwarf". The existence of brown dwarfs (BDs) was predicted since the 1960s [e.g. Kumar, 1963]. However the detection of such objects came only 20 years later and the first unambiguous example of a BD was the companion Gl229 B [Nakajima et al., 1995] to an early-type

M dwarf. Since then, BDs have been observed as free floating objects, as companions to stars, and as BD-BD binaries [e.g. Burgasser et al., 2003, Chauvin et al., 2005b, Dupuy & Liu, 2011]. In the case of BD companions, the presence of stellar primaries is crucial to determine the properties (age, mass, composition) of these objects. In this introduction we will only focus on BDs companions, since the study of BDs in general goes beyond the scope of this thesis.

In the same years as the first confirmed detection of a BD, the first extrasolar planet orbiting the solar analog 51 Pegasi was also detected [Mayor & Queloz, 1995]. Since then, more than 1000 planets have been found. Two are the remarkable features of these discoveries. The first is that planets are common. Figure 1.1 (from `http://www.exoplanet.eu`) shows how the number of known planets has increased over time. Second, the sample of detected planets presents a wide variety of orbital parameters, totally unexpected on the basis of our Solar System. For instance, there are planets much more massive than Jupiter, giant planets on really close orbits (also known as Hot Jupiters), planets on highly eccentric orbits or orbiting components of stellar binaries, etc. Theories that attempt to explain mechanisms of planet formation need to take into account this large variation in outcomes. In this thesis, however, we will mainly focus on giant extrasolar planets.

1.1.1 Orbital parameters

Stellar systems (star+star, star+BD, star+planet) represent one of the best examples in nature of the two-body problem from classical mechanics [fur further details see e.g. Horch, 2013, Wright & Gaudi, 2013]. The force of each component on the other is given by Newton's equation:

$$\mathbf{F}_{12} = -G\frac{m_1 m_2}{|\mathbf{r}|^2}\hat{\mathbf{r}}, \tag{1.1}$$

where $\mathbf{r}$=$\mathbf{r}_1$-$\mathbf{r}_2$ and $\hat{\mathbf{r}}$ is the unity vector in the $\mathbf{r}$ direction. This means that the force is attractive and directed along the line joining the two

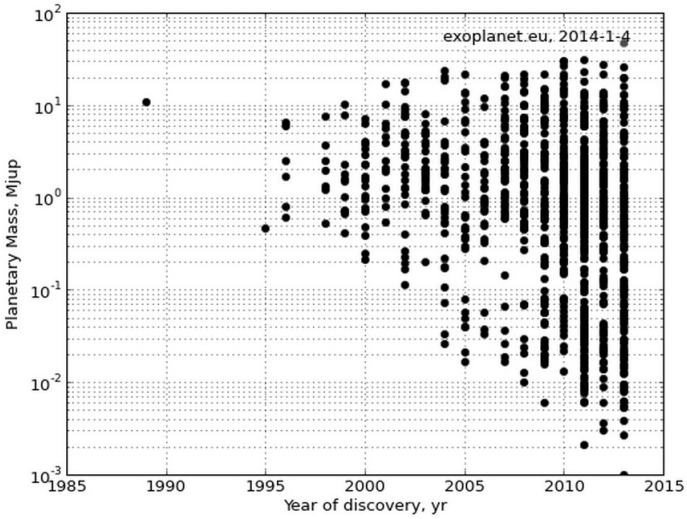

Figure 1.1 — *From* `http://www.exoplanet.eu`*: Planet discoveries since 1995.* The diagram represent the mass of the known planets as a function of year of discovery. From 1995 until January 2014, an continuously increasing number of planet have been detected. In total 1055 planets (in 801 planetary systems) have been discovered.

bodies. As the force is radial, in absence of external forces, the angular momentum and the total energy (potential, U + kinetic, K) are conserved. Defining the center of mass $\mathbf{r}_{CM}$ and the reduced mass μ of the system as:

$$\mathbf{r}_{CM} = \frac{m_1}{m_1 + m_2}\mathbf{r}_1 + \frac{m_2}{m_1 + m_2}\mathbf{r}_2, \quad \mu = \frac{m_1 m_2}{m_1 + m_2}, \tag{1.2}$$

the total energy of the system can be written as follows:

$$E_{TOT} = \frac{1}{2}\mu\left(\frac{d\mathbf{r}}{dt}\right)^2 - G\frac{\mu m_{TOT}}{r}, \tag{1.3}$$

where $m_{TOT} = m_1 + m_2$ is the total mass of the system and $\mathbf{r}$ in this case is the relative coordinate vector with respect to the center of mass. If

$E_{TOT} < 0$, the solution of this differential equation is an ellipse, yielding a bound orbit. In this case the system is in a periodic motion with period

$$P = \frac{4\pi^2}{Gm_{TOT}} a^3, \tag{1.4}$$

where a is the semi-major axis of the ellipse. This shows for example that, if the semi-major axis and the period are known, the total mass of the system can be calculated. A system in an elliptical orbit is therefore described by five physical parameters: the semi-major axis, a, the inclination, i, the eccentricity, e, and the masses, M_1 and M_2, of the primary and secondary components, respectively. It is common to define mass-ratio for a binary system the quantity $q = \frac{M_2}{M_1}$.

In reality, what we observe is a projection of the true ellipse on the plane of the sky. For visual binaries, for instance, the angular separation, orientation and brightness can be observed over time. Defining the brighter star in the system as primary star and the dimmer as secondary, we can indicate as orientation the angle θ between the line joining the primary to the secondary and the line drawn from the primary to the celestial north pole. As time passes, orientation and separation describe an apparent ellipse on the plane of the sky. The observed ellipse however needs to be converted to the true elliptical orbit, if we want to determine the physical parameters of the system. A nice solution of this problem is given in the book by Docobo [1985]. It is necessary to introduce three angular quantities (i, Ω, and ω) in order to perform this transformation (see also Figure 1.2). The inclination angle, i, is defined as the angle between the plane of the true orbit and the plane of the sky. The line of intersection of these two planes is called line of nodes and contains the position of the primary star (focus of the true ellipse). The two points of contact between the true and the projected ellipses are called nodes. The position of the line of nodes on the sky is at an angle Ω, which represents the angle (measured east of north) of the so-called "nodal point", where the secondary star cross the plane of the sky moving away from Earth. Finally, ω describes the angle in the plane of the true orbit between the nodal point and the periastron (closest approach of the two

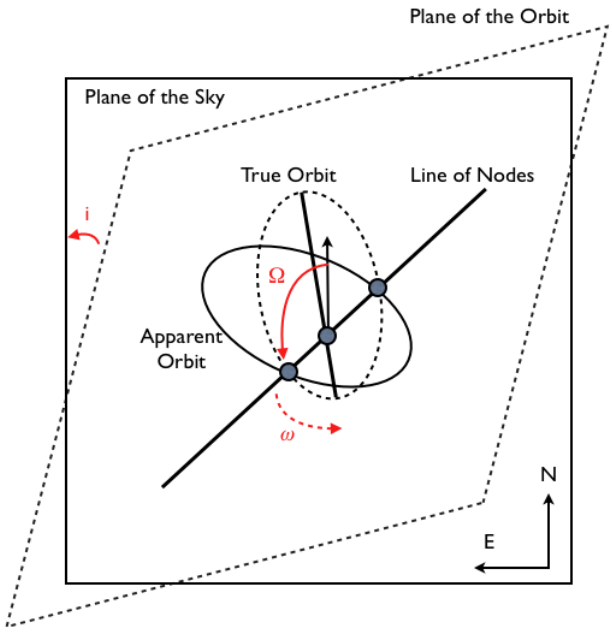

Figure 1.2 — *Geometry of the orbit* The figure shows the geometry for the calculation of a true orbit of a binary. The solid lines indicate the plane of the sky and the projection of the real orbit onto this plane, whereas dashed lines are used for the true orbit on the plane of the orbit.

stars). The positions of the two bodies at any time can be expressed in polar coordinates (r, ν), where r is the separation between them and ν (also called "true anomaly") is the angle between the location of the secondary and the periastron. The computation of the secondary's position in its orbit with time is usually carried out through the variable E, called the "eccentric anomaly". This quantity is related to the time and the periastron passage, T, through the "mean anomaly", M:

$$M = \frac{2\pi(t-T)}{P} = E - e\sin E, \tag{1.5}$$

where e is the eccentricity of the ellipse, ranging from 0 to 1. E allows

to calculate ν and r through the simple relations:

$$\tan\frac{\nu}{2} = \sqrt{\frac{1+e}{1-e}}\tan\frac{E}{2}, \quad r = a(1-e\cos E). \tag{1.6}$$

1.2 Observational Techniques

As mentioned above, there are three main groups of binary systems: visual binaries, spectroscopic binaries and eclipsing binaries. Many high resolution techniques for detecting visual binaries have been developed over the years, since the first observations performed with visual micrometers, eye-devices that allow to measure position angles and separations of binary components. Speckle and long baseline optical interferometry, lunar occultation measurements, and adaptive optics (AO) are the most commonly used today. Concerning spectroscopic binaries, the variety of techniques is not as vast as for visual binaries and the radial velocity (hereafter RV) method both in the optical and in the infrared is the most common approach. Finally, eclipsing binaries are detected through photometry of the system. A monitoring of the flux of a star over time can reveal the presence of a companion.
Since the discovery of the first BD companions and exoplanets, the observational techniques developed for stellar binaries have been taken to their extreme limits. Beside the aforementioned methods, three other techniques, namely gravitational microlensing, astrometric (positional) shifts and orbital timing methods, have also been adopted. Here is a brief description of the different methods.

Speckle Interferometry

The resolution limit, R, of a telescope is generally given by the wavelength of observation, λ, and the mirror size, D, with a larger telescope being able to resolve smaller angles (the Reyleigh Criterion, $R = 1.22\frac{\lambda}{D}$).

This is due to Fraunhofer diffraction and means that images of point sources are spread out to a diffraction pattern, also called the Airy pattern. This relation breaks down due to the limits imposed by the Earth atmosphere (seeing). Turbulence introduces phase and amplitude shifts in the wavefront. With some techniques, such as speckle interferometry and adaptive optics, it is possible to overcome this limitation and resolve very close systems, like binaries. The main principle of speckle imaging is to take a large number (from hundred to few thousands) of very short exposure images of the target in order to "freeze" the fluctuations of the atmosphere. If the exposures are shorter than the coherence time of fluctuations in the atmospheric turbulence, the images of the star contain many small bright points, or speckles, whose size is that of the diffraction limit of the telescope. In case of a double star, a double speckle-pattern is expected. With image processing techniques (and Fourier analysis) it is then possible to reconstruct a diffraction-limited image and determine the position of the second star.

Long Baseline Interferometry

This is another method that takes advantage of the use of interferometry to resolve binary systems. This technique coherently combines the light received by two or more telescopes, resulting in a fringe pattern of constructive and destructive interference. The fringe pattern (visibility) of a point source is distinguishable from that of a resolved double or an extended source with the aid of a model. The resolution of the instrument corresponds to that of a single mirror with a diameter equivalent to the distance between the telescopes. With interferometry also some spectroscopic binaries have been detected. In the few cases of visual/spectroscopic systems it is possible to have a complete determination of the parameters of interest, such as masses, luminosities and temperatures.

Lunar Occultations Measurements

This method exploits the dark limb of the moon acting as a diffracting edge when it happens to pass in front of a star. When such an event takes place, a typical light curve with a diffraction pattern is observed. In the case the occulted source is a binary star, it would result in the superposition of two interference patterns. With this technique, it is possible to detect companions that are much fainter than their primaries and at angular separations smaller than the classical diffraction limit. Moreover, the displacement of the two patterns gives the angular separation of the two stars along the line of the Moon's motion. Even though it offers better resolution than speckle interferometry and better sensitivity than long baseline interferometry, this method has the drawback of lacking full-sky coverage.

Adaptive Optics (AO)

This technique, similarly to speckle interferometry, aims at overcoming the limitations on resolution imposed by the atmospheric fluctuations to achieve the diffraction limit of the telescope. In this case, a bright source (or the target itself) is used to measure the shape of the wavefront. In real time, a computer calculates the best mirror shape to correct for the distortions and a deformable mirror system adjusts accordingly (at a rate up to hundreds or a thousand Hz). In this way it is possible to obtain high-resolution images and detect much fainter companions. As it does not offer any advantage over speckle interferometry for bright companions, it is widely and successfully used for exoplanet detections, but not so exploited in binary star measurements.

Radial Velocity Measurements

Compared to visual binaries, spectroscopic systems have high orbital velocities and very small separations. The presence of two components is gathered indirectly from a line shift in the spectrum due to the Doppler effect observed over time. The formula for the Doppler effect is

$$\frac{\Delta\lambda}{\lambda_0} = \frac{v}{c}, \tag{1.7}$$

where $\Delta\lambda$ is the shift in wavelength relative to the rest wavelength of the the line λ_0, and v is the velocity along the line of sight (radial velocity). The shift is positive when the observed object is receding from the observer and negative when approaching. When the two binary components are comparable in mass and present the same spectral features, spectral lines from both stars are visible. Such systems are called double-lined spectroscopic binaries. The lines shift first toward the blue, then toward the red, as each of the component moves first toward the observer, and then away from it, in its orbit around the center of mass. In other cases, only the lines from one of the components (the brightest of the pair) are visible in the spectrum but they still shift periodically towards the blue and towards red, indicating the presence of a companion. These stars are known as single-lined spectroscopic binaries. Orbits of spectroscopic binaries are therefore determined with a long series of observations. The radial velocity of one or both components of the system is measured by observing the Doppler shift of the spectral lines. The velocity is then plotted against time and the periodicity of the curve is the same as that of the orbit. The exact shape of the velocity curve depends on the eccentricity and the inclination of the orbit. In the particular case of a circular orbit and a 90° inclination, the individual masses and the semi-major axis can be obtained. Without knowing the inclination of a system however only the mass-ratio, q, and a lower limit for the separation, $a \sin i$, can be determined. In many cases the mass of the primary can be estimated from its observed properties (e.g. temperature and luminosity). In the lucky case of a visual/double-lined spectroscopic binary, the inclination angle can be obtained by the visual

orbit, as well as the sum of the masses, wheres spectroscopic observations can give information on the mass-ratio and on the quantity $a \sin i$. Thus, the semi-major axis is also known and an independent measure of the distance of the system is obtained as well.

Light Curve Measurements

This technique only applies to binary systems whose orbit is perpendicular to the plane of the sky or roughly so. The basic idea is that, when the two components of a binary are orbiting each other, they will eclipse. Dips in the brightness of the binary star can be observed if the magnitude of the object is monitored over time. There are two dips per orbital period. The deepest dip, also known as primary eclipse, takes place when the secondary star passes in front of the primary. The so-called secondary eclipse occurs when the secondary goes behind the primary star. If the two stars differ in size, we have total eclipse, if the larger star is in front, and annular eclipse, if the smaller one is in front. Partial eclipse occurs when the inclination angle is different from 90°. The spacing and length of the eclipses are determined by the geometry of the orbit. From the light curve it is possible to determine the period, and radii of the stars in terms of the semi-major axis of the orbit. If the binary is also a double-lined spectroscopic binary, all parameters can be determined unambiguously. These rare objects are fundamental to calibrate all we know about the physical properties of stars as a function of their mass.

Gravitational Microlensing

Gravitational microlensing has also been employed for determining the frequency of BDs, as well as planets, as companions to stars. A microlensing event occurs when a foreground star, called "the lens", aligns closely with a background source. As the star moves across the line

of sight, the light of the background source is focused gravitationally and the apparent flux is amplified. Its brightness peaks when it is at its closest separation with the lens and declines as the angular separation increases. If the lens star has a companion with an appropriate orientation, the brightness of the background object is amplified by the companion as well, and a secondary spike appears in the light curve. Microlensing events are usually unique and it is often difficult to obtain direct information (such as luminosity, temperature, composition) on the lens star or the companion. However, the duration and magnification of the microlensing event depends on the mass and distance of the lens, and transverse speed of the relative lens-source motion. For double systems it is relatively easier to measure these quantities and the mass-ratio, q, of the lens components, and thus derive their physical parameters.

Astrometry

Astrometry consists of precisely measuring the position of a star on the sky and how it varies over time with respect to a set of (presumably) fixed background stars. If the star has a companion (e.g. a planet), it will move on an elliptical orbit around the center of mass. This method is particularly effective for massive planets (and BDs) or with low-mass host stars.

Timing

Timing methods take advantage of time variations in periodic phenomena of stars due to the presence of planetary companions. This method is used in particular with pulsars, eclipsing binary stars, or even stars with transiting planets. When it is applied to systems with transiting planets, it is called "transit timing variations".

1.3 Statistics

1.3.1 Stellar Binary Statistics

Since the 1970s, the study of binary properties has been a topic of great interest in the star formation community, as it can provide a tool for discriminating between different formation mechanisms. A common way of expressing the number of binary or higher order systems in a sample is the multiplicity fraction, MF [Reipurth & Zinnecker, 1993]. MF is simply the sum of the binary systems, B, triple systems, T, quadruple systems, Q, etc. divided by the total number of single stars, S, binary systems, triple systems, quadruple systems etc.:

$$MF = \frac{B + T + Q + ...}{S + B + T + ...}. \tag{1.8}$$

Alternatively, one can define the companion frequency [see e.g. Reipurth & Zinnecker, 1993] as:

$$CF = \frac{2B + 3T + 4Q + ...}{S + 2B + 3T + ...}. \tag{1.9}$$

The period (or the semi-major axis) distribution has been frequently parametrized as a power law $dN/dP \propto P^{\beta}$. The particular case of $\beta = -1$, is known as Öpik's law [Öpik, 1924]. A log-normal parametrization, characterized by a mean period $\bar{P}$ and a width $\sigma_{\log P}$, is also widely used. Alternatively, it is expressed in terms of a semi-major axis distribution and thus characterize by mean separation $\bar{a}$ and width $\sigma_{\log a}$. Concerning the mass-ratio, q, a power law distribution $dN/dq \propto q^{\alpha}$ is commonly used.

Several observational surveys have attempted to measure the frequency of multiple systems and the distributions of orbital parameters for binary stars both in the field and in star forming regions. The results of all these studies have been recently collected in Duchêne & Kraus [2013]. In this introduction we only summarize the most recent updates

on these properties for both main sequence (MS) stars in the field as a function of primary mass and young pre-main sequence solar-type objects .

Solar-type MS Stars (0.7 - 1.3 $M_{\odot}$)

Sun-like stars represent the ideal population for multiplicity studies. They are numerous and bright enough to enable us to build statistically significant samples of binaries. In addition to that, the contrast with their companions is modest. Raghavan et al. [2010] conducted the most recent and complete multiplicity study for solar type stars to date (down to q=0.1). It is a volume-limited survey of 545 solar type stars within 25 pc. They found a multiplicity fraction of MF=44 $\pm$ 2%, with hint of a dependence on stellar mass ($MF_{1-1.3\,M_{\odot}}$=50$\pm$4% and $MF_{0.7-1\,M_{\odot}}$=41$\pm$3%). The distribution of semi-major axis follows a log-normal function centered at $\bar{a}$ $\sim$50 AU and with a width $\sigma_{\log a}$= 1.68. The observed CMRD appears to be flat down to $q = 0.1$, but with close binaries more peaked towards equal masses than large separation ones.

Low-mass MS Stars (0.1 - 0.5 $M_{\odot}$)

As the distribution of stellar masses peaks at $\sim$0.3 $M_{\odot}$, low-mass stars constitutes the majority of all stars. They have been widely studied in the past decades with a large number of techniques (RV, speckle interferometry, direct imaging). However, for a long time a volume-limited multiplicity survey of low-mass stars was not available. Recently a few studies [e.g. Delfosse et al., 2004, Janson et al., 2012] have been conducted and a multiplicity fraction of MF=26$\pm$3% for mass-ratios between 0.1 and 1 has been measured. Similar to solar-type systems, the semi-major axes appears to be log-normally distributed with $\bar{a}$ $\sim$16 AU and with a width $\sigma_{\log a}$= 0.8 [Janson et al., 2012]. Although the CMRD

is generally flat, a tendency of short-period binaries more peaked toward 1:1 is observed for low-mass primaries, too [Delfosse et al., 2004].

Very Low-mass MS Stars (<0.1 $M_{\odot}$)

Multiplicity studies of very low-mass (VLM) objects are generally challenging, as these objects are faint and difficult to observe both spectroscopically or through direct imaging. Due to the lack of SB and VB volume-limited surveys, the properties of VLM binaries are still poorly understood. Reviews of substellar binary properties have been recently provided by Burgasser et al. [2007] and Luhman [2012]. The frequency of SBs binaries estimated by dedicated surveys [e.g. Basri & Reiners, 2006, Blake et al., 2010, Tanner et al., 2012] is at least $MF = 5.2^{=3.8}_{-1.5}$ for $a \leq 1$ AU. For VBs MF is measured to be 15%±3 for a≥2 AU and $q = 0.5 - 1$[Bouy et al., 2003] and no more than 2% in the separation range 40-1000 AU and mass ratio range 0.6-1 [Allen et al., 2007]. By adding up these results, the overall frequency is 20-25%. Unfortunately, due to the paucity of VLM stars observed, it is difficult to infer a robust estimate on the distributions of orbital parameters. The semi-major axis distribution seems to be narrower and peaked at smaller separation (4-7 AU) compared to low-mass stars. The CMRD is peaked to 1:1 (most of $q \geq 0.7$) but different surveys report different values for the slope of the distribution [Allen et al., 2007, Burgasser et al., 2006]. The CMRD for VLM stars appears to be inconsistent with higher-mass primary CMRDs [Goodwin, 2013].

Intermediate-mass MS Stars (1.5 - 5 $M_{\odot}$)

Detecting faint companions around intermediate-mass stars is more challenging than for lower-mass primaries, and due to their larger distance, there is an unprobed gap in orbital radius between SBs and VBs. The VAST survey [De Rosa et al., 2011, 2012] represents the most most com-

plete and thorough multiplicity study for A-type stars to date. They found a multiplicity of MF=33.8% between $30 - 10^4$ AU and $q \geq$0.05. The q-distribution is flat for close binaries ($<$ 125 AU) and tends towards smaller mass-ratios for wider systems. Similar to sun-like primaries, the semi-major axis distribution is log-normal, but peaked at ∼390 AU.
Another approach of determining binary properties for intermediate-mass stars is to study rich stellar associations. By an age of a few million years, in fact, these stars have already reached the main sequence. The most studied region for both SBs and VBs [Brown & Verschueren, 1997, Kouwenhoven et al., 2005] is the Scorpius-Centaurus (Sco-Cen) OB association. Combining SBs and VBs, Kouwenhoven et al. [2007] derived a CMRD that can be fitted with a power law with exponent α=-0.45±0.15. For many years this result has been considered as representative of all intermediate-mass binaries.

High-mass MS Stars ($>$ 8 $M_\odot$)

Multiplicity studies for high-mass stars are even more difficult than for intermediate-mass primaries. Due to their large distances, high contrasts in brightness and high rotational velocities, it is challenging to have unbiased estimates. Furthermore, most of O star binaries need to be studied in their birth environment, since only $\sim$ 20% of them are found in the field. Recently, Sana et al. [2012] conducted a rigorous multiplicity study of high-mass SBs down to q=0.2 in young clusters, whereas VBs have been studied for both galactic samples [e.g. Mason et al., 2009] and clusters or associations [e.g. Duchêne et al., 2001, Peter et al., 2012]. In general the multiplicity is $MF \geq$70% for both SBs and VBs. The orbital separation distribution is most likely a combination of a sharp distribution for short period binaries and a power law function extending out to 10^4 AU [Mason et al., 2009, Sana et al., 2012]. According to Sana et al. [2012], the CMRD for SBs is essentially flat. More controversial is instead the q-distribution for VBs. Combining different surveys, Duchêne & Kraus [2013] fitted a power-law with exponent α=-0.55±0.13.

Open Clusters (50 Myr - 1 Gyr)

The objects that belong to open clusters represent a population of relatively young stars. These clusters are generally dynamically old, and binaries have already been processed and wide binaries disrupted [Kroupa, 1995, Parker et al., 2009]. The best-studied open clusters are the Pleiades, Praesepe, the Hyades and α Per. Concerning solar-type primaries in open clusters, they share the same binary properties and are consistent with the field population. Combining both SBs and VBs, Patience et al. [2002] found a multiplicity fraction of $\sim$48% for separation up to 580 AU and $q \geq 0.25$. The distribution of semi-major axis is in good agreement with the field distribution and the CMRD is consistent with flat for both VBs [Patience et al., 2002] and SBs [e.g Bender & Simon, 2008].

Pre Main-Sequence stars (1 - 5 Myr)

Young (1-5 Myr) PMS stars have also been widely studied to characterize their multiplicity properties. PMS stars with masses below 2 $M_{\odot}$ are generally called T Tauri stars. They can be found in dense star forming regions (e.g. the Orion Nebula Cluster, ONC), OB associations (e.g. Sco-Cen) or "loose" associations (also know as T associations, like Taurus-Auriga or Chamaeleon). Around those stars, many VBs have been detected with several techniques. In T associations, the frequency of binary systems is twice as high as in the field [e.g. Duchêne, 1999, Ghez et al., 1993, Leinert et al., 1993]. In dense clusters, instead, the MF is much lower, suggesting a dependence of the fraction of binaries with stellar density. The semi-major axis distribution is consistent both with a log-normal distribution [Kraus et al., 2011] and a slowly declining power-law distribution [King et al., 2012]. Further it seems to be truncated with a maximum separation that varies with stellar mass [Kraus & Ireland, 2012]. The mass-ratio distribution for PMS stars is found to be roughly flat by most surveys [e.g. Kraus et al., 2011].

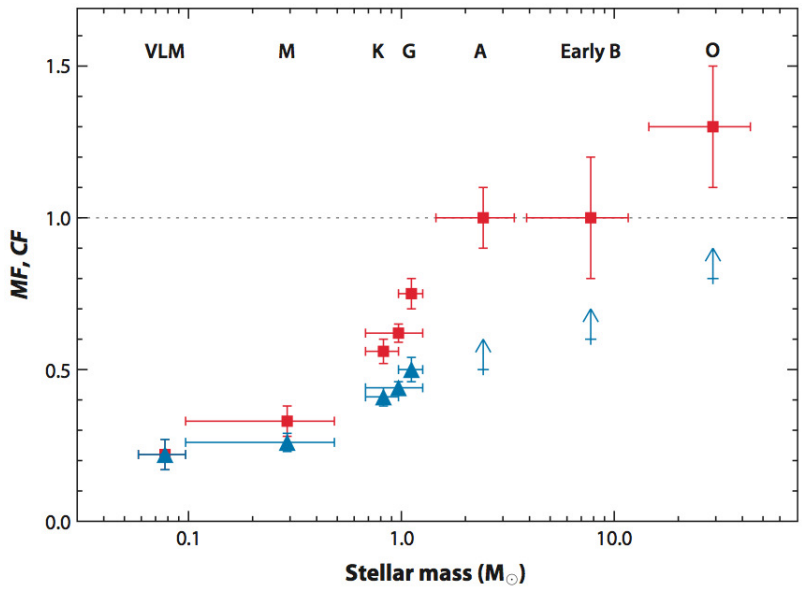

Figure 1.3 — *From Duchêne & Kraus [2013]: Dependency of the CF and MF with primary mass.* The companion frequency is represented by red squares and the multiplicity fraction by blue triangles. The horizontal error bars indicate the approximate mass range for each sample. The values of the MF and CF plotted here can be found in Table 1 of Duchêne & Kraus [2013]

Overall Stellar Companion Statistics

Although using the system mass instead of the primary mass may be more appropriate for comparing binary properties [Goodwin, 2013], it is interesting to evaluate the primary-mass dependence of these properties based on the most recent observations [for a more detailed description see Duchêne & Kraus, 2013]. As shown in Figure 1.3, the MF increases with stellar mass, with a multiplicity fraction that approaches to 100% for high mass primaries. The separation distribution is unimodal for low mass stars and sun-like primaries, but the mean and width of the distribution decreases with decreasing stellar mass (see Figure 1.4). For

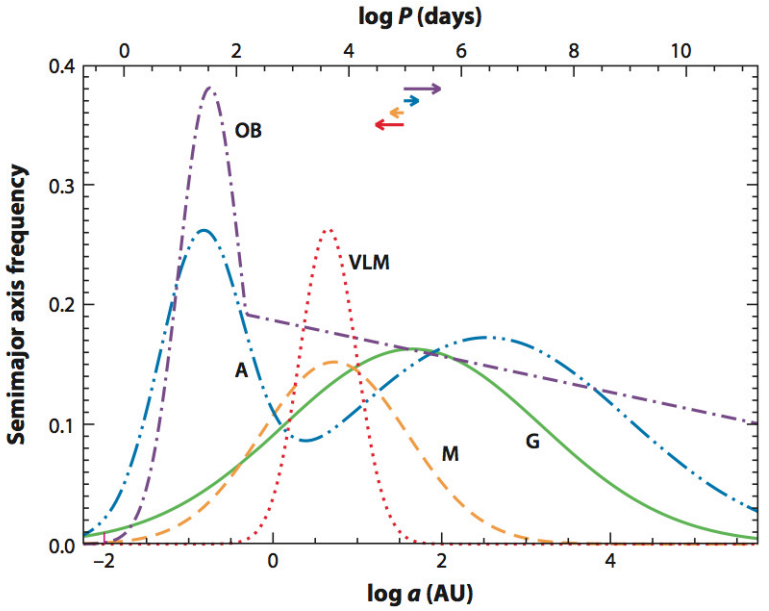

Figure 1.4 — *From Duchêne & Kraus [2013]: Approximate forms of the orbital period distribution for field multiple systems.* The bottom horizontal axis shows the semi-major axis. The top horizontal axis represents the corresponding orbital periods for sun-like binaries. Orbital periods for the other mass ranges are offset from the axis values due to their different total masses. The offsets in period are shown as arrows with the corresponding color for each sample.

intermediate- and high-mass star the distribution is more complicated and presents a peak at short separations. The CMRD is essentially flat, as presented in Figure 1.5, for masses above $0.3M_{\odot}$ and $q > 0.1$. For lower mass primaries the q-distribution becomes skewed to equal-mass systems. According to these results, the multiplicity properties of VLM, low-mass and sun-like stars seem to be a smooth function of stellar mass, indicating a common formation mechanism for these systems. If we ignore the population of short-period high mass binaries, this is also valid for higher mass systems.

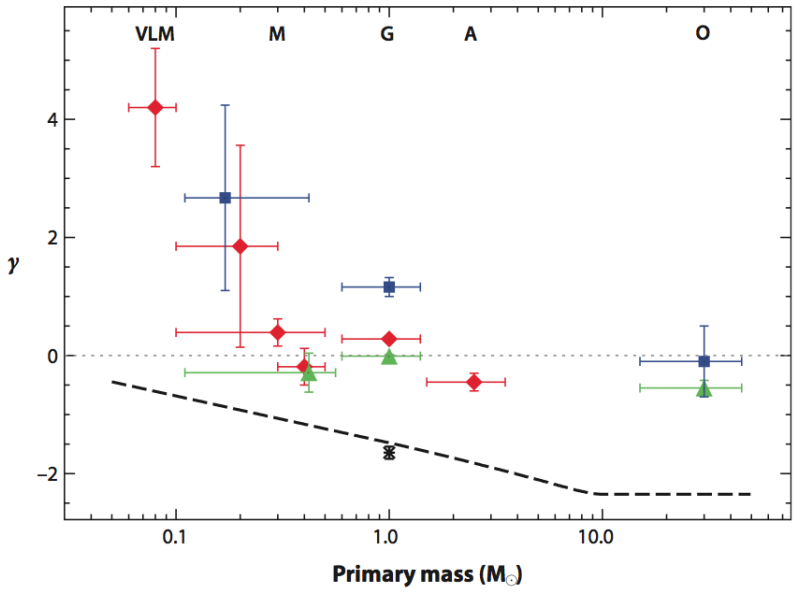

Figure 1.5 — *From Duchêne & Kraus [2013]: CMRD power-law index as a function of primary mass.* Red diamonds represent fits to the population of multiple systems for different primary masses, whereas blue squares and green triangles indicate the power-law index for the subsets of tight ($P \leq \bar{P}$) and wide ($P \geq \bar{P}$) binaries, respectively. The horizontal error bars represent the mass range spanned by each subsample. The horizontal dotted line represents a flat mass-ratio distribution, whereas the dashed curve represents the index that would correspond to companions drawn randomly from the single-star initial mass function (IMF) of Chabrier [2003]. The power-law indexes can be found in Table 1 of Duchêne & Kraus [2013]

1.3.2 BD Companion Statistics

The occurrence of BDs as companions and their mass distribution has been mostly investigated for sun-like stars. Concerning SBs, a low frequency ($< 1\%$) of BDs companions has been observed [Grether & Lineweaver, 2006, Marcy & Butler, 2000] at close separations (< 3 AU). This rare occurrance of close-in companions has been referred to as the

"brown dwarf desert". Recent RV measurements have revealed a minimum in the substellar companion mass function (CMF) between 25 and 45 $M_{Jupiter}$ [Sahlmann et al., 2011]. Direct imaging surveys [Metchev & Hillenbrand, 2009, Tanner et al., 2010] observed a frequency of BD companions among VBs that is in agreement with RV statistics, although potentially consistent with higher frequency, too [Carson et al., 2006]. As suggested by Metchev & Hillenbrand [2009], the observed frequency at large separations (>28 AU) is consistent with an extrapolation of the stellar binary statistics to lower mass-ratios. Whether this paucity of companions with respect to planets and low-mass stellar companions is a true lack of objects, or it is simply due to the shape of the CMF in the substellar regime, will be discussed in Chapter 4.

1.3.3 Planet Statistics

Concerning sun-like stars, RV surveys provide large enough and well defined (e.g. volume-limited) samples of planets that statistics of planetary properties can be derived. Among the different planet-search programs, we adopt Cumming et al. [2008] as a reference for solar- type host stars in this thesis. One of the typical properties measured in such a survey is the fraction of detected planets among the targeted stars. Generally, by using Monte Carlo simulations it is possible to measure the survey completeness and determine the occurrence of planet in a certain range of masses and separation. Cumming et al. [2008] estimated a 10.5% probability of solar type stars having a planet with mass between 0.3-10 $M_{Jupiter}$ and period between 2-2000 days, which is consistent with previous determinations [e.g. Marcy et al., 2005]. The distributions of masses and orbital periods are other important properties of a planet population. They are generally fitted with a double power law, $dN \propto m^{\alpha_1} P^{\beta_1} d\log m\, d\log P$ [e.g. Tabachnik & Tremaine, 2002]. In this case, Cumming et al. [2008] found values of $\alpha_1 = -0.31 \pm 0.2$ and $\beta_1 = 0.26 \pm 0.1$, for solar-type host stars.
Unfortunately, no analogous statistical analysis for M-dwarfs is currently available [see e.g. Delorme et al., 2012]. However, from direct imaging

and microlensing results it is possible to place some constraints on the occurrence of planets around low-mass stars and on the orbital period distribution [Quanz et al., 2012].
Regarding intermediate-mass stars, RV surveys of evolved A-stars [e.g. Johnson et al., 2007, 2010b] show significant differences in the planetary distributions compared to RV-measured statistics around lower-mass stars. Moreover, these results suggest a higher frequency of planets around more massive stars and also more massive detected planets [Johnson et al., 2010a].

1.4 Formation Mechanisms

The processes that lead to the formation of stars have been widely investigated in the past decades. Although we have a general understanding of how individual stars form [e.g. Ballesteros-Paredes & Hartmann, 2007, Hartmann, 2008, Shu et al., 1987], our knowledge regarding the formation of binary systems is still not complete. We know however that at least half of the stars in our Galaxy formed as multiple systems, and that the pre main-sequence population distribution of semi-major axes is consistent with the field distributions [Mathieu, 1994]. This implies that the formation of binaries must be a primary branch of star formation [Mathieu, 1994]. The binary formation mechanisms that have been proposed in the past decades can be divided into three main categories: capture, prompt fragmentation, and delayed breakup [Tohline, 2002].
In the capture scenario, stars preferentially form as isolated objects from molecular cloud cores. Only after the formation process is completed, stars become bound due to dynamical encounters. This means that capture occurs on a timescale that is long compared to the collapse time of each component [e.g. McDonald & Clarke, 1993]. Clarke [1992] has shown that in order to create a bound orbit (total negative energy) there must be some energy loss. This could happen either in the case of three-body interaction, where the extra energy produced in the formation of the binary is transferred as kinetic energy to a third object that escapes

the interaction, or if there is tidal interaction of one component with the circumstellar disk of the other [Larson, 2002]. However the probability of such encounters to occur is too low for capture to be the main mechanism of forming binary systems.
Fragmentation mechanisms (prompt fragmentation and delayed breakup) are thought to be the preferred mechanism for the formation of binaries, as they seem to be able to produce enough of these systems.
In the prompt fragmentation scenario [e.g. Bonnell & Bastien, 1992, Boss, 1986], both components form by fragmentation of the same collapsing molecular cloud core during or soon after its free-fall collapse. The details of the collapse (homologous or non-homologous) are still subject of debate. Delayed breakup, also know as disk fragmentation [e.g. Bonnell, 1994, Stamatellos & Whitworth, 2009] or gravitational instability [e.g. Boss, 1997, Mayer et al., 2002], takes place when the star-disk system has already formed. If the infall onto the disk from the surrounding cloud core material is higher than the accretion rate onto the star from the disk, the circumstellar disk may become gravitationally unstable and consequently fragment. This mechanism is thought to be a viable process for the formation of low-mass stars, BDs and giant planets. Both fragmentation models, however, are still unable to produce close (a <10 AU) binary systems, suggesting that other processes maybe relevant for forming such objects.
Concerning the formation of wide binaries, capture in dissolving cluster [Kouwenhoven et al., 2010, Moeckel & Bate, 2010] has been proposed. In these models, pairs of stars could become bound during the dissolution phase of stellar clusters, giving origin to the small population of large separation binaries ($a = 10^4$ - 10^5 AU) observed in the field.

It is generally believed that the mechanisms for forming brown dwarfs are not different from those creating low-mass stars [Whitworth et al., 2007]. The statistical properties of BDs (such as the mass function, the binary properties, etc.) constitute a smooth continuum with those of low-mass stars [Kraus & Hillenbrand, 2012]. However, for many years several theories have tried to explain the paucity of close BD companions to solar-type stars, including ejection from multiple stellar systems

[Reipurth & Clarke, 2001], disk fragmentation [Rice et al., 2003], subsequent ejection [Bate et al., 2003, Goodwin & Whitworth, 2007], etc. Recently, Jumper & Fisher [2013] have shown that a single turbulent fragmentation model could be able to explain both stellar and BD binary distributions.

Whereas BDs companions are thought to form in a star-like scenario, different theories have been proposed for the formation of giant extrasolar planets. What has been suggested, already since the 18th century, is that planets may form out of the circumstellar material around newly formed stars (the Nebula Hypothesis, Laplace 1796). How to grow from micron-sized particles of dust and ice through more than 10 orders of magnitude up to bodies of thousands or tens of thousands of km in diameter is still not fully understood [for further explanations see Armitage, 2010]. Moreover, gas or ice giant planets present substantial gas envelopes. The presence of these envelopes implies that such objects must form relatively quickly, before the gas in the circumstellar disk is dispersed. According to observations, the gas disk lifetime is in the range between 3-10 million years [e.g. Meyer et al., 2007]. Theories of planet formation need to meet this constraint.
The theory that is considered the most plausible mechanism for the formation of gas giants is core accretion [e.g. Alibert et al., 2004, Pollack et al., 1996]. In this scenario cores of giant planets form by accretions of solids up to a mass of ∼10-15 Earth masses. Whereas in the inner regions of a protoplanetary disk there is not enough material to form such massive bodies, at wider separation both ice and rocky materials condense. This allows the formation of large solid cores at large orbital radii. An increasingly massive atmosphere grows and surrounds the core, as the gas contracts onto it. If the core exceeds a critical core mass, beyond which a it cannot maintain an hydrostatic envelope, gas begins to "collapse" onto the core. The more massive the planet is the more rapidly this process becomes. The core accretion process ends either when the disk of gas dissolves, or because the planet opens a gap in the disk.
As mentioned above, an alternative theory is direct gravitational col-

lapse of the gas within the disk [e.g. Boss, 1997, Mayer et al., 2002]. First, a gas disk becomes unstable if the Toomre's Q parameter, defined as

$$Q = \frac{c_s \Omega}{\pi G \Sigma} \tag{1.10}$$

is less then unity [Toomre, 1964], where Σ is the surface density of the disk, c_s the sound speed and Ω its angular velocity. Second, if the disk cools on an orbital timescale, the instability leads to fragmentation of the disk creating bound objects. These objects, in the case of circumstellar disks, would have masses similar to giant planets. Unlike core accretion, gravitational instability is able to form giant planets extremely rapidly. However, even though young protoplanetary disks may be massive enough to be unstable, it is unlikely that they cool rapidly enough to fragment.
Although core accretion seems to explain the existence of ice giant planets and the observed correlation between the metallicity of the host star the planet frequency, many other unresolved problems indicate that a complete understanding of giant planet formation is yet to be obtained. In the future, the continuously increasing number of known planets may allow us to observe features in the planetary property distributions that can place constraints on planet-formation models.

Despite our incomplete knowledge on the formation of stellar and planetary companions, it appears clear that the mechanisms for the formation of stars and planets overlap in the substellar regime. In addition to that, each theory makes predictions for the q-distribution in different mass ranges. In Table 1.1 we summarize the range of q in which the different formation mechanisms are able to produce companions. This thesis aims at determining the shape of the CMF in the stellar and substellar regime, with the purpose of discriminating among the different theories and determining which formation scenario produces most companions in each mass range.

Tab. 1.1 — Formation Mechanisms

Theory	Mass-Ratio Range	Ref. [a]
PROMPT FRAGMENTATION	$0.003 < q < 1$	1
DISK FRAGMENTATION	$0.001 < q < 0.2$	2
CORE ACCRETION	$q \lesssim 0.006$	3

[a]References: (1) Boyd & Whitworth [2005] , (2) Stamatellos et al. [2011], (3) Matsuo et al. [2007].

1.5 Goals and Outline of this Thesis

The main goal of this thesis is to place some constraints on the formation mechanisms of stellar companions (stars, BDs and planets) by comparing observations of binary properties with MonteCarlo simulations.
Among the other orbital parameters of binary systems, the CMRD appears to be independent of dynamical processing in clusters, thus providing the ideal tool for discriminating among different star formation events [Parker & Reggiani, 2013]. In Chapter 2, we compare observations of the CMRD for different primary masses in the field and star forming regions with the most recent estimates of the Initial Mass Function and predictions from theories of binary formation. In Chapter 3, we discuss the universality of the CMRD in the galactic field and provide the best fit to the distribution.
Assuming that the "universal" CMRD for solar-type stars can be extrapolated to extremely low q values ($q \leq 0.08$), the substellar CMF could result in the superposition of the extrapolation of the stellar CMRD into the BD regime and the RV-measured planet CMF. Such model for the CMF in the substellar-mass range is presented in Chapter 4. A comparison between the predictions from this model and the outcome of direct imaging surveys, probing the occurrence of BDs and planets

around solar-type stars, allows us to place some constraints on the orbital parameter distributions and investigate the existence of the "BD desert" at large ($\geq$ 5 AU) separations. We find no observable quantity that enables us to distinguish whether a particular substellar companion formed in a star- or planet-like mechanism. On a statistical basis, this simple model indicates the probability of a companion having formed as a BD or as a planet in each mass range.
Finally, in Chapter 5, we present as an example of a directly image protoplanet candidate around the Herbig Ae/Be star, HD 169142. Among the different methods, high contrast imaging represents an effective technique for the detection of planetary mass companions at large orbital separation, a key region to distinguish formation mechanisms. Imaging planets in their birth environment, and possibly still embedded in their circumplanetary disk, is another avenue for investigating how such objects might have formed. Furthermore, with a rich disk structure and the hypothesis of a second protoplanet forming in the disk, this planetary system may enable us to explore sequential planet formation and planet evolution in the near future.

CHAPTER 2

BINARY FORMATION MECHANISMS: CONSTRAINTS FROM THE COMPANION MASS-RATIO DISTRIBUTION

This chapter is based on Reggiani & Meyer [2011] (`http://adsabs.harvard.edu/abs/2011ApJ...738...60R`).

Abstract

We present a statistical comparison of the mass-ratio distribution of companions, as observed in different multiplicity surveys, to the most recent estimate of the single object mass function [Bochanski et al., 2010]. The main goal of our analysis is to test whether or not the observed companion mass-ratio distribution (CMRD) as a function of primary star mass and star formation environment is consistent with having been

drawn from the field star IMF. We consider samples of companions for M dwarfs, solar type and intermediate mass stars, both in the field as well as clusters or associations, and compare them with populations of binaries generated by random pairing from the assumed IMF for a fixed primary mass. With regard to the field we can reject the hypothesis that the CMRD was drawn from the IMF for different primary mass ranges: the observed CMRDs show a larger number of equal-mass systems than predicted by the IMF. This is in agreement with fragmentation theories of binary formation. For the open clusters α Persei and the Pleiades we also reject the IMF random-pairing hypothesis. Concerning young star forming regions, currently we can rule out a connection between the CMRD and the field IMF in Taurus but not in Chamaeleon I. Larger and different samples are needed to better constrain the result as a function of the environment. We also consider other companion mass functions (CMF) and we compare them with observations. Moreover the CMRD both in the field and clusters or associations appears to be independent of separation in the range covered by the observations. Combining therefore the CMRDs of M and G primaries in the field and intermediate primary binaries in Sco OB2 over the separation range 1-2400 AU and mass-ratios, $q = M_2/M_1$, from 0.2 to 1, we find that the best chi-square fit follows a power law $dN/dq \propto q^{\alpha}$, with $\alpha = -0.50 \pm 0.29$, consistent with previous results. Finally we note that the KS test gives a $\sim$1% probability of the observed CMRD in the Pleiades and Taurus being consistent with that observed for solar type primaries in the field over comparable primary mass range. This highlights the value of using CMRDs to understand which star formation events contribute most to the field.

2.1 Introduction

The study of binary stellar systems and their properties is one of the most important topics in star formation. Since many stars form in multiple systems, both in the field [e.g Duquennoy & Mayor, 1991, Fischer & Marcy, 1992] and in star forming regions [e.g Patience et al., 2002],

a correct understanding of the binary fraction and companion mass distribution for different primary masses represents a fundamental test for star formation theories. Binary populations, in fact, may carry an even wider amount of information concerning star formation processes than the IMF [Goodwin & Kouwenhoven, 2009]. By conventional definition, in a binary system of stars with masses M_1 and M_2, with $M_1 > M_2$, M_1 and M_2 indicate the primary and secondary mass, respectively. Consequently one can define the ratio of the secondary over the primary mass as $q = M_2/M_1$. Analogous to the initial mass function (IMF) for single objects, one can define the companion mass-ratio distribution (hereafter CMRD) as the distribution of q for a chosen primary mass.

Different binary formation models predict different mass-ratio distributions and dependencies of the CMRD on the primary mass. Traditionally these classes of models have been divided into capture and fragmentation scenarios. Capture refers to the tidal capture of two unbound objects on a timescale that is long compared to the collapse time of each component [e.g. McDonald & Clarke, 1993]. For each primary star the mass of the secondary is chosen randomly from the single star mass function and the secondary-mass distribution would reflect the IMF. While tidal capture appears to be too inefficient in reproducing high binary fractions, it has been noticed that, particularly in small groups of stars, star-disk encounters may form binaries [McDonald & Clarke, 1995]. In any case even this disk assisted capture, whereby a star passing through the disk of another which dissipates enough kinetic energy to form a bound system, is unlikely to be the most relevant binary formation mechanism [Boffin et al., 1998].

Fragmentation scenarios are the preferred mechanism for the formation of multiple systems. The so-called fragmentation models are usually classified as prompt fragmentation [e.g. Bonnell & Bastien, 1992, Boss, 1986] and disk fragmentation [e.g. Bonnell, 1994, Stamatellos & Whitworth, 2009]. In the prompt fragmentation scenario both primary and secondary star form by fragmentation of the same collapsing molecular cloud core. Disk fragmentation takes place in a newly formed star-disk

system in which the disk subsequently fragments due to density perturbations. The latter mechanism is a process by which low-mass stars and BDs (e.g. companions with $q \leq 0.25$) may form. In both cases fragmentation is only the first step in binary formation and processes such as disk accretion and dynamical interactions all contribute to determine the final properties of binary systems [Bate, 2004]. In general, continued accretion onto both objects from a common reservoir tends in the long term to equalize the masses, moving the q distribution towards unity, and this effect seems to be more significant for high mass primaries and in closer binaries [Bate, 2000].

Recently, a variation on capture has been proposed as mechanism for forming wide binaries [Kouwenhoven et al., 2010, Moeckel & Bate, 2010]. In this scenario wide binaries (10^4 - 10^5 AU) would form during the dissolution phase of star clusters, especially during the quick expansion of clusters after gas expulsion. This mechanism could perhaps explain the substantial population of wide binaries observed in the field and, to the first order approximation, the mass ratio distribution could be similar to that expected from random pairing of individual stars [Kouwenhoven et al., 2010].

However, at the moment no model is able to reproduce all of the observed binary properties, in particular, the predicted distributions of separations and mass-ratios tend not to match the observations very well [Goodwin et al., 2007]. Even if no observation will definitely confirm one theory, observations of CMRDs in disparate environments can at least put constraints on theoretical binary formation models. Beginning with the pioneering multiplicity survey of G stars in the solar neighborhood by Duquennoy & Mayor [1991], there have been several studies of binary properties in the field (e.g. Fischer & Marcy [1992], Reid & Gizis [1997] for M dwarfs, Metchev & Hillenbrand [2009] and Raghavan et al. [2010] for solar-type stars) and in clusters or associations [e.g. Ghez et al., 1993, Kraus et al., 2011, Leinert et al., 1993, Patience et al., 2002]. Curiously in young clusters the binary fractions overall are higher but little is known about the CMRD.

Furthermore observations of different star forming regions revealed that the mass distribution of cores usually has a form similar to the IMF [Alves et al., 2007, Motte et al., 1998, 2001], leading to the suggestion that IMF and the core mass function are directly related. At the same time the majority of observations of single objects from the field, local young clusters, old globular clusters and associations suggest a universal IMF [Bastian et al., 2010]. What is the role played by binaries and multiple systems? Is there a connection between the CMRD and the IMF? Metchev & Hillenbrand [2009] present an analytical form of the companion mass function (CMF) and reject the hypothesis that the CMRD of solar-mass stars in the field is consistent with having been drawn from random pairing of the single star IMF. However, the most recent estimate of the log-normal IMF for isolated objects [Bochanski et al., 2010] is peaked at higher masses than those they considered, and might be in closer agreement with the CMRD they derived. It is also interesting to study CMRDs as a function of primary mass as well as in different environments and look for variations in the CMRD among regions where the IMF varies.

Finally, another crucial question that the CMRD could address is the origin of the field. Matching properties of the field to star forming regions could give insights into what sort of regions contribute most to the field. Binaries are subject to dynamical evolution and disruption [Parker et al., 2009], changing the overall binary fraction. The extent of these dynamics depends on the environment in which they were born. Recent results from N-body simulation also predict that some binary properties (e.g. the CMRD for low-mass binaries) might be independent of dynamical processing [Parker & Goodwin, 2011], making them excellent tracers of origins.

A rigorous approach to answering these questions requires a careful account of the completeness of observational data and potential biases as a function of separation, besides a proper choice of the IMF. *So far, a complete analysis of the CMRD over a broad range of primary masses and as a function of separation and environment has not been done.* In

this paper we address the problem of the connection between IMF and CMRD by considering samples of binaries with primaries of different masses and using the most recent evaluation of the IMF. We first describe the datasets we have used in our analysis (Section 2.2). Then in Section 2.3 we discuss the methodology we adopt while the results obtained are shown in Section 2.4. Finally, Section 2.5 and Section 2.6 are left to the discussion of the results and to our conclusions.

2.2 Datasets

2.2.1 Samples from the field and Sco OB2

As mentioned before, the multiplicity of stars in the field has been investigated in the past years by different groups. Among these surveys we have selected for our analysis three studies, each of which surveyed companions for a restricted range of primary masses (M dwarfs, solar-type stars and intermediate-mass stars). In this section we give a brief overview of the datasets we have chosen while in Section 2.2.2 we describe the samples of binary systems from young clusters/associations that we have also considered in our analysis. A full summary of the main properties of all these samples is given in Table 2.1. We already said that to obtain reliable results it is important to account for completeness and possible biases. However also the estimate of completeness and observational biases is not free from uncertainties. Therefore, instead of considering completeness-corrected samples, we decided to limit our investigation to the mass and separation range where the completeness of the samples is flat (so the sample is *representative* in mass, if not complete) and exceeds a certain level ($\geq 65\%$).

The sample of M dwarfs we have considered is the set of binary systems collected by Fischer & Marcy [1992] (hereafter FM92) from several high-quality surveys of M dwarfs with distances within 20 pc from the

Tab. 2.1 — Sample Properties

Sample	Ref. [a]	Primaries	No. Systems	Sep. (AU)	q_{lim}
Field	1	M	27	1-2400	0.2
Field	2	F/G	30	28-1590	0.1
ScoOB2	3	A/late-B	60	29-1612	0.05
Pleiades	4	F/G	22	11-910	0.2
α Persei	5	F/G	18	26-581	0.25
Chamaeleon I	6	G/K[b]	13	20-800	0.1
Taurus	7	G/K[c]	40	5-5000	0.1

[a]References: (1) Fischer & Marcy [1992] , (2) Metchev & Hillenbrand [2009], (3) Kouwenhoven et al. [2005], (4) Bouvier et al. [1997], (5) Patience et al. [2002], (6) Lafrenière et al. [2008], (7) Kraus et al. [2011].

[b]The mass range is 0.55 and 2.2 $M_\odot$, comparable to MH09

[c]The mass range is 0.7 and 2.7 $M_\odot$, comparable to MH09

Sun (ages $\geq$ Gyr). Each one of these surveys covers a different angular separation range, but the complete sample extends from roughly 1 to 2400 AU in separation and down to $q = 0.2$ in mass-ratio. Generally, M dwarfs with masses < 0.2 $M_\odot$ show mass-ratios biased towards unity due to sensitivity limitations (Fischer & Marcy [1992]). For this reason we have considered only binary systems with primaries having masses between 0.2 to 0.55 $M_\odot$, where the sample is 85% complete. The sample consists then of 27 systems.

Regarding solar-mass stars we selected the work presented in Metchev & Hillenbrand [2009] (hereafter MH09). MH09 report results from an adaptive optics survey of stellar and substellar companions to solar analogs (range in primary mass between 0.7 to 1.3 $M_\odot$) within 10-190 pc and in the 3 Myr - 3 Gyr age range. The orbital separation interval covered is 28-1590 AU. The choice of this survey, with respect to previous

works (e.g. Duquennoy & Mayor [1991]), is due to the higher sensitivity to low-mass companions, meaning small mass-ratios ($q \leq 0.1$). In order to have a 65% complete sample we considered the set of 30 binary systems with $q \geq 0.1$ and companions between 28 and 1590 AU from the primary which was defined as minimally-biased sample (AD_{30}) in their paper.

Finally, we chose a sample of companions to A-type and late B-type primaries. Due to the shorter lifetime of more massive stars and the difficulty to find a statistically large and complete survey of intermediate-mass primaries in the field, we selected a dataset in the young (5-20 Myr) and nearby (∼140 pc) Scorpius OB2 association (ScoOB2). This binary population was observed in the near-infrared adaptive optics multiplicity survey described by Kouwenhoven et al. [2005] (hereafter K05) and the properties of the 60 stellar systems we have used in our analysis are taken from Kouwenhoven et al. [2007]. This survey is sensitive to very low mass-ratios (down to $q \sim 0.05$) over the orbital separations range 29-1612 AU between primaries and companions. Despite the fact that Sco OB2 is not a sample from the field and it is young, it is still the best sample ($\geq 90\%$ complete) of intermediate mass primary binaries we can study. Therefore we will include it in the analysis of the other datasets from the field.

We emphasize that the three datasets span similar separation ranges. Even though the study of the detailed dependence of the CMRD on angular separation goes beyond the purpose of the present work, in Section 2.4.1 we will show that our results should not be affected by any possible change in the shape of the CMRD with orbital separation.

2.2.2 Clusters or associations

We considered also four datasets of companions to solar-type stars from nearby clusters or associations that over similar separation ranges have

a reasonable number of binary systems. We have selected observations of binaries in two open clusters, Pleiades and α Persei (α Per), and in two T associations, Chamaeleon I and Taurus.

The Pleiades is one of the best studied open clusters, due to its proximity and richness (roughly 1000 stars at a distance of $\sim$ 120 pc). With an age of 125-150 Myr [Burke et al., 2004, Stauffer et al., 1998] it is just old enough to be dynamically evolved. The sample from the Pleiades [Bouvier et al., 1997] consists of 22 binary systems with G and K primaries observed in the near-IR using adaptive optics. The separation range covered by this survey is 11-910 AU and the mass-ratio distribution is more than 70% complete down to 0.2 over this separation range.

α Per is a younger cluster, with an age of $\sim$90 Myr [Stauffer et al., 1999], at a distance of $\sim$ 190 pc [Robichon et al., 1999]. We selected a sample of 18 solar type stars within the dataset presented in Patience et al. [2002]. They were nearly complete in the separation range from 26 to 581 AU and were sensitive to mass-ratios $q > 0.25$.

Chamaeleon I, instead, is one of the nearest [$\sim$170 pc, Bertout et al., 1999] low-density young [$\sim$1 Myr, Luhman, 2004] star forming regions. It consists of $\sim$230 stars and has a stellar density that is low compared to other young regions [Luhman, 2008]. We have considered the results of a multiplicity survey presented by Lafrenière et al. [2008]. The primaries span the mass range from $\sim$ 0.1 to 3 $M_\odot$ and the separation range $\sim$20-800 AU. We have selected a subsample with only K and G primary binaries with masses between 0.55 and 2.2 $M_\odot$ and mass-ratios down to $q \sim 0.1$ ($\sim$ 90% complete), comparable to MH09 (13 systems in total).

Finally we selected a sample of solar-type primary binaries in Taurus from the almost complete sample by Kraus et al. [2011]. Taurus is another young (1 Myr) low-density star-forming region close to the Sun (d = 140 pc) with more than 300 PMS stars and brown dwarfs [Kenyon et al., 2008]. We considered 40 systems with primary masses between 0.7 and 2.5 $M_\odot$, mass-ratio $q \geq 0.1$ and angular separation in the range

$5 - 5000$ AU.

We will discuss the dependence of the CMRD on separation in Section 2.4.1.

2.3 Methodology for our analysis of these surveys

2.3.1 Monte Carlo simulations

Our goal is to explore whether the observed mass-ratios in the field and young clusters or associations as function of primary mass could be the outcome of random pairing of stars from the stellar IMF. To this end we have created a Monte Carlo tool able to generate artificial companion mass-ratio distributions as expected by random sampling of secondaries from a chosen function, for fixed primary mass. Through these simulations one can reproduce a population of N binaries by fixing the mass of the primary and the analytic form to be tested, and then compare this simulated CMRD with the observations.

2.3.2 Initial Mass Function

The Initial Mass Function we have considered in our analysis is the single objects IMF from Bochanski et al. [2010] (hereafter Bo2010). Below 1 $M_{\odot}$ it is a log-normal function of the mass, defined as $\xi(\log m) = dn/d\log m$. Except for a normalization constant, it can be parametrized (in $(\log M_{\odot})^{-1}pc^{-3}$) as:

$$\xi(\log m) \propto \exp\left\{-\frac{(\log m - \log m_c)^2}{2\sigma^2}\right\} \tag{2.1}$$

where $m_c = 0.18$ and $\sigma = 0.34$.

For m>1 $M_\odot$ we assumed the classical "Salpeter slope":

$$\xi(\log m) \propto m^{-1.35}. \tag{2.2}$$

The study by Bochanski et al. [2010] is based on the observational work presented in Covey et al. [2008] which represents the largest field investigation of the luminosity function to date constructed from a catalog of matched Sloan Digital Sky Survey (SDSS) and Two Micron All Sky Survey (2MASS) sources. Note that in Bo2010 the log-normal peak of the mass distribution is shifted toward higher masses compared to Chabrier [2003] ($m_c = 0.08$ and $\sigma = 0.69$).

In each run of our Monte Carlo simulations, the assumed IMF is normalized to the primary mass that we choose, to the appropriate range of q for the dataset with which we compare the results, and to the number of binaries N that we want to reproduce. We typically run each simulation 10^5 times.

2.3.3 KS test

To evaluate the probability that the observed CMRDs and the simulated ones come from the same parent distribution we use the the Kolmogorov-Smirnov test (KS test). The KS test in fact is a statistical test which returns the probability that two distributions were drawn from the same parent sample by examining the maximum difference in the cumulative distribution functions.

For our purposes, we have tested how well this statistical tool can distinguish differences in the shape of the distributions and evaluated the extent to which results depend on sample size.

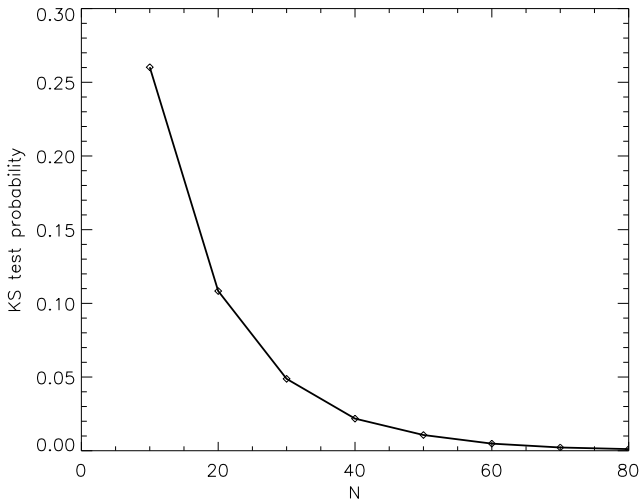

Figure 2.1 — *Capability of the KS test to distinguish flat and log-normal distribution.* The solid black line describes how varies the probability given by the KS that a log-normal differs from a flat distribution, as function of sample size. We computed this probability for samples of 10, 20, 30, 40, 50, 60, 70 and 80 objects.

First, we tested the reliability of the KS test to distinguish two populations of stars distributed in mass according to power law distributions with different slopes as a function of sample size. With larger populations, the KS test is able to detect smaller differences in slope. From the comparison of distributions of only 10 objects the KS test gives a probability of $\sim 10^{-2}$ for a difference of 5 in the slopes while when the number of objects increases to 30 the same probability is already obtained with a difference of 2.5.

Second, we checked the capability of the KS test to distinguish a log-normal and a flat distribution, again as function of sample size. This test is of great importance because, on one hand, we want to test the hypothesis of a log-normal CMRD, on the other, the linearly flat distri-

bution of q is a commonly made assumption in numerical simulations [e.g. Kouwenhoven et al., 2009, Parker et al., 2009]. In Figure 2.1 we show our results. In this comparison, with a sample of $\sim$50 objects the KS test returns a 1% chance of having been drawn from the same parent. A KS probability of 1% is the threshold we adopt equal to or below which we reject the hypothesis of two distributions being consistent.

2.4 Results

Here, we report our findings regarding the comparison of the observed CMRDs with the simulations. We begin describing in Section 2.4.1 the results for the samples of M dwarfs, G stars in the field and intermediate mass stars in ScoOB2. In Section 2.4.2 we summarize the outcome of our tests for the Pleiades, α Per, Chamaeleon I and Taurus. We compare the observed CMRDs with other commonly assumed companion mass functions in Section 2.4.3. Finally (Section 2.4.4) we give our best fit estimate of the distribution.

2.4.1 Results from the field and Sco OB2

The top panel of Figure 2.2 shows the CMRD for the sample of 27 M dwarf primary binary systems from Fischer & Marcy [1992]. The hatched histogram represents the observed distribution of q, while the dashed line is the CMRD generated by random pairing through Monte Carlo simulations from Bo2010 for the same range of mass-ratios ($q \geq$0.2). The KS test gives a probability of $\sim$ 1% that the observations are consistent with the IMF in the separation range 1-2400 AU. From the figure it appears that there is an overabundance of equal mass binaries in the observed sample compared to the predictions of random pairing from the IMF.

Tab. 2.2 — KS test probabilities (%)

Sample	Ref. [a]	Bo2010	Flat CMF	$dN/dM_2 \propto M_2^{-0.4}$
Field - M	1	1	58	24
Field - F/G	2	10^{-3}	2	58
ScoOB2 - A/late-B	3	10^{-13}	0.4	30
Pleiades - F/G	4	10^{-4}	34	17
α Persei - F/G	5	0.1	27	89
Chamaeleon I - K/G	6	17	30	76
Taurus- K/G	7	10^{-11}	45	2

[a]References: (1) Fischer & Marcy [1992] , (2) Metchev & Hillenbrand [2009], (3) Kouwenhoven et al. [2005], (4) Bouvier et al. [1997], (5) Patience et al. [2002], (6) Lafrenière et al. [2008], (7) Kraus et al. [2011].

In Figure2.2 (central and bottom panels) we also present the results obtained for the other two datasets. In both cases we compare the observations (hatched histograms) with the simulated CMRDs (dashed line histograms) over the same range of q. On the basis of the KS test for the samples of solar type from the field and A type stars from Sco OB2 we get probability of 10^{-3} and 10^{-13} respectively that the CMRD is consistent with the field IMF in the separation range ∼30-1600 AU. The results are summarized in Table 2.2. We find again that the observed mass-ratios are more strongly peaked towards unity than in the simulations from the IMF.

This overall result suggests that we can reject the hypothesis that the CMRD is consistent with having been drawn from the IMF over the separation range ∼30-1600 AU and this statement seems to hold true independent of the primary mass and angular separation. In fact we checked with the KS test whether for each sample we see variations in the CMRD as a function of the angular separation. Practically, for

each one of the datasets we have considered different values of the angular separation within the range covered by the observations, and we evaluated for each of these separations the KS test probability of the CMRD inside this value being consistent with the CMRD outside. For any given separation we find probabilities less than 0.1%. Therefore we did not see any evidence for dependence on orbital separation in any of the samples under study.

Therefore we can compare with the KS test the observed CMRDs for these three datasets over the common range of q. The distributions of mass-ratios for M dwarfs and solar type stars are consistent at the 6% level. On the other hand the probability of the sample of intermediate mass stars from ScoOB2 being consistent with G/K stars and M dwarfs in the field is 36% and 53% respectively. These results suggest that we cannot reject the hypothesis they are all drawn from the same parent distribution.

2.4.2 Results from clusters and associations

We also compared the datasets of solar type stars from the Pleiades, α Per, Chamaeleon I and Taurus with the results of the MC simulations of the IMF over the range of q spanned by each sample. In Figure 2.3 we show the CMRD for the Pleiades. The KS test probabilities that the observed CMRDs of all samples are consistent with having been drawn from the IMF are given in Table 2.2. With regard to the Pleiades, α Per and Taurus (KS test probabilities of 10^{-4}%, 0.1% and 10^{-11}%, respectively) we can reject the hypothesis of random pairing, while the higher probability (17%) between the IMF and CMRD in Chamaeleon I does not allow us to rule out the null hypothesis in this case. However, the number of objects (13) in Chamaeleon I sample is quite low. As we have shown in Section 2.3.3 the KS test can only distinguish extreme differences in distributions from such small samples.

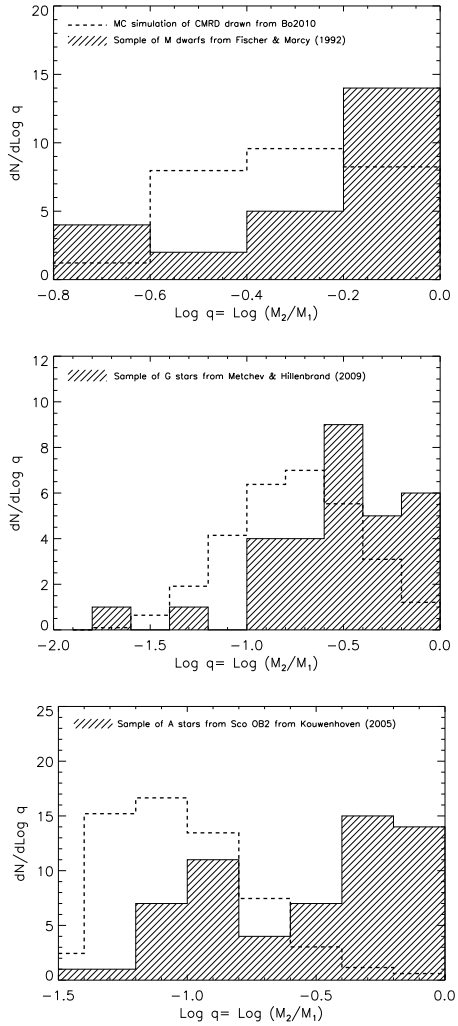

Figure 2.2 — *Companion mass-ratio distributions and the IMF in the field.* From top to bottom the comparison between the observed CMRD and the log-normal field IMF is shown for M dwarfs, G stars in the field and for the sample of intermediate stars in Sco OB2 respectively. The hatched histogram represents the observed CMRD for the relative dataset of binary systems (see Section 2.2). Superimposed with a dashed line is the CMRD generated for the same number of objects through random pairing from Bo2010. The KS probabilities are summarized in Table 2.2.

We should also note that in Taurus the IMF is peaked toward higher masses with respect to the field IMF [Luhman et al., 2009]. The use of the proper mass distribution would bring the CMRD in Taurus in closer agreement with random pairing from the IMF. Hence we should be cautious in interpreting this preliminary result.

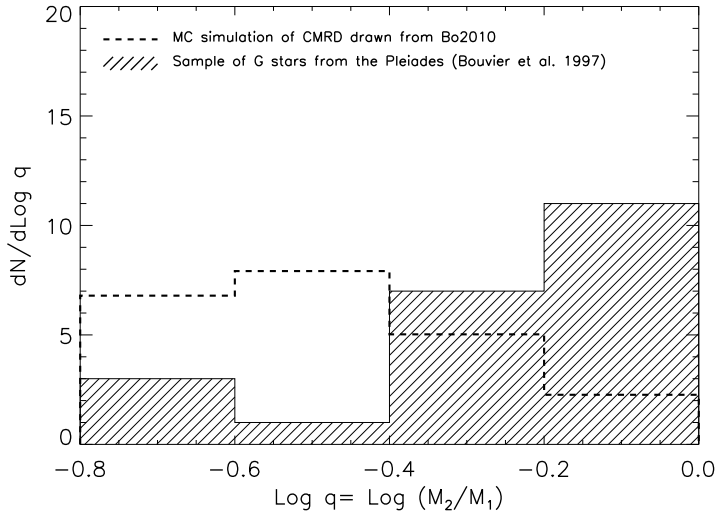

Figure 2.3 — *Companion mass-ratio distribution for solar-type stars in the Pleiades.* The image shows the comparison between the observed CMRD in the Pleiades and the predictions from the IMF. We adopt the same legend as in figure 2.2. The probability from the KS test that observations are consistent with the IMF is less than 1%.

To summarize, at the moment in the Pleiades and α Per we can reject the possibility of the CMRD being drawn from the IMF for orbital separation between 20 and 600 AU, whereas concerning much younger regions, we rule out the random pairing from the field IMF only in Taurus in the separation range 5-5000 AU. Data from larger and different samples are needed to better constraint the result as a function of age and environment.

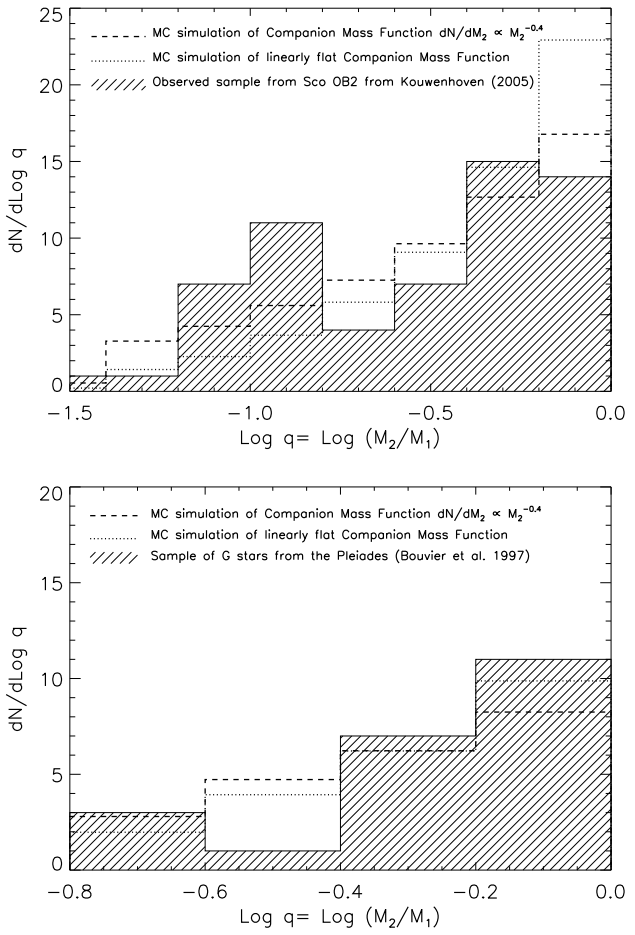

Figure 2.4 — *Test of other CMFs.* Top: the figure shows the comparison between the observed CMRD for intermediate stars in ScoOB2 with a flat CMRD (dotted line) and a companion mass function of the form $dN/dM_2 \propto M_2^{-0.4}$ (dashed line). We found a probability of less then 1% that the observations are consistent with the flat CMF while a 30% level of agreement with the CMF by MH09. Bottom: Comparison for the observed CMRD for solar-type stars in the Pleiades with the two choices of CMF. The KS test probabilities we obtained are 34% and 17% for the flat CMRD and MH09 CMF, respectively. The probabilities for all the other samples we have considered are given in Table 2.2.

Tab. 2.3 — KS test probabilities

Sample	Ref. [a]	Bo2010 (%)
Field - M	1	1
Field - F/G	2	10^{-3}
ScoOB2 - A/late-B	3	10^{-13}
Pleiades - F/G	4	10^{-4}
α Persei - F/G	5	0.1
Chamaeleon I - K/G	6	17
Taurus- K/G	7	10^{-11}

[a]References: (1) Fischer & Marcy [1992] , (2) Metchev & Hillenbrand [2009], (3) Kouwenhoven et al. [2005], (4) Bouvier et al. [1997], (5) Patience et al. [2002], (6) Lafrenière et al. [2008], (7) Kraus et al. [2011].

2.4.3 Different Companion Mass Functions

Using the same Monte Carlo method, we have tested also whether the observed CMRD as function of primary mass and environment is consistent with other analytic forms of the CMRD. First of all we have considered a linearly flat companion mass-ratio distribution (see Section 2.3.3) and second we have tested the companion mass distribution $dN/dM_2 \propto M_2^{-0.4}$ suggested by MH09. In Table 2.3 we report the KS probabilities for each dataset. Concerning the flat distribution, only for the sample of A and late B-type primary binaries in Sco OB2 we can reject the hypothesis that the two distributions are consistent. The comparison in this case is shown in the top panel of Figure 2.4. Note that the ScoOB2 is the largest sample, placing the strongest constraints on possible differences. The MC simulations of flat CMF for the young regions match well the observations (see e.g. bottom panel of Figure 2.4). Regarding the CMRD provided by MH09 we find a KS probability exceeding 15% for all samples (see Table 2.2) except for Taurus (2%).

We should keep in mind that the KS test is not suited to evaluate which is the best fit distribution. If we take as an example the results for the FM92 sample, the difference in the probability from 58% to 24% between the flat and M09 CMF in the context of the KS test does not have any significance. Furthermore, the sample size of our datasets in the majority of cases prevents us from discriminating between log-normal, flat or other distributions (see Section 2.3.3). For this reason we have utilized a chi-square procedure to determine the best fit for the CMRD for a combined sample including all primary masses.

2.4.4 Chi-square best fit

Motivated by the fact that the CMRD appears to be independent of angular separation over the range we are considering, we combined together, over the common range of mass-ratios (q=0.2-1), the samples of M dwarfs and G stars in the field and intermediate mass stars in ScoOB2 even thought the separation ranges vary across the samples. We then used the composite q distribution to find the best fit. According to the chi-square test for M_1=0.25-6.5 $M_\odot$ the total mass-ratio distribution follows a power-law $dN/dq \propto q^\alpha$, with α=-0.50±0.29 (χ^2= 0.7 with 7 degrees of freedom; see Figure 2.5). This result is also in agreement with the value of α=-0.50 (45-900 AU) for B star primaries [Shatsky & Tokovinin, 2002] or with α=-0.4 for K dwarfs primaries [Mazeh et al., 2003] in the orbital range 0-4 AU. Metchev & Hillenbrand [2009] and Kouwenhoven et al. [2005], already included in the sample under discussion, found α=-0.39±0.36 and α=-0.33 respectively.

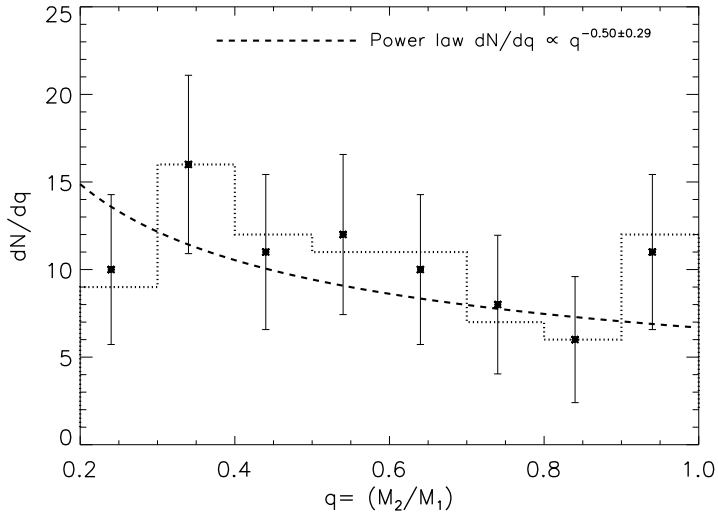

Figure 2.5 — *Chi-square best fit* mass-ratio distribution for the sample of primaries in the field with masses between 0.25-6.5 $M_{\odot}$ over the separation range 1-2400 AU. The best chi-square fit is a power-law $dN/dq \propto q^{\alpha}$, with $\alpha = -0.50 \pm 0.29$ (χ^2= 0.7 with 7 degrees of freedom).

2.5 Discussion

The results from the field and Sco OB2 described in Section 2.4.1 show an overall trend of CMRDs more peaked towards equal mass values than predicted by random pairing from Bo2010. This result suggests that the capture hypothesis, at least for primary stars in the mass range 0.25-7 $M_{\odot}$ and orbital separation range 1-2400 AU, is not the major mechanism for binary formation.

Our findings appear to be in agreement with predictions from fragmentation theories of binary formation, even though we cannot discriminate between different fragmentation mechanisms. In general, near-

equal mass binaries are the most likely outcome of fragmentation in hydrodynamical simulations [e.g. Bate, 2000, Kouwenhoven et al., 2009]. In these simulations, companions are expected to form by the fragmentation of massive accretion regions around stars in very early phases of star formation [Goodwin et al., 2007] and to gain mass from the gas reservoir around them. In this process, even though a secondary star forms with an initial mass close to the opacity limit for fragmentation, it will accrete from the circumstellar material, reaching a mass roughly similar to the primary [Kouwenhoven et al., 2009]. These calculations generally predict a relation between mass-ratio and separation, showing closer binaries with higher mass-ratios than wider systems [Bate, 2000, 2009]. This outcome differs from the observational evidence of a CMRD which is independent of separation from few to few thousands AU and suggests that some key element is still missing in our models of multiple formation.

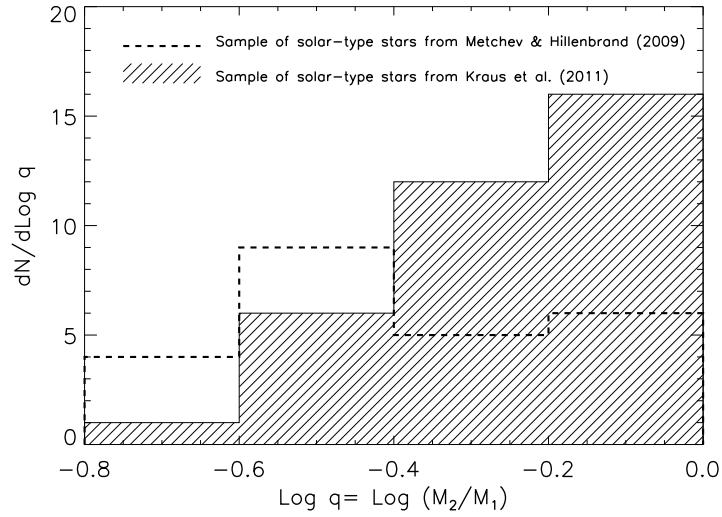

Figure 2.6 — *Companion mass-ratio distribution for solar-type stars in Taurus [Kraus et al., 2011] and in the field (MH09).* The image shows the comparison between the observed CMRD in Taurus for the sample of solar type stars primaries and the one observed in the field over the common range of q.

It should be also noted that the field is likely a mixture of systems coming from very different environments [Goodwin, 2010]. Binaries might have been processed in different ways [Parker et al., 2009] and diverse star forming regions may contribute in different degrees to the field. Recent results from N body simulations [Parker & Goodwin, 2011] show that the CMRD for very low mass binaries is independent of dynamical evolution. If this preliminary evidence holds for a broader range of primary masses, we can rule out the hypothesis that the CMRD was drawn from the IMF at any evolutionary stage, suggesting the current CMRD corresponds to the birth mass-ratio distribution. If this is the case variations in the CMRD can be used to trace how different star formation regions contribute to the field.

Interestingly, if we compare the CMRD for solar-type primaries in the Pleiades and in the field (MH09) we obtain a probability of $\sim$1%. Likewise (see also Figure 2.6), we find a probability of $\sim$1% with the KS test between the CMRDs for solar-type primaries in Taurus and the field (MH09). Perhaps bound open clusters like the Pleiades or extremely low density Taurus-like SFs do not contribute significantly to the field stellar population [e.g. Adams, 2010, Kroupa, 1995, Portegies Zwart, 2009]. This points toward using binary properties to understand which star formation events contribute most to the field. Furthermore the comparison between the mass-ratio distribution in Taurus and Pleiades return a 37% KS probability, suggesting they are drawn from the same parent population. However the reason why the CMRD turns out to be similar in so different environments remains an open question.

2.6 Conclusions

We have explored the connection between the CMRD and the IMF as a function of primary mass in the field and in few examples of clusters and low density associations through Monte Carlo simulations. Using the KS test we determined the probability that the two distributions

are consistent. We have also examined the probabilities that observed samples are consistent with having been drawn from a linearly flat mass-ratio distribution and a CMF of the form $dN/dM_2 \propto M_2^{-0.4}$. Finally we have found the best chi-square fit for a composite CMRD in the primary mass range 0.25-6.5 $M_\odot$ ($q \geq 0.2$) over the angular separation range 1-2400 AU.

Our main results can be summarized as follows:

- We can reject the hypothesis that the CMRD was drawn from the single object IMF for solar type stars and M dwarfs in the field and A and late-B type stars in Sco OB2 in the separation range ∼30-1600 AU. The observed CMRDs show a larger number of equal-mass systems than would be predicted by the IMF. This is in agreement with fragmentation theories of binary formation.

- We do not see evidence for variation of the CMRD with orbital separation in the ranges explored by the observations.

- Concerning the observed CMRDs for M dwarfs and G stars in the field, we obtain a probability of 6% that they are consistent with each other over the same range of mass-ratios. The CMRD for the sample of A and late-B type primaries in Sco OB2 is consistent with both the CMRDs of M and G stars with a probability of 36% and 53% respectively. In other words, they all appear to be consistent with each other.

- The inconsistency between the CMRD observed in the Pleiades and Taurus and that observed in the field suggests Pleiades- and Taurus-like SF events do not contribute significantly to field.

- Regarding the combined CMRD of M and G primaries in the field and intermediate primary binaries in Sco OB2 over the separation range 1-2400 AU and mass range 0.25-6.5 $M_\odot$, we obtain a chi-square best fit following a power law $dN/dq \propto q^\alpha$, with $\alpha = -0.50 \pm 0.29$, consistent with previous studies.

Certainly further binary studies in young clusters are needed to study the dependence of the CMRD on dynamical processes and to test possible variations in the mass-ratio distribution as tracers of different star formation mechanisms.

CHAPTER 3

THE UNIVERSALITY OF THE COMPANION MASS-RATIO DISTRIBUTION

This chapter is based on Reggiani & Meyer [2013] (`http://adsabs.harvard.edu/abs/2013A%26A...553A.124R`).

Abstract

We present new results regarding the companion mass-ratio distribution (CMRD) of stars, as a follow-up of our previous work. We used a maximum-likelihood-estimation method to re-derive the field CMRD power law avoiding dependence on the arbitrary binning. We also considered two new surveys of multiples in the field for solar-type stars and M dwarfs to test the universality of the CMRD. We found no significant differences in the CMRD for M dwarfs and solar-type stars compared with previous results over the common mass-ratio and separation range.

The new best-fit power law of the CMRD in the field, combining two previous sets of data, is $dN/dq \propto q^{\alpha}$*, with* $\alpha = 0.25 \pm 0.29$*.*

3.1 Introduction

A large portion of stars, both in the field [Janson et al., 2012, Raghavan et al., 2010] and in star-forming regions [Patience et al., 2002], are formed in multiple systems. Therefore understanding multiple star formation is necessary to investigate star formation in general [Duchêne & Kraus, 2013, Goodwin et al., 2007]. Because binary properties reflect the main characteristics of binary formation, they may help us determining the most common mechanisms for the formation of multiple stars. In a binary system of stars with masses M_1 and M_2 ($M_1 > M_2$), the mass-ratio is conventionally defined as $q = M_2/M_1$. Similar to the initial mass function (IMF) for single objects, the companion mass-ratio distribution (CMRD) is the distribution of q values as a function of primary mass. Tidal capture models predict that for each primary star the mass of the secondary is chosen randomly from the single-star mass function, and the CMRD reflects the IMF [Kroupa et al., 2003, McDonald & Clarke, 1993]. In fragmentation scenarios subsequent continued accretion onto both objects from a common reservoir tends to equalize the masses, resulting in a q distribution peaked toward unity [Bate, 2000]. Capture is unlikely to be the most relevant binary formation mechanism, but it may still occur during the dissolution phase of star clusters, causing differences in the shape of the CMRD as a function of orbital separation [Moeckel & Bate, 2010, Moeckel & Clarke, 2011]. Motivated by the fact that every theoretical model predicts a different shape of the mass-ratio distribution and of dependency of the CMRD on the primary mass, we used Monte-Carlo simulations to compare the CMRD for different samples and to study the relationship between the IMF and the CMRD (Reggiani & Meyer [2011], hereafter, RM11). This research note represents a follow-up to RM11, in which we reanalyze the "universal" CMRD by adopting a different statistical approach (Section 3.2) and some new results on

the CMRD on the basis of recent datasets (Section 3.3).

3.2 Universal companion mass-ratio distribution

The CMRD appears to be universal over a wide range of q values and primary masses [e.g. Metchev & Hillenbrand, 2009]. According to RM11, the CMRD follows a single-slope power law $dN/dq \propto q^{\alpha}$ over the separation range 1-2400 AU and primary mass range 0.25-6.5 $M_{\odot}$, and there is no evidence for variation of the CMRD with orbital separation.

In previous work we combined samples of M dwarfs [Fischer & Marcy, 1992] and G stars [Metchev & Hillenbrand, 2009] in the field and intermediate mass stars in ScoOB2 [Kouwenhoven et al., 2005] adopting a χ^2 fit of the combined binned distribution to derive the power law slope, obtaining $\alpha = -0.50 \pm 0.29$ [Reggiani & Meyer, 2011]. The choice of the statistical method was motivated by the need of comparing our results with previous studies of the CMRD [e.g. Kouwenhoven et al., 2005, Metchev & Hillenbrand, 2009]. However, the χ^2 fit of a binned distribution can lead to a biased estimate, in particular for small samples. A more robust analysis is instead achieved through a maximum-likelihood estimation method [Feigelson & Babu, 2011]. This approach gives a new best-fit power law $dN/dq \propto q^{\alpha}$, with $\alpha = -0.18 \pm 0.33$ to the data described in RM11. Although the two values are consistent with each other within the errors, the new estimate is flatter than previously thought.

3.3 Updates to the CMRD in the field

Recently, two new studies of the CMRD for solar-type [Raghavan et al., 2010] and M-dwarf primaries [Janson et al., 2012] in the field have been carried out. Since they represent the most complete samples to date for

sun-like stars and M dwarfs, respectively, we applied the same statistical analysis as was presented in RM11 to follow up this preliminary work.

In the first study [Raghavan et al., 2010], roughly 200 binaries with primary masses between 0.5-3 $M_{\odot}$ were considered to determine the CMRD over a wide range of separations (10^{-1}-10^{5} AU) and mass-ratios (0.02-1). The new CMRD appears to be more peaked toward unity than previously observed and the period distribution is unimodal and roughly log-normal with a peak at around 50 AU. Following the methodology described in RM11, we used a KS test to compare the newly observed CMRD with the CMRD by Metchev & Hillenbrand [2009], over the common range of mass-ratios (0.02-1) and separations (28-1590 AU). The KS test returns a probability of $\sim 30\%$, therefore we cannot reject the hypothesis that the data were drawn from the same parent population. However, when we compare the two samples over the common range of mass-ratios, irrespective of separation, the probability is only $\sim 1\%$, pointing toward a change of the CMRD with orbital radius, because that of Raghavan et al. [2010] covers a wider range than that of Metchev & Hillenbrand [2009]. We therefore tested the possibility of a variation of the CMRD with angular separation. To do this we considered break points in the angular separation distribution between 10^{-1} and 10^{5} AU and used a KS test for each of them to determine the probability that the CMRD inside the break point is consistent with the CMRD outside. Because we found probabilities greater than 1% for any possible choice of break point, we conclude that we have no strong evidence for a dependence of the CMRD on angular separation. Moreover, because we do not expect to see random pairing from cluster dissolution models inside 10^{4} AU [Kouwenhoven et al., 2010] and these widest binaries are relatively rare, we need larger samples in the future to test these models.

The second study [Janson et al., 2012] consists of 85 systems with primary masses between 0.15-0.5 $M_{\odot}$, separations in the range 3-227 AU and mass-ratios between 0.1 and 1. For M dwarfs, the CMRD appears to be flat and the period distribution is narrower and peaks at lower values than for solar type primaries, indicating a continuous transition

from higher- to lower-mass stars [Burgasser et al., 2007]. In this case as well, we tested the newly observed CMRD with the CMRD from Fischer & Marcy [1992] over the common range of mass-ratios and separations. With a probability of ∼56% the KS test does not allow us to reject the hypothesis that the newer data were drawn from the same parent sample. Finally, we used the same procedure as we adopted for sun-like stars, but in the range 3-227 AU, to explore the dependence of the observed CMRD on separation. We saw no evidence of this dependence either for this sample.

Moreover, we compared the CMRD for solar-type primaries from Raghavan et al. [2010] with the new sample of M-dwarf primary binaries [Janson et al., 2012]. The KS test returned a probability of 30% that the two distributions are consistent with each other (Figure 3.1). Motivated by this result and because the CMRD is independent of angular separation, we combined the two CMRDs over the common range of mass-ratios. We again used a maximum-likelihood method to fit the distribution and found a power law $dN/dq \propto q^{\alpha}$, with α=0.25±0.29. While this slope α is formally consistent with the one derived in Section 3.2 (within the errors), the change in sign is significant. It is also worth mentioning that this fit is consistent with the mass-ratio distribution with power-law exponent α=-0.10±0.58 presented in a recent study of O-type spectroscopic binaries [Sana et al., 2012], whereas the observed CMRD for brown dwarfs (α ∼1.5) points toward a different formation mechanisms for these objects [Goodwin, 2013].

3.4 Summary

In this research note we have presented some updates to the study of RM11. First, we adopted a maximum-likelihood estimation method to re-derive the field CMRD power law, based on the combination of samples [Fischer & Marcy, 1992, Kouwenhoven et al., 2005, Metchev & Hillenbrand, 2009] described in RM11, to show how the dependence on

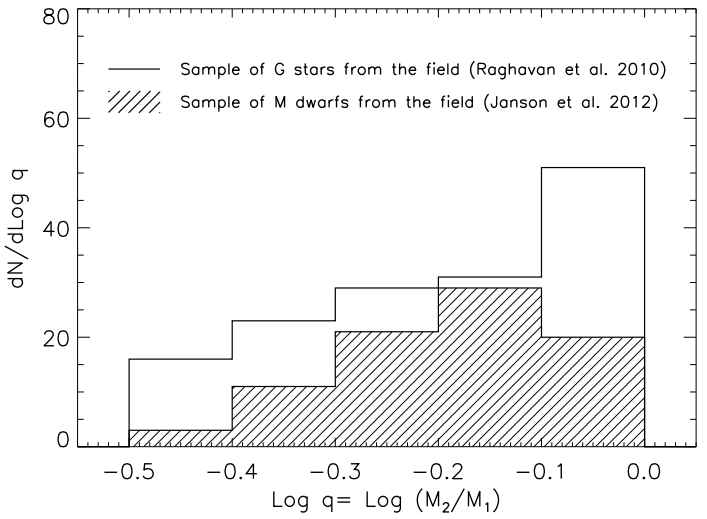

Figure 3.1 — *Comparison between the observed CMRDs for solar-type primaries and M-dwarf primaries in the field.* The open histogram represents the CMRD from Raghavan et al. [2010], whereas the hashed histogram represents the distribution from Janson et al. [2012]. The KS test returns a probability of 30% that the two distributions are drawn from the same parent sample.

the bin size can bias the result.

Secondly, we analyzed recent binarity studies from the field [Janson et al., 2012, Raghavan et al., 2010] adopting the same methodology as in RM11. The new results from Raghavan et al. [2010] appear to be consistent with Metchev & Hillenbrand [2009] over the common range of mass-ratios and angular separations. The recent updates on the M-dwarf CMRD [Janson et al., 2012] are also consistent with past results. The KS test does not allow us to reject the hypothesis that the CMRDs from Raghavan et al. [2010] and Janson et al. [2012] are drawn from the same parent sample. In both studies we uncovered no evidence for a dependence of the CMRD on separation. Therefore we combined the two distributions and obtained a new maximum-likelihood fit to the field

CMRD $dN/dq \propto q^{\alpha}$, with α=0.25±0.29.

Since the CMRD appears to be independent of separation and dynamical evolution [see also Parker & Reggiani, 2013], it represents a measurable parameter of binary stars to focus on when investigating binary formation mechanisms. However, we need larger samples to look for subtle variations of the CMRD with separation. In the future we aim to study the CMRD in other star-forming regions (e.g. the ONC) and test its dependence on separation for wide systems.

CHAPTER 4

BROWN DWARFS AND GIANT PLANETS AS COMPANIONS TO SOLAR-TYPE STARS: NO GAP BUT LOCAL MINIMUM

This chapter is based on a paper to be submitted to Astronomy & Astrophysics

Abstract

In recent years there have been many attempts at characterizing the occurrence and distribution of stellar, brown dwarf (BD) and planetary-mass companions to solar-type stars, with the aim of constraining formation mechanisms. Although the mass and semi-major axis distributions are quite well established for stellar companions, in the substellar regime they are not fully understood. From radial velocity observations a dearth

of companion with masses between 10-40 $M_{Jupiter}$ has been noticed at close separations, suggesting the possibility of a distinct formation mechanism for objects above and below this range. Several direct imaging surveys have reported non-detections of both giant planets and BDs at larger separations (>5 AU). In this paper we present a new model for the substellar companion mass function. It consists of the superposition of the planet and BD companion mass distributions, assuming that we can extrapolate the radial velocity measured companion mass function for planets to larger separations and the stellar companion mass-ratio distribution over all separations into the BD mass regime. By using both the results of the VLT/NaCo large program (NaCo-LP, P.I. J. L. Beuzit) and the complementary archive datasets that probed the occurrence of planets and BD in wide orbits around solar-type stars, we place some constraints on the planet and BD distributions. To this purpose, we developed a MonteCarlo simulation tool to predict the outcome of a given survey, depending on the shape of the orbital parameter distributions (mass, semi-major axis, eccentricity and inclination). Through the comparison of the predictions with the results of the observations, we can calculate how likely different models are and which can be ruled out. Current observations are consistent with the proposed picture for the CMF, if we assume the radial velocity measured quantities for the planet distributions, as long as a sufficiently small outer truncation radius (≤80 AU) is introduced for the planet separation distribution. Some models can be excluded by the observations. We conclude that the results of the direct imaging surveys searching for substellar companions around Sun-like stars are consistent with a combined substellar mass spectrum of planets and BDs. This mass distribution has a minimum between 10 and 40 $M_{Jupiter}$, in agreement with radial velocity measurements. In this picture the dearth of objects in this mass range would naturally arise from the shape of the mass distribution, without the introduction of any distinct formation mechanism for BDs. This model for the CMF allows to determine what is the probability for a substellar companion as a function of mass to have formed in a planet- or BD-like process, as they overlap in this mass range.

4.1 Introduction

Binary systems have been observed and characterized for almost 100 years [see e.g. the study by Aitken, 1935]. Since the seminal work by Duquennoy & Mayor [1991] and Fischer & Marcy [1992], the properties of stellar binaries have also been widely studied. One of the most interesting parameter of a binary system is the mass-ratio $q = M_2/M_1$, defined as the ratio of the secondary (M_2) over the primary mass (M_1). The distribution of q values for a sample of binaries is the companion mass-ratio distribution (CMRD). Several surveys in the past decades focused on the detection of stellar binaries with the purpose of characterizing the occurrence of companions and their mass distribution both in the field [e.g. Janson et al., 2012, Raghavan et al., 2010] and in star forming regions [e.g. Patience et al., 2002]. Reggiani & Meyer [2013], as an update of Reggiani & Meyer [2011], have shown that in the field the CMRD is consistent with being universal, independent of separation in the range covered by the observations, and can be fitted by a single power-law slope $dN/dq \propto q^{\beta}$, with $\beta = 0.25 \pm 0.29$. In addition, N-body simulations suggest that only modestly affected by dynamics, even in dense cluster, as opposed to the semi-major axis (SMA) distribution [Parker & Reggiani, 2013]. The CMRD seems therefore a good diagnostic for different star formations.

Whereas the distributions of masses and orbital parameters are quite well established for stellar companions, the shape of the companion mass function (CMF) and of the SMA distribution in the substellar regime is still poorly understood. The ~ 500 extrasolar planets discovered by using the radial velocity (RV) method allowed us to fit power-law slopes to the mass and semi-major axis distributions for planets with masses between 0.3-10 $M_{Jupiter}$ and within $\sim$3 AU [see e.g. Cumming et al., 2008]. However, nothing guarantees that the same behavior holds at larger separations or higher masses. Currently, direct imaging is the only method that allows us to characterize large-separation exoplanets. In the past decade many direct imaging surveys [e.g. Biller et al., 2007,

Chauvin et al., 2010, Heinze et al., 2010, Lafrenière et al., 2007, Lowrance et al., 2005] have been carried out to evaluate the occurrence of giant planets in wide orbits (10-500 AU). Besides a few brown dwarfs (BDs) detected [e.g. Chauvin et al., 2005b, Mugrauer et al., 2010], no planet has been found around those targets. Although this result cannot be used to fit power-laws to the distributions beyond 10 AU, it suggests a truncation of the semi-major axis distribution at a few tens of AU in order to reproduce the RV statistics below 3 AU (assuming the same power-law slopes hold).

Regarding the substellar companion mass spectrum, BDs were originally proposed as a separate class of objects, with intermediate masses between stars and planets. Recent high contrast observations have unambiguously revealed the presence of several substellar objects, some as companions to nearby star, some resolved as binary systems and some in isolation in the field [e.g. Burgasser et al., 2003, Chauvin et al., 2005b, Dupuy & Liu, 2011]. Their existence indicates that the formation mechanisms proposed to form stars (turbulent fragmentation, collapse and fragmentation, disk fragmentation) can actually form objects down to a few Jupiter masses. Star and planet formation mechanisms therefore overlap in the planetary-mass regime. Companions in this mass range could be the lower mass tail of the stellar CMRD as well as the higher mass end of the planet CMF. Currently no observable quantity enables us to distinguish definitely whether a given object detected formed by one process or another. Different features in the frequency of BD companions and planets as a function of mass and semi-major axis could help distinguish different formation mechanisms. Large surveys are needed to assess in which companion mass range a stellar-like or planet-like process contribute most to the CMF, particularly if strong discontinuities were observed.

As a project within the VLT/NaCo large program (hearafter NaCo-LP, P.I. J. Beuzit, Chauvin et al. 2014, submitted), the work presented in this paper represents a first attempt to place some constraints on the full CMF in the substellar regime. It takes into account both BDs and

planets as companions to solar-type stars and makes use of the results of most of the direct imaging surveys of solar-type primaries currently available. In the first and second section (Section 4.2 and 4.3) we present our model for the mass distribution of substellar companions and the MonteCarlo simulation tool that we developed to test it. Then, we describe the datasets that we adopted for the analysis (Section 4.4) and the results of the MonteCarlo simulations based on these data (Section 4.5). Finally, we discuss the results in Sect 4.6 and summarize the conclusions in Sect 4.7.

4.2 Model for the substellar CMF

As mentioned in the introduction, our model for the CMF is based on the hypothesis that both BDs and planets contribute to the substellar mass distribution. In this context, we consider as "BDs" all objects that, having formed through a "stellar-like mechanism", constitute the lower mass tail of the CMRD, assuming that it can be extrapolated into the BD regime as suggested by Metchev & Hillenbrand [2009]. We define as "planets", instead, all the companions that formed in "standard planet-formation scenarios" and resulting in the RV measured CMF but extrapolated to higher masses and larger separations. There are of course some caveats to these assumptions. For instance, we do not take into account how GI and core accretion contribute to the distributions of orbital parameters. The fact that there are multiple binary formation mechanisms, that both planets and BDs migrate, etc. make everything more complicated. Here we make a simple, but complete model and see whether it works.

The overall frequency of substellar companions is therefore the sum of the two contributions:

$$dN_{BD} = C_0\, q^{\alpha_0}\, d\log q\, e^{-\frac{(\log a - \log a_0)^2}{2\,\sigma_0^2}}\, d\log a, \tag{4.1}$$

$$dN_{planet} = C_1\, m^{\alpha_1}\, d\log m\, a^{\beta_1}\, d\log a \tag{4.2}$$

for BDs and planets, indicated with the 0 and 1 subscripts, respectively. $\alpha_{0,1}$ and β_1 are the exponents of the power-law mass and semi-major axis distributions [c.f. Cumming et al., 2008], whereas a_0 and σ_0 are the mean and the standard deviation of the BD separation distribution, if log-normally distributed as for solar type primaries [see e.g. Raghavan et al., 2010]. C_0 and $C1$ are normalization constants that can be obtained from measurements of the BD and planet frequency $f_{0,1}$ over a range of masses and semi-major axes.

In this paper we assume values for the parameters that we think would be appropriate for solar-type primaries, typical of the dataset that we use to test this model. Our choices are presented in Table 4.1. Some of these values are measurement based, and some are extrapolations (e.g. the CMRD in the BD regime). Notes in Table 4.1 explain the extrapolations that have been made. Moreover, several physical mechanisms or observational constraints place upper and lower limits to the maximum and minimum mass and separation for these distributions. For our analysis we assume:

- the minimum and maximum masses for the BD mass distribution are given by the opacity limit for fragmentation [Low & Lynden-Bell, 1976] and the hydrogen burning limit [e.g. Burrows et al., 2001],
- the minimum and maximum separations for the BD separation distribution can be set in order to exclude less than 1% of companions from the measured stellar separation distribution,
- the maximum mass for the planet mass distribution is constrained by the disk mass (e.g. 10% of the mass of the star),
- the maximum separation for the planet separation distribution is possibly set by an outer truncation radius (as suggested by previous direct imaging surveys).

The corresponding values are listed in Table 4.1.

The combined CMF in the substellar regime for this choice of parameters is shown in Figure 4.1. It is interesting to mention that the opacity limit for fragmentation, which sets a lower limit to the BD mass distribution, creates a discontinuity in the CMF. The opacity limit for fragmentation occurs when the gravitational potential energy that is released during the collapse of a molecular cloud core exceeds the energy that can be radiated away [Low & Lynden-Bell, 1976]. Theories of core fragmentation predict that fragmentation cannot take place at densities higher than 10^{-13} g cm^{-3}, corresponding to a minimum mass of a few Jupiter masses [e.g. 1-10 $M_{Jupiter}$, Boss, 2001, Low & Lynden-Bell, 1976, Silk, 1977]. Future observations, that may enable us to characterize with high precision the substellar mass function and to detect such a feature, would also provide a test for these theories.

4.3 Methodology

In this section we present the methodology that we developed to test the model for the substellar CMF presented in Section 4.2. We created a MonteCarlo simulation tool with the aim of predicting the frequency of planets and BDs around a given list of targets and the probability of detection in a given survey, assuming the combined CMF. The probability of existence of substellar companions around a star depends on their mass and semi-major axis distributions. The probability of detecting them instead depends on the orbital parameters of the companions (mass, separation, eccentricity, inclination), on the properties of the star (age, distance, mass), and on the sensitivity (and contrast limits) of the instrument used.

The first step in our methodology is therefore to calculate the expected number of existing companions, both BDs and planets, per star. This quantity is generally expressed as the expectation value of the num-

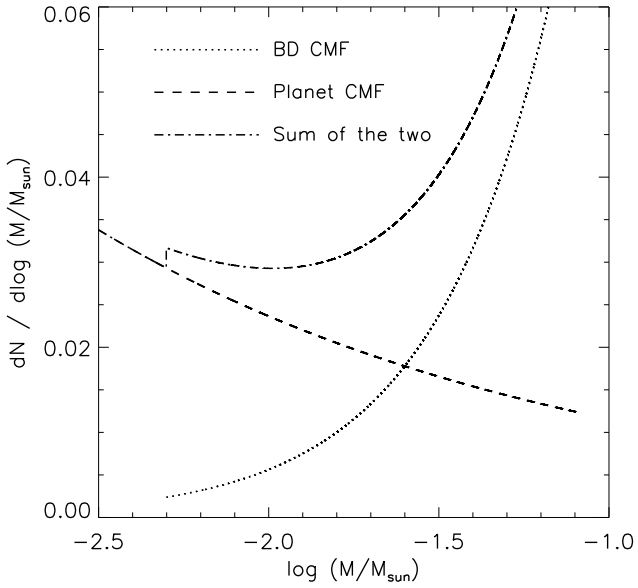

Figure 4.1 — Combined substellar CMF.

ber of BDs or planets per star in a given range of masses and separations:

$$P_{BD} = C_0 \int_{q_{min_0}}^{q_{max_0}} q^{\alpha_0}\, d\log q \int_{a_{min_0}}^{a_{max_0}} e^{-\frac{(\log a - a_0)^2}{2\sigma_0^2}}\, d\log a, \qquad (4.3)$$

$$P_{pl} = C_1 \int_{m_{min_1}}^{m_{max_1}} m^{\alpha_1}\, d\log m \int_{a_{min_1}}^{a_{max_1}} a^{\beta_1}\, d\log a, \qquad (4.4)$$

where the integral limits indicate the mass and semi-major axis ranges of interest for BDs (0 subscript) and planets (1 subscript), respectively. The other parameters are described in Section 4.2.

Once we have calculated the average number of planets and BDs per star in the mass and semi-major axis ranges that we are interested in, we run N simulations of the survey, in each of which every target star is

randomly assigned a number of planets and a number of BDs, based on Poisson statistics with mean P_{pl} and P_{BD} for planets and BDs, respectively. In case the Poisson probability returns a number smaller than 0.5, the number of planets or BDs for the given star is zero. However, if the star turns out to have one or more planets (or BDs), the mass and semi-major axis for each one of them is randomly selected from the input planet (or BD) distributions (see Section 4.2). The eccentricity is randomly selected from the Jurić & Tremaine [2008] distribution, of the form $P(\epsilon) = \epsilon * e^{[-\epsilon^2/2\sigma^2]}$ with $\sigma = 0.3$, and an inclination is randomly assigned. Time spent, as a function of orbital location, is explicitly taken into account as a function of orbital parameters when converting the semi-major axis into a projected separation in AU.
Once every simulated planet or BD is assigned all its orbital properties, we compare its mass and separation with the sensitivity limits of the survey to determine which planets or BDs could have been detected. Generally, the sensitivity limits are given for each star as a contrast curve, meaning apparent magnitude (or contrast) as a function of the angular separation. In order to perform a direct comparison of the simulated properties with the contrast curves, we use a family of substellar evolutionary models [e.g. COND models, Baraffe et al., 2003] and the information about distance and age of the stars to transform companion masses and projected separations into apparent magnitudes and angular separations. If the combination of magnitude and separation for a given companion falls below the sensitivity limits for the target, the companion is not detected.
At the end of the N runs of the artificial survey, we know how many planets or BDs we have "created" and how many we would have detected in each simulation. Finally, we can define the total probability for the survey of having found zero, one or more objects, given the model that we assumed, and can compare it with the real outcome of the survey. Examples of applications of this tool are presented in Section 4.5.

4.4 Dataset

The dataset that we used to test the model for the substellar CMF described in Section 4.2 mainly consists of the targets of the NaCo-LP (Chauvin et al. 2014, submitted; Desidera et al. 2014, submitted). This program is a direct imaging survey that aimed at providing a homogeneous statistically significant study of the occurrence of giant planets and BDs in wide (5-500 AU) orbits around young, nearby stars. It focused on a carefully selected list of stars, chosen with declinations $\delta \leq 25°$, ages $t \leq 200$ Myr, distances $d \leq$100 pc, and R-band brightnesses $R \leq 9.5$. The sample was initially comprised of 84 targets, none of which had been observed before. Those stars were then observed with VLT/NaCo in the H band in a series of observing runs spread between end 2009 and 2013, for a total of 16.5 nights. A complete description of the sample and its properties (distance, age, mass) can be found in Desidera et al.. The summary of the program and of the observations is instead provided in Chauvin et al.. As a result of the campaign, no substellar companions were detected around the targets. The statistical analysis regarding the constraints on the planet distributions will be presented in a separate paper (Vigan et al., in preparation). In the present work we use the statistical sample (57 objects) described in Vigan et al. 2014, in preparation, to place some constraints on the BD and planet populations together. For simplicity we will refer to the statistical sample as "NaCo-LP sample".

As it is presented in Vigan et al., we also built an archive sample to complement the NaCo-LP dataset. We took into account several surveys that in the past years imaged stars with similar properties to the NaCo-LP targets: Lowrance et al. [2005], Masciadri et al. [2005], Biller et al. [2007], Kasper et al. [2007], Lafrenière et al. [2007], Chauvin et al. [2010], Heinze et al. [2010], Vigan et al. [2012], Brandt et al. [2013], and Rameau et al. [2013]. From these programs we included in the archive sample those targets that share the same range of spectral types (from early-mid F to late K) and distance ($\leq$ 100 pc) as the NaCo-LP stars,

for a total of 154 objects. No age or declination limit was applied in this case. While the outcome of the NaCo-LP was a non-detection, around 4 targets in the archive sample substellar companions have been found:

GSC 08047-00232 B is a 25±10 $M_{Jupiter}$ mass BD with a derived spectral type M9.5±1 [Chauvin et al., 2005a] at a projected separation of 278 AU. It is a probable member of the Tucana-Horologium association with an age of 10-50 Myrs.

AB Pic b is a $\sim$ 13 $M_{Jupiter}$ mass objects at the planet/brown dwarf boundary [Chauvin et al., 2005b] and separation of 275 AU. It is also member of the Tucana-Horologium association.

HD 130948 BC is a BD binary system, companion to HD 130948. The total mass was estimated to be 0.1095±0.0022 $M_{\odot}$ [Dupuy & Liu, 2011] and the age 0.93 Gyr.

PZ Telescopii B is a BD companion with a mass of 24-40 $M_{Jupiter}$ at a projected separation of 15 AU [Mugrauer et al., 2010]. It is member of the β Pic moving group.

The complete sample (NaCo-LP + archive) is therefore constituted of 211 nearby ($d \leq$100 pc) solar-mass stars that have been observed in deep imaging with sensitivity down to planetary companions.

4.5 MonteCarlo simulation results

To test our model for the substellar CMF, we used the tool described in Section 4.3 to compare our predictions with real observations. In this section we present the results that we obtained after applying our methodology to the set of data presented in Section 4.4, beginning with the results from the NaCo-LP sample only and then with the comparison with the full archive sample.

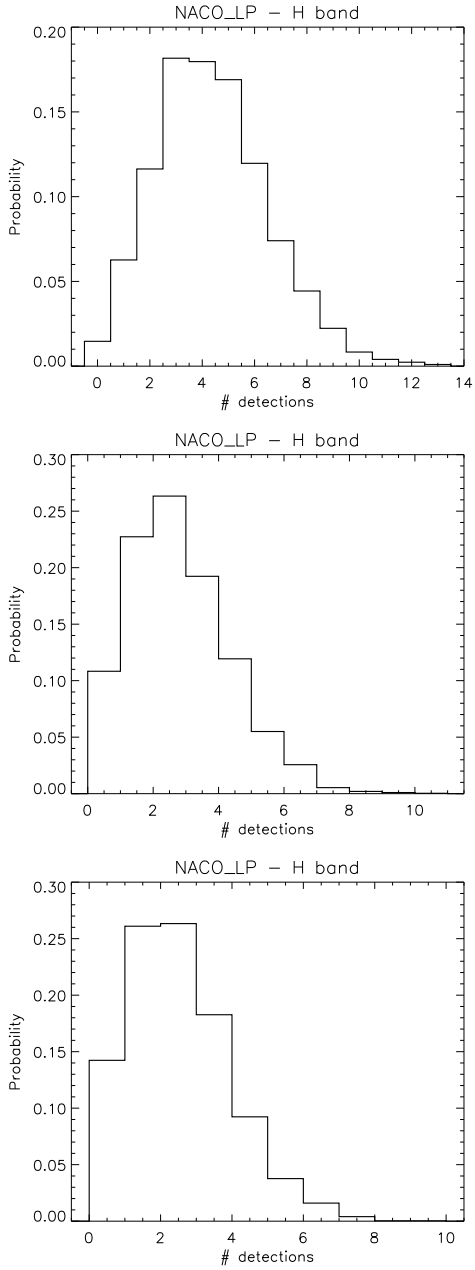

Figure 4.2 — Detection probability for the NaCo-LP sample for r_{cutoff} =100, 30, 20 AU (from left to right).

4.5.1 Results from the NaCo-LP

Concerning the targets (57) from the NaCo-LP, we run initially 3000 MonteCarlo simulations of the survey, with the set of parameters shown in Table 4.1 and with an outer radius cutoff of r_{cutoff} = 100 AU to quantify how likely the null result of the survey would be, according to this model. In the 3000 simulations 506905 planets and 14443 BDs were created, of which 7939 and 5153 were detected, respectively. The overall probability distribution of detections is shown in Figure 4.2(a). In 1.5% of the realizations, our survey found zero companions, while in 6% of the cases it found one and 92% of the time it found two or more planets or BDs. The average outcome of the survey is a detection of 3 planets and 2 BDs in total, for this choice of parameters. Given the probability of 1.5% of having a null detection with this choice of parameters, we can rule out this model with a 98.5% confidence. We then verified the dependence of this results on the choice of r_{cutoff}. We repeated the set of 3000 MonteCarlo simulations for both r_{cutoff}=20 AU and r_{cutoff}=30 AU, but leaving all the other parameters unchanged. In this case, the probability of a null results is 14% and 11% for r_{cutoff}=20 AU and 30 AU, respectively (see Figure 4.2). The average number of detections is 0 planets and 2 BD for r_{cutoff}=20 AU and 1 planets and 2 BD for r_{cutoff}=30 AU. This result clearly show that introducing a lower value for the outer radius cutoff reproduces the outcome of the observations, assuming that the mass and SMA distributions from RV surveys [Cumming et al., 2008] are a good representation even at larger separations.

4.5.2 Results from the full archive sample

In the case of the full archive sample (211 targets), we repeated the same sets of simulations that we carried out for the NaCo-LP dataset. Besides the size, the main difference between the NaCo-LP subsample and the full archive dataset is in the outcome of the observations.

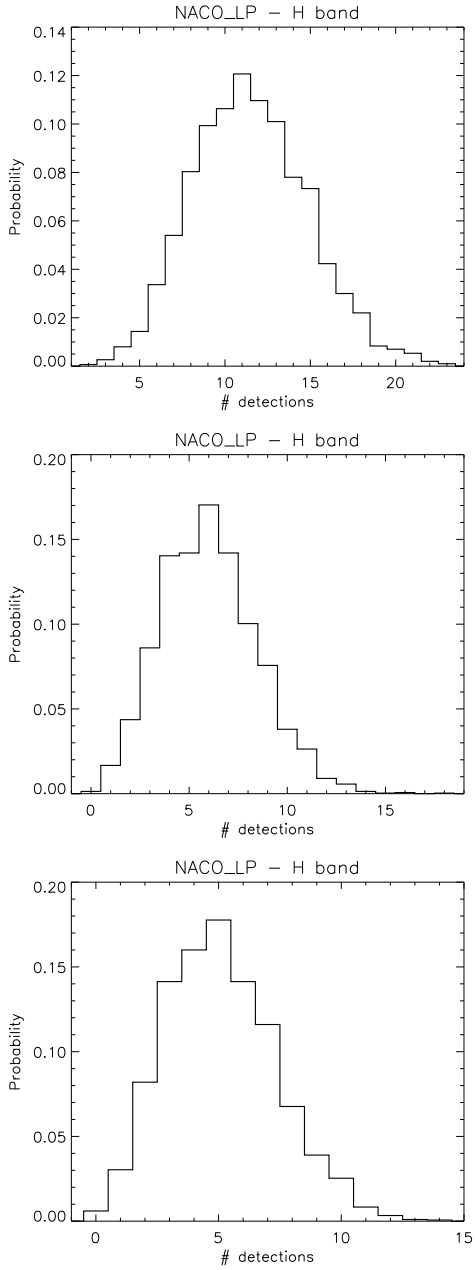

Figure 4.3 — Detection probability for the full archive sample for r_{cutoff} =100, 30, 20 AU (from left to right).

In this case, because of the detection of 4 BD companions presented in Section 4.4, we are interested in the probability of detecting 4 objects. Analogously to what has been done for the NaCo-LP sample, we simulated 3000 artificial observations of the targets in the archive sample for the same three values of r_{cutoff}= 20,30 and 100 AU. The detection probability distributions are shown in Figure 4.3 The probability of detecting of 4 objects is 1%, 14% and 16% for r_{cutoff}= 100, 30 and 20 AU, respectively. The results from the archive sample are therefore consistent with what was obtained for the NaCo-LP dataset only. The model described in Section 4.2 cannot be ruled out by the observations, as long as we introduce a sufficiently small truncation radius in the planet separation distribution.

In order to quantify this statement and assess which planet distributions could instead be excluded, we explored the β_1-r_{cutoff} parameter space. Having fixed the BD mass and semi-major axis distributions, we varied β_1 from 0 to 1, with steps of 0.1, and r_{cutoff} from 10 to 200 AU with steps of 10 AU. For each pair of β_1 and r_{cutoff}, we run 300 simulations of the survey and we calculated the probability of detecting 4 objects. Regardless of the choice of values for β_1 and r_{cutoff}, every simulation was normalized to match the RV statistics within 3 AU. Figure 4.4 shows the probability of detecting 4 substellar companions as a function of β_1 and r_{cutoff}. Each grid cell point represents the 300 Monte Carlo simulations of the survey. The overall probability is normalized to be 1 within the figure. The 3-σ confidence level shown in Figure 4.4 indicates where the probability is lower than 0.3%. The region above the 3-σ therefore can be ruled out at a 99.7% confidence level. For example, in the case of β_1=0.39, as suggested by RV measurement [Cumming et al., 2008], all models with r_{cutoff} >80 AU can be ruled out.

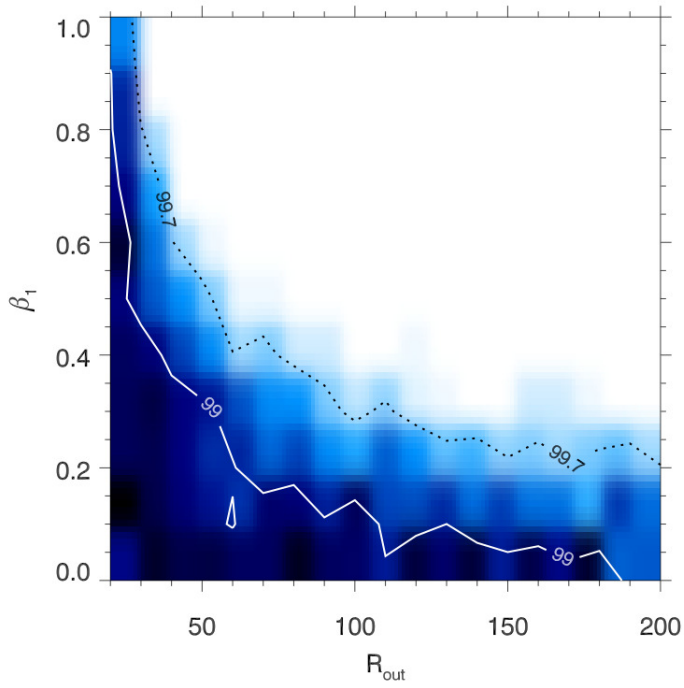

Figure 4.4 — Probability of our surveys detecting 4 substellar companions, as a function of the power-law slope of the semi-major axis distribution β_1, and the outer radius cutoff of the semimajor axis distribution. The region above the solid line is rule out at the 99.7% confidence level.

4.6 Discussion

The results presented in Section 4.5 clearly show that the current measurements of the occurrence of planets and BDs in wide orbits around solar-type stars do not rule out the model for the substellar CMF, presented in Section 4.2. Moreover the Kolmogorov-Smirnov test returns a probability of 16% that the distribution of masses of the 4 detected BD is drawn from the proposed CMF. If the RV statistics [Cumming et al., 2008] provide a good estimate of the normalization and the power-law

slopes of the planet distributions, an outer truncation radius of at most 80 AU is necessary to reproduce the observations. These constraints on the planet population are consistent with previous surveys analyses [Biller et al., 2007, Chauvin et al., 2010, Nielsen & Close, 2010].

In the past years, the observed dearth of close ($\leq$ 5 AU) BD companions to solar-mass stars [e.g. Marcy & Butler, 2000], also known as the "brown dwarf desert", has been used as evidence for a separate formation mechanism for brown dwarfs with respect to stars. Grether & Lineweaver [2006], in an attempt to quantify the relative number of stellar companions, planets and BDs in close orbit (period $\leq$ 5 yrs) around nearby sun-like stars, found a paucity of objects in the BD mass regime compared to planetary and stellar companions, with the driest part of the "desert" being at 31^{+25}_{-18} $M_{Jupiter}$. Sahlmann et al. [2011] also measured the CMF for close BD companions to solar-type stars and found a minimum in the distribution between 25 and 45 $M_{Jupiter}$ and claimed to have detected the high mass tail of the planet mass distribution.

According to the results presented in this paper, the mass distribution of substellar companions seems to be consistent with a superposition of the planet CMF and the stellar CMRD extrapolated into the BD mass regime. This suggests that objects from the Hydrogen burning limit down to a few Jupiter masses may still form as stellar companions, without the need of introducing a separate formation mechanisms. From the theoretical point of view, recent turbulent fragmentation models have also explained the binary brown dwarf properties in terms of a single core fragmentation mechanism [Jumper & Fisher, 2013]. The paucity of companions in the mass range 10-40 $M_{Jupiter}$ even at large (>10 AU) separations would naturally arise from the superposition of the two mass distributions (see Figure 4.1).

In the next couple of years, new instruments, like the VLT Spectro-Polarimetric High-contrast Exoplanet REsearch (VLT/SPHERE) or the Gemini Planet Imager (GPI), will enable us to find few new planetary-mass companions. Unfortunately this will not allows us to place more

stringent constraints on the distributions of orbital parameters, unless of big and unexpected discontinuities in the distributions. With the next generation of extremely large telescopes instead (e.g. the European Extremely Large Telescope, E-ELT), our understanding of planet statistics will make a real step forward. It will be possible to directly measure the shape of substellar CMF and locate with higher precision the minimum even for wide companions. In this context, it will be interesting to study how the distribution of companion masses in the substellar regime varies not only with respect to separation but also as a function of primary mass.

4.7 Conclusions

In this paper we propose a simple model for the substellar mass spectrum, as a combination of the planet CMF and an extrapolation of the stellar CMRD into the BD mass regime. Taking advantage of the largest and most complete sample to date of solar-type stars observed with direct imaging, we ran MonteCarlo simulations to compare predictions of our model with the observations from the NaCo-LP and archival data. We conclude that:

- the outcome of the direct imaging surveys is consistent with a superposition of the CMF derived by RV measurements and of the stellar CMRD down to 5 $M_{Jupiter}$, as long as $r_{cutoff} \leq 80$ AU,
- when all the other parameters are fixed, some combinations of β_1-r_{cutoff} can be ruled out by the observations with a 99.7% confidence,
- the proposed CMF has a minimum between 10-40 $M_{Jupiter}$, in agreement with the results from RV observations [Sahlmann et al., 2011].

- in this picture the so-called "BD desert" would naturally arise from the shape of the mass distribution, without having to introduce any different formation mechanism for BDs.

Future observations may allow us to measure directly the shape of the distribution and the precise location of the minimum in the substellar mass spectrum. The detection of features in the substellar CMF, such as the discontinuity predicted at the opacity limit for fragmentation, may enable us to test fragmentation theories.

Tab. 4.1 — Planet and BD distributions: model values

Parameter	Values
α_0	1.25[a]
α_1	-0.31[b]
$\log a_0$	1.70[c]
σ_0	1.68[c]
β_1	0.39[b]
f_0	0.032 between [12-72 M_J] and [28-1590 AU][d]
f_1	0.0329 between [1-13 M_J] and [0.3-2.5 AU][b]
BD min mass	1-10 $M_{Jupiter}$
BD max mass	80 $M_{Jupiter}$
BD min sep.	0.1 AU
BD max sep.	10000 AU
planet min mass	—
planet max mass	0.1 x M_{star}
planet min sep.	—
planet max sep.	r_{cutoff}

[a]Reggiani & Meyer [2013], measured for stellar companions but extrapolated to the BD regime.

[b]Heinze et al. [2010], based on Cumming et al. [2008] and extrapolated to larger separations.

[c]Raghavan et al. [2010], measured for stellar companions but extrapolated to the BD regime.

[d]Metchev & Hillenbrand [2009].

CHAPTER 5

DISCOVERY OF A PROTOPLANET CANDIDATE IN THE HD 169142 TRANSITION DISK

This chapter is based on Reggiani et al., to be submitted to Astrophysical Journal Letters

Abstract

We present L′-band high-contrast observations of HD 169142, obtained with the VLT/NACO AGPM vector vortex coronagraph. A source located at 0".156±0".032 north of the host star (PA=7.4° ±11.3°) appears in the final reduced image. At the distance of the star (∼145 pc), this angular separation corresponds to a physical separation of 22.7±4.7 AU, locating the source within the recently resolved inner cavity of the transition disk. The source has a brightness of L′=12.2±0.5 mag. If it arose solely from the photosphere of a companion, it would correspond

to a 35-80 $M_{Jupiter}$ object at the age of the star, according to the COND models. Ongoing accretion activity of the star suggests, however, that gas is left in the inner disk cavity from which the companion could also be accreting. In this case the object could be significantly lower in mass and its luminosity enhanced by the accretion process. A lower mass object is more consistent with the observed cavity width. If confirmed, HD 169142 b would represent one of the first and best laboratories to test brown dwarf/planet formation and evolution theories. Finally, the observations enable us to place an upper limit on the L′-band flux of a second companion candidate orbiting in the disk annular gap at ∼50 AU, as suggested by millimeter observations. If the second companion is also confirmed, HD 169142 might be forming a planetary system, with at least two companions opening gaps and possibly interacting with each other.

5.1 Introduction

To understand how planet formation proceeds and in which chemical and physical conditions it occurs, young, gas rich disks have been studied by numerous observing programs. The so-called "transition disks" show the presence of inner holes, bright rims and annular gaps, which could be tracing on-going planet formation. A few planet candidates have been found by looking at these disks. Some of them have been detected with sparse aperture masking (SAM) observations in the gaps around their host stars [e.g. LkCa15 b, TCha b; Huélamo et al., 2011, Kraus & Ireland, 2012]. HD100546 b has been found with coronagraph supported angular differential imaging [ADI, Marois et al., 2006], still embedded in the gaseous disk [Quanz et al., 2013a]. Additional support for a suspected second companion candidate in the inner cavity of HD 100546 was recently provided by spectroastrometry of CO rovibrational lines [Brittain et al., 2013]. For some of the candidates detected with SAM, other disk features or scattered light from the inner disk rims have been suggested to explain the observations [e.g. Cieza et al., 2013]. So far,

Tab. 5.1 — Stellar Parameters

Parameter	Value	Reference [a]
R.A. (J2000)	18h 24m 29.785s	1
Dec. (J2000)	-29° 46' 49.829"	1
Distance (pc)	145-151	6; 3
J (mag)	7.31±0.02	1
H (mag)	6.91±0.04	1
K_s (mag)	6.41±0.02	1
L' (mag)	5.66±0.03	7
Sp. Type	A9III/IVe/A7V	2; 3
$v\ sin\ i$ (km s^{-1})	55±5	2
Age (Myr)	1-5/12/3-12	2; 3; 4
T_{eff}	7500±200/6500/7650±150	2; 3
Mass ($M_\odot$)	∼1.65	3
L_* ($L_\odot$)	∼8.6-13	3; 8
R_* ($R_\odot$)	∼1.6	3; 5
$\dot{M}$ ($10^{-9} M_\odot yr^{-1}$)	$\sim 3.1 / \leq 1.25 \pm 0.55$	3; 4
log g	3.7 ±0.1/4.0-4.1	2; 5
μ_α, μ_δ ($mas\ year^{-1}$)	-2.1, -40.2	9

[a]References: (1) From 2MASS point source catalog [Cutri et al., 2003] and corrected for proper motions to the epoch of our VLT observations; (2) Guimarães et al. [2006]; (3) Blondel & Djie [2006]; (4) Grady et al. [2007]; (5) Meeus et al. [2010]; (6) Sylvester et al. [1996]; (7) van der Veen et al. [1989]; (8) Mariñas et al. [2011]; (9) Høg et al. [2000].

no planet candidate has been found in a disk gap with standard high contrast imaging.

HD 169142 is a young Herbig Ae/Be star (see Table 5.1 for the stellar properties). It possesses a circumstellar disk with a quite complex structure, that has been extensively studied [e.g., Dent et al., 2006, Grady et

al., 2007, Honda et al., 2012, Meeus et al., 2010, Quanz et al., 2013b]. In particular, it has a small central disk (< 0.7 AU) with either hot-dust halo [Honda et al., 2012] or a hot inner wall [Osorio et al., 2014], an inner cavity, a bright rim ($\sim$25 AU), and an annular gap extending from 40 to 70 AU. The latter features have recently been resolved with polarimetric differential imaging (PDI) in the H band [Quanz et al., 2013b]. Furthermore, EVLA 7-mm observations of the disk detected the thermal dust emission of the bright rim, seen in polarized light, and revealed a compact emission source inside the annular gap [at $\sim$ 50 AU Osorio et al., 2014]. These recent observations as well as the morphology of the disk suggest that HD 169142 could be hosting (or forming) planetary companions.

In this letter we present L'-band high-contrast imaging observations of HD 169142[1], which reveal the presence of a companion candidate in the inner cavity of its transition disk.

5.2 Observations and Data Reduction

The observations of HD 169142 were carried out on June 28, 2013 with the VLT/NACO annular groove phase mask (AGPM) vector vortex coronagraph [Mawet et al., 2013] in pupil stabilized mode. All images were taken with the L27 camera (plate scale $\sim$27.15 mas pixel^{-1}) using the L' filter ($\lambda_c = 3.8\mu$m, $\Delta\lambda = 0.62\mu$m). The detector reads were recorded in "cube" mode and the integration time per read was set to 0.25 s. The sky was observed every $\sim$ 20 minutes and unsaturated images of the star were acquired to calibrate the photometry. The unsaturated reads had an exposure time of 0.05 s. Table 5.2 summarizes the observations.

We subtracted the background from each frame adopting for each

[1]Based on observations made with ESO Telescopes at the Paranal Observatory under program 291.C-5020(A)

Tab. 5.2 — Summary of L' Imaging Observations

Parameter	Value
No. of detector reads × exp. time	$60 \times 0.25s$
No. of data cubes	444
Parallactic angle start/end	-84.29/74.70
Airmass range	1.097 -1.038

cube the mean of the closest sky measures in time that were taken right before and after it. We applied a bad pixel/cosmic ray correction, adopting a 5-sigma threshold and replacing every anomalous pixel with the mean value of the 8 surrounding pixels. Since the AGPM already requires a mandatory centering accuracy of ∼0.3 pixel, which has been checked every 10-30 minutes during the observations, we did not apply any further centering to our images. Additional centering was performed in a second data reduction with a separate pipeline (see Section 2.4), which obtained consistent results. Finally from each image we created a ∼2"×2" sub-image (75×75 pixels) centered in the star, resulting in a stack of ∼25000 sub-images.

To subtract the stellar PSF from all the sub-images we used the principal component analysis (PCA) based package `PYNPOINT` [Amara & Quanz, 2012]. After scaling up the images by a factor of 2 in size, `PYNPOINT` creates a set of orthogonal basis functions to reproduce the stellar PSF and fits it to the individual frames with a chosen number of PCA coefficients. Then it subtracts the PSF from each frame, de-rotates the frames to the same field rotation, averages them and convolves them with a Gaussian kernel (FWHM = $0.5 \times \mathrm{FWHM_{PSF}}$) to get the final image of the stack. We adopted the 20 PCA `PYNPOINT` image as final reference, as it shows lower residual noise compared to images obtained with higher or lower numbers of PCA coefficients.

5.3 Results

5.3.1 Detection of an Emission Source

An emission source is revealed north of HD 169142 (see, Figure 5.1a). To assess the reliability of this detection, we performed a series of tests.

1. We varied the number of PCA coefficients used in `PYNPOINT` between 5 and 120.
2. We divided the dataset into different subsets containing either half or a third of the frames, but spanning the full field rotation.
3. We did two "blind" data reductions to confirm the result using both a separate PCA-based pipeline [Absil et al. 2013 (in press), Mawet et al., 2013] and the LOCI algorithm [Lafrenière et al., 2007].

In each case, we always found a bright emission source at the same location. To estimate the statistical confidence of the detection we used the final image and selected 28 pixels in 2 concentric rings around the star as noise reference. 10 pixels had the same separation from the star as the peak flux of the companion, the ring of the other 18 pixels had a radius of $0.23''$ and included the bright residual feature east of the central star. The separation of all these pixels was such that they are statistically independent in the convolved image. From these 28 pixel values we computed the mean, variance and skewness of the distribution and built a probability density function (PDF) assuming a log-normal as underlying distribution. From this PDF we then estimated the p-value, i.e., the likelihood of finding a pixel value equaling the companion's peak flux or higher, to be $p < 0.2\%$.

The results of all these tests give us confidence that the detection is real. None of the other features in the final image is a reliable detection,

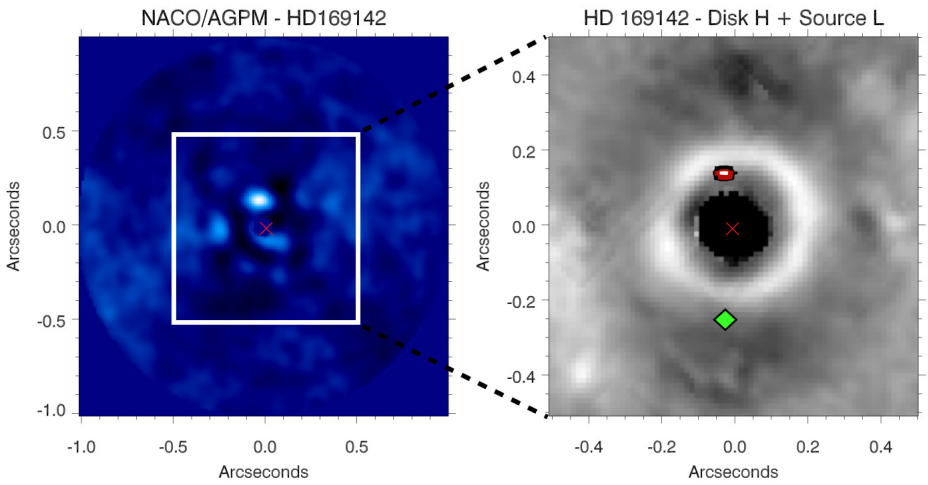

Figure 5.1 — a) NACO/AGPM L' image of HD 169142. This image is the final outcome of `PYNPOINT` with 20 PCA coefficients. A bright source is detected north of the central star. The image is linearly scaled with respect to the maximum flux. b) H-band PDI image of the circumstellar disk of HD 169142 [Quanz et al., 2013b]. The inner cavity (<25 AU), the bright rim, and the annular gap (40-70 AU) are clearly visible. Overplotted in red contours is the detected L' source. The green diamond indicate the expected location of the compact 7-mm emission.

based on these tests.

To derive the astrometry and photometry of the source, we inserted negative artificial planets in the individual exposures with different fluxes and at different locations, and then re-ran `PYNPOINT`. To generate the artificial objects we used a MonteCarlo photon generator with customizable FWHM. We adopted the FWHM measured from the unsaturated images of the photometric calibration dataset and we scaled the flux of the objects relative to the star, taking into account the difference in exposure time. We then inserted negative fake planets varying at the same time their brightness (with steps of 0.25 mag) and location (with

steps of 0.25 pixel). Each time, we used the final `PYNPOINT` image to calculate the deviation of the remaining flux at the object's location compared to the background noise in an annulus of 1 FWHM around the detection. We chose as brightness and astrometry of the source the combination of flux and position that yields the lowest deviation; i.e. the best subtraction. The errors on these measurements are the 1-σ deviation quantities.

To conclude, the source is located at 0".156±0".032 from the central star at a position angle of PA=7.4° ±11.3°. Our best estimate of the contrast for the object is ΔL' = 6.5±0.5 mag. These estimates are consistent with the expected performance of the AGPM at ∼0".16, based on past observations [see e.g. Mawet et al., 2013]. However, we also inserted an artificial positive planet of the same brightness at 0".156 from the central star (roughly 90° W of the detection). Figure 5.2 shows that we were able to recover a source with the same contrast at the same angular separation from the star. The observed magnitude for HD 169142 is L'=5.66±0.03 mag [van der Veen et al., 1989]. Thus, we derived an apparent magnitude of L'=12.2±0.5 mag for the newly detected source, where the uncertainty is the square-root of the sum of squares of the errors on the stellar and the object's magnitudes.

5.3.2 Non-Detection of the L' Counterpart of a Millimeter Emission Source in the Annular Gap

H-band PDI images of HD 169142 revealed many structures in the disk. In particular, there is evidence for a low surface brightness annular gap in polarized light which extends from ∼40 to 70 AU [Quanz et al., 2013b]. EVLA 7-mm observations have revealed an unresolved source (0.15 mJy) in this gap [Osorio et al., 2014]. Since this millimeter emission does not appear in the H-band intensity image or in the L'-band images (see Figure 5.1), we can place an upper limit on its luminosity.

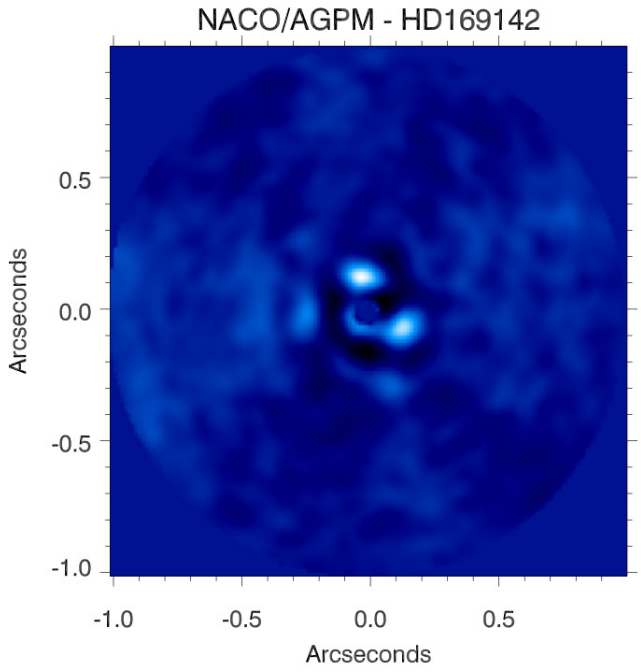

Figure 5.2 — NACO/AGPM L' image of HD 169142 with an artificial planet of the same brightness and at the same angular separation as the detection. This image shows the final outcome of `PYNPOINT` with 20 PCA coefficients. Besides the bright source detected north of the central star, we could recover the artificial planet at $PA \simeq 270°$. The image is linearly scaled with respect to the maximum flux.

To estimate our sensitivity at the expected location of this emission, we repeated the same procedure that we adopted in deriving the astrometry and photometry of the candidate companion. In this case, however, we inserted a positive artificial planet with increasing flux until we were able to detect it with `PYNPOINT` and the signal deviated more than 3σ from the mean background value. According to this calculation, the compact source has $L' > 14.0 \pm 0.5$ mag.

5.4 Discussion

5.4.1 The Emission Source in the Inner Cavity

According to the object's angular separation, the distance to HD 169142, and assuming the disk is seen face-on [Quanz et al., 2013b], the physical separation from the central star is 22.7±4.7 AU. This suggests that it is located within the inner cavity (see Figure 5.1b), right inside the inner edge of the bright rim [∼25 AU, Quanz et al., 2013b]. Different scenarios can explain these L'-band observations.

First, the detected source could have an instrumental origin. Such a feature could be an AO tip/tilt residual, but it should rotate and be subtracted with the PSF of the star. In case of bad centering behind the AGPM, point-like features can also be generated. In any case, as the signal appears in the final reduced image even when using subsets of the dataset or when applying further centering, and it is quite bright with $\Delta L' = 6.5$ mag, we can be confident on the physical origin of the detection.

The bright source could also be a background star. A single epoch of observations is not enough to completely rule out this possibility. However this scenario is highly unlikely. According to the Besancon galactic model [Robin et al., 2003], the number of objects with the apparent magnitude $L' \leq 12.2$ is 297 in a 1 deg^2 portion of the sky around HD 169142. This yields a probability of 2.3×10^{-6} of having an unrelated source in a 0.32"×0.32" region around the star.

An alternative explanation would be the detection of a disk feature, in scattered light or in thermal emission. Due to the limited precision in the astrometry for both the object and the nearby disk structures, we cannot exclude this possibility. However, the H-band PDI observations give the best indication of the morphology of the disk in scattered light. As shown in Figure 5.1b, the bright rim is mostly axisymmetric and

there is no maximum in polarized light in the direction of the PYNPOINT detection. On the other hand, if it was thermal emission from the disk, it should coincide with a peak in the 7-mm map obtained by Osorio et al. [2014], but it does not.

Fourth, we can assume that the emission is coming from the photosphere of a companion in quasi-hydrostatic equilibrium undergoing Kelvin-Helmholtz contraction in the inner cavity of the disk. Under this assumption, the L' luminosity suggests a mass of 35-80 $M_{Jupiter}$ for an age of 3-12 Myrs [Grady et al., 2007], according to the COND models [Baraffe et al., 2003]. Given the quite large mass estimate, the most favorable mechanisms to form such an object would be either formation through disk instability [e.g. Stamatellos et al., 2007] or core fragmentation in classical binary formation. The general disk structure and the possible existence of an extra (unresolved) component close to the star, such as a warm dust halo or a small inner disk [required for SED fitting Honda et al., 2012, Osorio et al., 2014], seem to prefer a disk-related formation mechanism. But even then, the fact that the star is accreting at a reasonable rate (see Table 5.1), indicating that material flows through the disk gap, appears difficult to reconcile with a 35-80 $M_{Jupiter}$ companion located in the gap.

A final possibility could be the detection of a lower mass planet during its formation, as it has recently been proposed for HD 100546b [Quanz et al., 2013a]. In this case, as the star is still accreting, the object itself might still be gathering gaseous material within the disk cavity. Such an accretion process would increase the observed luminosity, allowing a much lower mass for the object. A drastic increase in the planet luminosity during its formation and evolution is expected in cold-start models at a few million years [Marley et al., 2007, Mordasini et al., 2012].

From the theoretical point of view, the presence of a lower mass companion would more easily explain the morphology of the innermost 30 AU. According to classical gap opening theories [e.g. Lin & Papaloizou, 1993], we can estimate the expected width Δ of the gap if we assume

that a single body is carving out the cavity. Under several assumptions, such as the disk scale height at the object's location [2.8 AU from a disk model for HD 169142 by Meeus et al., 2010], the geometric factor [$f \approx$0.836, Lin & Papaloizou, 1993], and the effective disk viscosity ($\alpha =$ 0.001), we find a value of $\Delta =$ 60-102 AU, instead of the observed $\Delta \simeq$ 25 AU, for object masses in the range 35-80 $M_{Jupiter}$. A planet as small as 10 $M_{Jupiter}$ would already be enough to explain the observed cavity size. Recent 2-D hydrodynamical and dust evolution models of transitional disks [de Juan Ovelar et al., 2013] have shown that a morphology as the one observed for HD 169142 with PDI in H-band (e.g. an inner rim edge at 25 AU) could be reproduced with a 15 $M_{Jupiter}$ object at 20 AU. A strength of the latter models lies in their ability to predict what we should expect to see in observations at other wavelengths. If these models are correct, one should find a different spatial distribution of small and large dust grains, where the extent of the difference is proportional to the planet mass [Pinilla et al., 2012]. Future ALMA observations of this object might help us testing this theory and provide an independent estimate of the companion's mass.

5.4.2 The Non-Detection in the Annular Gap

Concerning the non-detection in the L'-band images of the compact 7-mm emission, our dataset allows us to put an upper limit on the mass of a possible object orbiting in the annular gap. At the distance of the star, our magnitude limit of $L' >$14.0$\pm$0.5 mag would correspond to <11-18 $M_{Jupiter}$ at 3-12 Myrs, according to the COND models [Baraffe et al., 2003]. Moreover, if we assume a single-temperature black-body with a 7-mm flux of 0.15 mJy, the non-detection in the L' band implies that the source of the millimeter emission must be cooler than $\sim$250 K and thus larger than $\sim$1.8 AU, consistent with it being unresolved by the EVLA. Therefore, if we assume a minimum Hill radius of r_H=1.8 AU at the expected location of the planet ($\sim$50 AU), we get a lower limit for its mass of 0.2 $M_{Jupiter}$.

The observations are then consistent with a planetary mass object (0.2-18 $M_{Jupiter}$) still surrounded by a circumplanetary disk cooler than ∼250 K (r_{disk} $\gtrsim$1.8 AU). With more (sub-)mm data of this disk we would be able to test this scenario.

5.4.3 Possible multiple planet interaction and evolution

If both objects are confirmed, it is interesting to speculate about the possibility of sequential planet formation and how it would affect the evolution of the disk. As suggested by Bryden et al. [2000], the accumulation of solid particles at the outer edge of a gap, that has been carved out by a protoplanet, could lead to the formation of an additional protoplanetary core at a larger orbital radius. In the future, more accurate measurements of the positions of the two companion candidates (currently ∼23 and ∼50 AU) may also allow us to constrain any possible mean motion resonances, if any, between the two objects.

Furthermore, Pierens & Nelson [2008] have shown that when two massive gap-opening planets are embedded in a disk, the gas in between the two gaps is cleared as the two gaps join together. The resulting positive torque from the inner disk slows down the inner planet's migration and allows the two planets to come into resonance. The bright rim seen in the scattered light may well be the region in between the gaps, before they merge. Such regions consist of gas surface density maxima (and hence pressure maxima) where dust can be trapped. In addition, such a scenario would also explain why the inner planet is so close to the peak in the scattered light, since the planet may well be closely "connected" to the region between the two gaps [see e.g. Figure 8 of Pierens & Nelson, 2008].

Such a system would thus represent the ideal laboratory to test planet migration theories, sequential formation and the importance of resonances at the early stages of planet formation.

5.5 Conclusions

In this letter, we present the first L'-band observations of HD 169142 with the VLT/NACO AGPM vector vortex coronagraph. These images suggest the presence of a low-mass companion in the inner cavity of the transitional disk, at a separation of ∼23 AU. Whether this object is a BD or a forming planet still remains to be investigated. In any case, it is likely that this companion affected the disk morphology. If confirmed, HD 169142b would be an extremely interesting laboratory to test BD and planet formation theories. Second epoch observations are needed to confirm it. Given the proper motion of HD 169142, observations will allow us to rule out the hypothesis of a background source as early as mid-2015. Upcoming instruments, such as VLT/SPHERE will be crucial for confirmation and follow-up.

Furthermore, our images do not exclude the possibility of a second object (0.2-18 $M_{Jupiter}$) forming in the annular gap (40-70 AU), as suggested by recent millimeter observations [Osorio et al., 2014]. If future observations (e.g. mm and sub-mm data) confirm this hypothesis, HD 169142 would be forming a planetary system with at least two planets, and would boost our understanding of multiple and possibly sequential planet formation.

CHAPTER 6

CONCLUSIONS AND OUTLOOK

To every man, in his acquaintance with a new art,
there comes a moment when that
which before was meaningless first lifts,
as it were, one corner of the curtain that hides its mystery,
and reveals, in a burst of delight
which later and fuller understanding can hardly ever equal,
one glimpse of the indefinite possibilities within.

C.S. Lewis, *Out of the Silent Planet*

In this last chapter, the main results of this thesis work are summarized. In Section 6.1 we discuss the conclusions provided at the end of every chapter in the broader context of star- and planet- formation. Finally, future projects and follow-up ideas, based on the results presented in this thesis, are described in Section 6.2.

Tab. 6.1 — Predictions from Binary Formation Mechanisms

Theory	Mass-Ratio Range	Ref. [a]
TIDAL CAPTURE	M_2 randomly chosen from IMF	1
PROMPT FRAGMENTATION	Equalization of masses	2; 3
CAPTURE IN DISPERSING CLUSTERS	Different CMRD for wide systems	4; 5

[a]References: (1) McDonald & Clarke [1993], (2) Bate & Bonnell [1997], (3) Bate [2000], (4) Moeckel & Bate [2010], (5) Moeckel & Clarke [2011].

6.1 Main Results

The Field CMRD

The results obtained in Chapter 2 and 3 can be compared with predictions from binary formation theories (see Table 6.1). In Chapter 2, we have demonstrated that observations of the CMRD in the field for different primary masses are inconsistent with random pairing from the most recent estimates of the field IMF [e.g. Bochanski et al., 2010, Chabrier, 2003]. Because in the tidal capture scenario the mass of the secondary component of a binary system is expected to be drawn randomly from the single star mass function and the CMRD would reflect the IMF [e.g. McDonald & Clarke, 1993], we can exclude this theory as the main mechanisms to create stellar binaries.
Furthermore, the CMRD appears to be independent of orbital separation. This feature is consistent with the idea that this distribution is not affected by dynamical processing in dense clusters, as shown by N-

body simulations [Parker & Reggiani, 2013]. Dynamical encounters in fact would alter the separation distribution [e.g. Parker et al., 2011], destroying preferentially wide binaries, but would leave the distribution of secondary masses unaffected. For this reason we believe that the CMRD is the ideal test of binary formation theory. In addition to that, the study of the CMRD as a function of the environment, from dense and rich star clusters to loose associations, could help in determining which type of star forming regions contribute the most to the field population.
The small difference in the CMRDs of close and wide binaries (see blue squares and green triangles in Figure 1.5), with more equal-mass companions at close separations is consistent with the equalizations of the masses of companions at close separations predicted by core fragmentation [Bate & Bonnell, 1997, Bate, 2000], indicating that this may be the principal binary formation process. A more careful analysis of the existing datasets and of the way in which triples and higher order multiple systems are taken into account when calculating the CMRD is needed to quantify the significance of this difference.
Capture in dissolving clusters, instead, predicts a different shape of the CMRD at wide separations [beyond 10^4 AU, Kouwenhoven et al., 2010]. In Chapter 3, we uncovered no evidence for such a variation. Although these widest binaries are relatively rare and we would need larger samples to test these models, capture in dispersing cluster does not appear to be a main mechanisms for the formation of binary systems.
Finally, the CMRDs for solar-type stars and M-dwarfs in the field are consistent with each other. A maximum likelihood fit of the combined companion mass distribution returns a power-law $dN/dq \propto q^{\alpha}$, with $\alpha = 0.25 \pm 0.29$.

The CMRD in Open Cluster and Loose Associations

Similarly to what we have found for the field CMRD, the q-distribution in the Pleiades, α Per and Taurus is inconsistent with random pairing from the IMF. We can therefore exclude the possibility that the inconsistency of the field CMRD with the IMF is the result of dynamical

evolution, as it is also shown by Parker & Reggiani [2013]. Currently, Chamaeleon I would represent the only exception. As mention in Chapter 2, due to the very small sample size, we should be cautious in interpreting this result. In the same chapter, we compared the CMRD for solar-type primaries derived by Metchev & Hillenbrand [2009] with the CMRD in Taurus and in the Pleiades and found a KS-test probability of $\sim 1\%$, in both cases. We concluded that perhaps low density associations (like Taurus) or bound open clusters (like the Pleiades) do not contribute significantly to the field stellar population. However, if we now compare them with the new binary sample of sun-like stars [Raghavan et al., 2010], the probability is 27% and 77%, respectively. The CMRD in α Per and Chamaeleon I is also in good agreement with the field CMRD from Raghavan et al. [2010] ($P_{KS} = 16\%$ and 9%, respectively). These outcomes simply indicate that at the moment we cannot exclude any of these star formation environments as contributor to the field. Hopefully, in the near future, measurements of the CMRD for larger and different samples (e.g. dense clusters, like the ONC) will better constrain the result as a function of age and environment.

The Substellar CMF

As the CMRD for Sun-like stars appears to be well-fitted by a single power-law function down to $q \sim 0.1$, it seems reasonable to assume that it can be extrapolated into the substellar mass regime ($q \lesssim 0.072$).
In Chapter 4 we have presented a functional shape for the substellar CMF, given by the superposition of the stellar CMRD [Reggiani & Meyer, 2013], extrapolated to lower q-values, and the RV measured planet mass function [Cumming et al., 2008]. This simple model implies that both star- and planet-like formation mechanisms contribute to the substellar CMF. Comparisons of the most recent direct imaging observations with MonteCarlo simulations for the simplest choices of the model parameters (see Section 4.5) show that the proposed CMF is in good agreement with the outcome of the surveys, as long as a sufficiently small (r_{cutoff} <80 AU) outer truncation radius for the planet distribu-

tion is adopted. According to this result, we can conclude that BDs as companions are consistent with being the lower mass tail of the stellar CMRD. As suggested by other binary properties [Kraus & Hillenbrand, 2012], BDs do not seems to be a different population with respect to stars. The observed paucity of companions to solar-type stars in the 10-40 $M_{Jupiter}$ range would naturally arise from the shape of the substellar CMF.
The great advantage of this simple CMF resides in the possibility of determining on a statistical basis what is the probability for a substellar companion of a given mass having formed in a planet- or BD-like process, as they overlap in this mass range. In the next years, spectra of these objects may allow us to constrain their formation mechanisms. Until then, a robust statistical analysis represents the only way of tackling the problem. Furthermore, the contribution from the BDs to the substellar CMF cannot be neglected when planning future surveys or analyzing already existing datasets: if we want to be able to exclude regions in the planet distribution parameter space (e.g. the $\beta_1 - r_{cutoff}$ space), the BD CMRD must be taken into account. The study of the distribution of companion masses is therefore a key for understanding stellar and substellar formation mechanisms.

Direct Imaging of Giant Exoplanets

The detection of a protoplanet candidate orbiting the Herbig Ae/Be star HD 169142, presented in Chapter 5, shows the great potential of high contrast imaging. Whereas at the moment we can only investigate on planet/BD formation theories with a statistical approach (like the one adopted in Chapter 4), imaging planets in their birth environment, perhaps still embedded in circumplanetary material, may bring hints on their formation. Understanding the connection between circumstellar disk structures and the presence of planets can also help in determining the role of disk-planet interaction in the planet formation process.
The L'-band images of HD 169142 indicate the presence of a low-mass companion in the inner cavity of the transitional disk. If we assume that

all the flux comes solely from the photosphere of the object, its L' luminosity indicates a mass of 35- 80 $M_{Jupiter}$ for an age of 3-12 Myrs [Grady et al., 2007], according to the COND models [Baraffe et al., 2003]. Alternatively, the observed L' emission could be explained with a lower mass planet caught in its formation and still gathering gaseous material within the disk cavity. At a few million years, drastic increases in the planet luminosity during its formation and evolution are expected by cold-start models [e.g. Mordasini et al., 2012]. Whether this object is a BD (although rare in this mass range, see Chapter 4) or a forming planet still remains to be determined. Future ALMA observations may enable the detection of circumplanetary material, if present, and confirm the hypothesis of a protoplanet in formation. Although less likely, as the cavity size and the accretion onto the star are harder to explain with a 35- 80 $M_{Jupiter}$ companion, the existence of a BD companion would support the disk instability scenario [e.g. Stamatellos et al., 2007]. Either way, if confirmed, HD 169142b would represent an extremely interesting laboratory to test BD and planet formation theories. Finally, the possibility of a second object (0.2-18 $M_{Jupiter}$) forming in the annular gap (40-70 AU) of HD 169142, as suggested by recent millimeter observations (Osorio et al., in preparation) and consistent with our L' images, raise many questions regarding multiple and possibly sequential formation in this systems. Follow up millimeter observations could shed light on this scenario. Although the effect of a planet in shaping the disk morphology has been widely investigated [e.g. de Juan Ovelar et al., 2013, Lin & Papaloizou, 1993, Pinilla et al., 2012], the shape and persistence of structures in the disk in the case of multiple planets represent a challenging topic that theories of planet formation still need to address in the coming future.

6.2 Future Work and Outlook

The Stellar CMRD

As mentioned in Section 6.1, the CMRD in the field and in several clusters and associations is "universal" and essentially flat. In order to test which SFRs contribute the most to the galactic field population, the study of the CMRD as a function of environment and age is needed. In particular, the determination of the CMRD in dense and rich clusters like the ONC could be an interesting way of evaluating whether such highly populated clusters bring a large contribution to the field. The ONC Treasury Program [P.I. M. Robberto, Robberto et al., 2013] provides a unique multi-band photometric catalog for a thousand of ONC stars. Thanks to this dataset, many studies have been carried out in the past years to determine for instance the Hertzsprung-Russel diagram of the cluster [Da Rio et al., 2010], the age spread for the stellar populations [Reggiani et al., 2011], the statistics of low mass stars and BDs [Andersen et al., 2011], the mass accretion rates [Manara et al., 2012, Robberto et al., 2004], etc. However, a complete determination of the binary population and its properties still needs to be performed.
In the coming years we plan to use this dataset to establish a census of binary systems, hopefully extending the separation range of previous studies [e.g. 67.5 to 675 AU, Reipurth et al., 2007]. Using the technique presented in Reggiani et al. [2011], we aim at determining the stellar parameters for the detected binary systems and measuring the CMRD for the ONC.

The Substellar CMF

The combined results of direct imaging surveys searching for planets and BDs around solar-type stars agree reasonably well with the model for the substellar CMF, described in Chapter 4. The advent of new

instruments in the next few years, like the Spectro-Polarimetric High-contrast Exoplanet REsearch (VLT/SPHERE) at the VLT, will allow us to discover new planetary-mass companions. However the constraints that we can place on the distribution of orbital parameters will not increase dramatically, unless unexpected discontinuities are found in the distributions. Only with the next generation of extremely large telescopes, such as the European Extremely Large Telescope (E-ELT), will our knowledge on the planet property statistics be boosted. Figure 6.1 shows how the number of planet detections for the same artificial sample of 100 solar-type stars (generated within 50 pc and younger than 300 Myrs) is expected to change with the different instruments. On average, with the E-ELT we aim at detecting as many as 20 planets and BDs in such a sample, if we assume the standard values presented in Chapter 4 and an outer truncation radius r_{cutoff}=30 AU for the planet separation distribution. This indicates that with the E-ELT we will be able to detect roughly 4 times as many substellar companions as what it is feasible now with NACO on the VLT. Moreover we should be sensitive to less massive planets. Figure 6.2 represents the mass-separation plane for the planets detected around 10 random targets in 3000 MonteCarlo simulations of an artificial survey with the E-ELT. Planets as small as a tenth of a Jupiter mass and closer than 0.1" could be imaged. This may enable us to characterize the substellar CMF down to very low companion masses and detect the discontinuity due to the opacity limit for fragmentation, presented in Section 4.2, leading to a definitive test for fragmentation theories. Concerning intermediate- and low-mass stars, instead, we begin now to build samples [e.g. Delorme et al., 2012, Vigan et al., 2012] that are large enough to perform statistically significant analyses on the planetary distributions. This will allow us in the near future to determine the shape of the substellar CMF as a function of primary mass. We can then evaluate whether the minimum observed in the CMF for sun-like primaries scales with primary spectral-type or not. The outcome of these analyses will provide constraints on planet and BD formation theories, as they will have to reproduce the observed dependence of companions properties as a function of host-star mass.

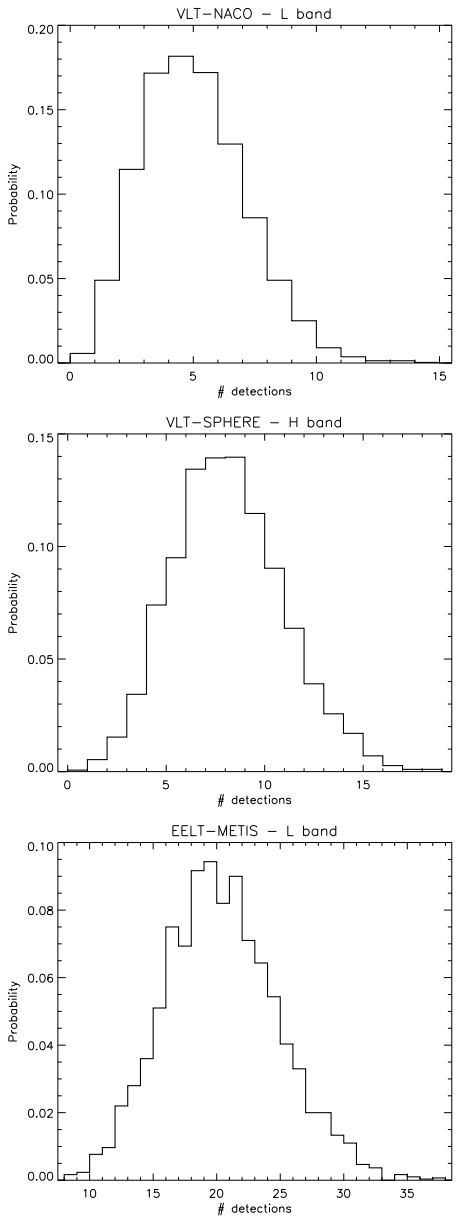

Figure 6.1 — *Planet detection: Forecasts for future instruments.* The three histograms represent the planet detection probability for VLT/NACO, VLT/SPHERE, and E-ELT/METIS (from top to bottom) in 3000 MonteCarlo simulations of an artificial survey of 100 solar-type stars within 50 pc and younger than 300 Myrs.

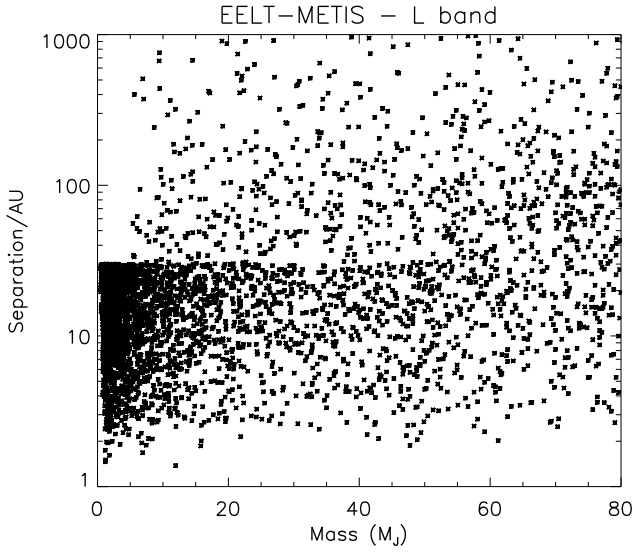

Figure 6.2 — *Planet Mass-Separation Diagram: Forecasts for future instruments.* The plot shows the distribution of masses and separations for the planets detected with the E-ELT in 3000 MonteCarlo simulated surveys of 10 Sun-like stars. A 39m-class telescope will allow us to detect really close-in planets down to tenth of a Jupiter mass. With the E-ELT we hope to detect the discontinuity in the CMF at $\sim$5 $M_{Jupiter}$, due to the opacity limit for fragmentation (see Section 4.2).

Planet Formation Mechanisms: the particular case of HD 169142

The discovery of a protoplanet candidate orbiting HD 169142 (see Chapter 5) makes this object one of the best star-disk systems for investigating perhaps not only planet formation and evolution but even multiple and sequential formation. As mentioned in Chapter 5, a second epoch of observations is needed to confirm the candidate. Given its proper motion, new observations as early as mid-2015 will enable us to rule out the hypothesis of a background source. Given the time frame, instruments

such as VLT/SPHERE will be crucial for the confirmation.
Concerning the second object in the gap (40-70 AU) of the transitional disk, 7-mm measurements and L' images are consistent with a planetary mass object (in the mass range 0.2-18 $M_{Jupiter}$) surrounded by a circumplanetary disk cooler than ∼250 K and larger than 1.8 AU. If granted, proposed ALMA observations will allow us to detect circumplanetary material for the first time. The circumplanetary disk can in fact be probed by searching for higher levels of continuum emission as well as CO emission at the location of the 7-mm detection. These observations could provide estimates of the disk mass and size. The direct detection of a circumplanetary disk around young forming giant planet and the determination of the disk-planet mass-ratio would represent a major step in constraining initial conditions of planet formation.

BIBLIOGRAPHY

Adams, F. C. 2010, ARA&A, 48, 4

Aitken, R. G. 1935, New York and London, McGraw-Hill book company, inc., 1935. 2d ed.,

Alibert, Y., Mordasini, C., & Benz, W. 2004, A&A, 417, L25

Allen, P. R., Koerner, D. W., McElwain, M. W., Cruz, K. L., & Reid, I. N. 2007, AJ, 133, 971

Alves, J., Lombardi, M., & Lada, C. J. 2007, A&A, 462, L17

Amara, A., & Quanz, S. P. 2012, MNRAS, 427, 948

Andersen, M., Meyer, M. R., Greissl, J., & Aversa, A. 2008, ApJ, 683, L183

Andersen, M., Meyer, M. R., Robberto, M., Bergeron, L. E., & Reid, N. 2011, A&A, 534, A10

Armitage, P. J. 2010, Astrophysics of Planet Formation, by Philip J. Armitage, pp. 294. ISBN 978-0-521-88745-8 (hardback). Cambridge, UK: Cambridge University Press, 2010.,

Ballesteros-Paredes, J., & Hartmann, L. 2007, Rev. Mexicana Astron. Astrofis., 43, 123

Baraffe, I., Chabrier, G., Barman, T. S., Allard, F., & Hauschildt, P. H. 2003, A&A, 402, 701

Basri, G., & Reiners, A. 2006, AJ, 132, 663

Bastian, N., Covey, K. R., & Meyer, M. R. 2010, arXiv:1001.2965

Bate, M. R., & Bonnell, I. A. 1997, MNRAS, 285, 33

Bate, M. R., Bonnell, I. A., & Bromm, V. 2003, MNRAS, 339, 577

Bate, M. R. 2000, MNRAS, 314, 33

Bate, M. R. 2004, Revista Mexicana de Astronomia y Astrofisica Conference Series, 21, 175

Bate, M. R. 2009, MNRAS, 392, 590

Bender, C. F., & Simon, M. 2008, ApJ, 689, 416

Bertout, C., Robichon, N., & Arenou, F. 1999, A&A, 352, 574

Biller, B. A., Close, L. M., Masciadri, E., et al. 2007, ApJS, 173, 143

Blake, C. H., Charbonneau, D., & White, R. J. 2010, ApJ, 723, 684

Blondel, P. F. C., & Djie, H. R. E. T. A. 2006, A&A, 456, 1045

Bochanski, J. J., Hawley, S. L., Covey, K. R., West, A. A., Reid, I. N., Golimowski, D. A., & Ivezić, Ž. 2010, AJ, 139, 2679

Boffin, H. M. J., Watkins, S. J., Bhattal, A. S., Francis, N., & Whitworth, A. P. 1998, MNRAS, 300, 1189

Bonnell, I., & Bastien, P. 1992, ApJ, 401, 654

Bonnell, I. A. 1994, MNRAS, 269, 837

Boss, A. R. 1986, ApJS, 62, 519

Boss, A. P. 1997, Science, 276, 1836

Boss, A. P. 2001, ApJ, 551, L167

Bouvier, J., Rigaut, F., & Nadeau, D. 1997, A&A, 323, 139

Bouy, H., Brandner, W., Martín, E. L., et al. 2003, AJ, 126, 1526

Boyd, D. F. A., & Whitworth, A. P. 2005, A&A, 430, 1059

Brandt, T. D., Kuzuhara, M., McElwain, M. W., et al. 2013, arXiv:1305.7264

Brittain, S. D., Najita, J. R., Carr, J. S., et al. 2013, ApJ, 767, 159

Brown, A. G. A., & Verschueren, W. 1997, A&A, 319, 811

Brown, A. G. A., Blaauw, A., Hoogerwerf, R., de Bruijne, J. H. J., & de Zeeuw, P. T. 1999, NATO ASIC Proc. 540: The Origin of Stars and Planetary Systems, 411

Bryden, G., Różyczka, M., Lin, D. N. C., & Bodenheimer, P. 2000, ApJ, 540, 1091

Burgasser, A. J., McElwain, M. W., & Kirkpatrick, J. D. 2003, AJ, 126, 2487

Burgasser, A. J., Kirkpatrick, J. D., Cruz, K. L., et al. 2006, ApJS, 166, 585

Burgasser, A. J., Reid, I. N., Siegler, N., et al. 2007, Protostars and Planets V, 427

Burke, C. J., Pinsonneault, M. H., & Sills, A. 2004, ApJ, 604, 272

Burrows, A., Hubbard, W. B., Lunine, J. I., & Liebert, J. 2001, Reviews of Modern Physics, 73, 719

Carson, J. C., Eikenberry, S. S., Smith, J. J., & Cordes, J. M. 2006, AJ, 132, 1146

Chabrier, G. 2003, ApJ, 586, L133

Chauvin, G., Lagrange, A.-M., Lacombe, F., et al. 2005, A&A, 430, 1027

Chauvin, G., Lagrange, A.-M., Zuckerman, B., et al. 2005, A&A, 438, L29

Chauvin, G., Lagrange, A.-M., Bonavita, M., et al. 2010, A&A, 509, A52

Cieza, L. A., Lacour, S., Schreiber, M. R., et al. 2013, ApJ, 762, L12

Clarke, C. 1992, Nature, 357, 197

Covey, K. R., et al. 2008, AJ, 136, 1778

Cumming, A., Butler, R. P., Marcy, G. W., et al. 2008, PASP, 120, 531

Cutri, R. M., Skrutskie, M. F., van Dyk, S., et al. 2003, VizieR Online Data Catalog, 2246, 0

de Juan Ovelar, M., Min, M., Dominik, C., et al. 2013, arXiv:1309.1039

Da Rio, N., Robberto, M., Soderblom, D. R., et al. 2010, ApJ, 722, 1092

De Rosa, R. J., Bulger, J., Patience, J., et al. 2011, MNRAS, 415, 854

De Rosa, R. J., Patience, J., Vigan, A., et al. 2012, MNRAS, 422, 2765

Delfosse, X., Beuzit, J.-L., Marchal, L., et al. 2004, Spectroscopically and Spatially Resolving the Components of the Close Binary Stars, 318, 166

Delorme, P., Lagrange, A. M., Chauvin, G., et al. 2012, A&A, 539, A72

Dent, W. R. F., Torrelles, J. M., Osorio, M., Calvet, N., & Anglada, G. 2006, MNRAS, 365, 1283

Docobo, J. A. 1985, Celestial Mechanics, 36, 143

Duchêne, G., & Kraus, A. 2013, arXiv:1303.3028

Duchêne, G., Simon, T., Eislöffel, J., & Bouvier, J. 2001, A&A, 379, 147

Duchêne, G. 1999, A&A, 341, 547

Dupuy, T. J., & Liu, M. C. 2011, ApJ, 733, 122

Duquennoy, A., & Mayor, M. 1991, A&A, 248, 485

Feigelson, E. D. & Babu, G. J. 2011, Modern Statistical Methods for Astronomy with R Applications, Cambridge Univ. Press

Fischer, D. A., & Marcy, G. W. 1992, ApJ, 396, 178

Ghez, A. M., Neugebauer, G., & Matthews, K. 1993, AJ, 106, 2005

Goodwin, S. P., & Kouwenhoven, M. B. N. 2009, MNRAS, 397, L36

Goodwin, S. P., & Whitworth, A. 2007, A&A, 466, 943

Goodwin, S. P., Kroupa, P., Goodman, A., & Burkert, A. 2007, Protostars and Planets V, 133

Goodwin, S. P. 2010, Royal Society of London Philosophical Transactions Series A, 368, 851

Goodwin, S. P. 2013, MNRAS, 430, L6

Grady, C. A., Schneider, G., Hamaguchi, K., et al. 2007, ApJ, 665, 1391

Grether, D., & Lineweaver, C. H. 2006, ApJ, 640, 1051

Guimarães, M. M., Alencar, S. H. P., Corradi, W. J. B., & Vieira, S. L. A. 2006, A&A, 457, 581

Hartmann, L. 2008, Accretion Processes in Star Formation, by Lee Hartmann, Cambridge, UK: Cambridge University Press, 2008,

Heinze, A. N., Hinz, P. M., Kenworthy, M., et al. 2010, ApJ, 714, 1570

Høg, E., Fabricius, C., Makarov, V. V., et al. 2000, A&A, 355, L27

Honda, M., Maaskant, K., Okamoto, Y. K., et al. 2012, ApJ, 752, 143

Horch, E. 2013, Planets, Stars and Stellar Systems, Volume IV, 653-692

Huélamo, N., Lacour, S., Tuthill, P., et al. 2011, A&A, 528, L7

Janson, M., Hormuth, F., Bergfors, C., et al. 2012, ApJ, 754, 44

Johnson, J. A., Fischer, D. A., Marcy, G. W., et al. 2007, ApJ, 665, 785

Johnson, J. A., Aller, K. M., Howard, A. W., & Crepp, J. R. 2010, PASP, 122, 905

Johnson, J. A., Howard, A. W., Bowler, B. P., et al. 2010, PASP, 122, 701

Jumper, P. H., & Fisher, R. T. 2013, ApJ, 769, 9

Jurić, M., & Tremaine, S. 2008, ApJ, 686, 603

Kasper, M., Apai, D., Janson, M., & Brandner, W. 2007, A&A, 472, 321

Kenyon, S. J., Gómez, M., & Whitney, B. A. 2008, Handbook of Star Forming Regions, Volume I, 405

King, R. R., Goodwin, S. P., Parker, R. J., & Patience, J. 2012, MNRAS, 427, 2636

Kouwenhoven, M. B. N., Brown, A. G. A., Zinnecker, H., Kaper, L., & Portegies Zwart, S. F. 2005, A&A, 430, 137

Kouwenhoven, M. B. N., Brown, A. G. A., Portegies Zwart, S. F., & Kaper, L. 2007, A&A, 474, 77

Kouwenhoven, M. B. N., Brown, A. G. A., Goodwin, S. P., Portegies Zwart, S. F., & Kaper, L. 2009, A&A, 493, 979

Kouwenhoven, M. B. N., Goodwin, S. P., Parker, R. J., Davies, M. B., Malmberg, D., & Kroupa, P. 2010, MNRAS, 404, 1835

Kraus, A. L., & Hillenbrand, L. A. 2012, ApJ, 757, 141

Kraus, A. L., & Ireland, M. J. 2012, ApJ, 745, 5

Kraus, A. L., Ireland, M. J., Martinache, F., & Lloyd, J. P. 2008, ApJ, 679, 762

Kraus, A. L., Ireland, M. J., Martinache, F., & Hillenbrand, L. A. 2011, ApJ, 731, 8

Kroupa, P., Bouvier, J., Duchêne, G., & Moraux, E. 2003, MNRAS, 346, 354

Kroupa, P. 1995, MNRAS, 277, 1522

Kumar, S. S. 1963, ApJ, 137, 1121

Lafrenière, D., Doyon, R., Marois, C., et al. 2007, ApJ, 670, 1367

Lafrenière, D., Jayawardhana, R., Brandeker, A., Ahmic, M., & van Kerkwijk, M. H. 2008, ApJ, 683, 844

Larson, R. B. 2002, MNRAS, 332, 155

Leinert, C., Zinnecker, H., Weitzel, N., Christou, J., Ridgway, S. T., Jameson, R., Haas, M., & Lenzen, R. 1993, A&A, 278, 129

Lin, D. N. C., & Papaloizou, J. C. B. 1993, Protostars and Planets III, 749

Low, C., & Lynden-Bell, D. 1976, MNRAS, 176, 367

Lowrance, P. J., Becklin, E. E., Schneider, G., et al. 2005, AJ, 130, 1845

Luhman, K. L., Mamajek, E. E., Allen, P. R., & Cruz, K. L. 2009, ApJ, 703, 399

Luhman, K. L. 2004, ApJ, 602, 816

Luhman, K. L. 2008, Handbook of Star Forming Regions, Volume II, 169

Luhman, K. L. 2012, ARA&A, 50, 65

Manara, C. F., Robberto, M., Da Rio, N., et al. 2012, ApJ, 755, 154

Marcy, G. W., & Butler, R. P. 2000, PASP, 112, 137

Marcy, G., Butler, R. P., Fischer, D., et al. 2005, Progress of Theoretical Physics Supplement, 158, 24

Mariñas, N., Telesco, C. M., Fisher, R. S., & Packham, C. 2011, ApJ, 737, 57

Marley, M. S., Fortney, J. J., Hubickyj, O., Bodenheimer, P., & Lissauer, J. J. 2007, ApJ, 655, 541

Marois, C., Lafrenière, D., Doyon, R., Macintosh, B., & Nadeau, D. 2006, ApJ, 641, 556

Masciadri, E., Mundt, R., Henning, T., Alvarez, C., & Barrado y Navascués, D. 2005, ApJ, 625, 1004

Mason, B. D., Hartkopf, W. I., Gies, D. R., Henry, T. J., & Helsel, J. W. 2009, AJ, 137, 3358

Mathieu, R. D. 1994, ARA&A, 32, 465

Matsuo, T., Shibai, H., Ootsubo, T., & Tamura, M. 2007, ApJ, 662, 1282

Mawet, D., Absil, O., Delacroix, C., et al. 2013, A&A, 552, L13

Mayer, L., Quinn, T., Wadsley, J., & Stadel, J. 2002, Science, 298, 1756

Mayor, M., & Queloz, D. 1995, Nature, 378, 355

Mazeh, T., Simon, M., Prato, L., Markus, B., & Zucker, S. 2003, ApJ, 599, 1344

McDonald, J. M., & Clarke, C. J. 1993, MNRAS, 262, 800

McDonald, J. M., & Clarke, C. J. 1995, MNRAS, 275, 671

Meeus, G., Pinte, C., Woitke, P., et al. 2010, A&A, 518, L124

Metchev, S. A., & Hillenbrand, L. A. 2009, ApJS, 181, 62

Meyer, M. R., Backman, D. E., Weinberger, A. J., & Wyatt, M. C. 2007, Protostars and Planets V, 573

Moeckel, N., & Bate, M. R. 2010, MNRAS, 404, 721

Moeckel, N., & Clarke, C. J. 2011, MNRAS, 415, 1179

Mordasini, C., Alibert, Y., Klahr, H., & Henning, T. 2012, A&A, 547, A111

Motte, F., Andre, P., & Neri, R. 1998, A&A, 336, 150

Motte, F., André, P., Ward-Thompson, D., & Bontemps, S. 2001, A&A, 372, L41

Mugrauer, M., Vogt, N., Neuhäuser, R., & Schmidt, T. O. B. 2010, A&A, 523, L1

Nakajima, T., Oppenheimer, B. R., Kulkarni, S. R., et al. 1995, Nature, 378, 463

Nielsen, E. L., & Close, L. M. 2010, ApJ, 717, 878

Öpik, E. 1924, Publications of the Tartu Astrofizica Observatory, 25, 1

Osorio, M., Anglada, G., Carrasco-González, C., et al. 2014, IAU Symposium, 299, 145

Parker, R. J., & Goodwin, S. P. 2011, MNRAS, 411, 891

Parker, R. J., & Reggiani, M. M. 2013, MNRAS, 432, 2378

Parker, R. J., Goodwin, S. P., Kroupa, P., & Kouwenhoven, M. B. N. 2009, MNRAS, 397, 1577

Parker, R. J., Goodwin, S. P., & Allison, R. J. 2011, MNRAS, 418, 2565

Patience, J., Ghez, A. M., Reid, I. N., & Matthews, K. 2002, AJ, 123, 1570

Peter, D., Feldt, M., Henning, T., & Hormuth, F. 2012, A&A, 538, A74

Pierens, A., & Nelson, R. P. 2008, A&A, 482, 333

Pinilla, P., Birnstiel, T., Ricci, L., et al. 2012, A&A, 538, A114

Pollack, J. B., Hubickyj, O., Bodenheimer, P., et al. 1996, Icarus, 124, 62

Portegies Zwart, S. F. 2009, ApJ, 696, L13

Prosser, C. F. 1992, AJ, 103, 488

Quanz, S. P., Lafrenière, D., Meyer, M. R., Reggiani, M. M., & Buenzli, E. 2012, A&A, 541, A133

Quanz, S. P., Amara, A., Meyer, M. R., et al. 2013, ApJ, 766, L1

Quanz, S. P., Avenhaus, H., Buenzli, E., et al. 2013, ApJ, 766, L2

Raghavan, D., McAlister, H. A., Henry, T. J., et al. 2010, ApJS, 190, 1

Rameau, J., Chauvin, G., Lagrange, A.-M., et al. 2013, A&A, 553, A60

Reggiani, M. M., & Meyer, M. R. 2011, ApJ, 738, 60

Reggiani, M., & Meyer, M. R. 2013, A&A, 553, A124

Reggiani, M., Robberto, M., Da Rio, N., et al. 2011, A&A, 534, A83

Reid, I. N., & Gizis, J. E. 1997, AJ, 113, 2246

Reipurth, B., & Clarke, C. 2001, AJ, 122, 432

Reipurth, B., & Zinnecker, H. 1993, A&A, 278, 81

Reipurth, B., Guimarães, M. M., Connelley, M. S., & Bally, J. 2007, AJ, 134, 2272

Rice, W. K. M., Armitage, P. J., Bonnell, I. A., et al. 2003, MNRAS, 346, L36

Robberto, M., Song, J., Mora Carrillo, G., et al. 2004, ApJ, 606, 952

Robberto, M., Soderblom, D. R., Bergeron, E., et al. 2013, ApJS, 207, 10

Robichon, N., Arenou, F., Mermilliod, J.-C., & Turon, C. 1999, A&A, 345, 471

Robin, A. C., Reylé, C., Derrière, S., & Picaud, S. 2003, A&A, 409, 523

Sahlmann, J., Ségransan, D., Queloz, D., et al. 2011, A&A, 525, A95

Sana, H., de Mink, S. E., de Koter, A., et al. 2012, Science, 337, 444

Shatsky, N., & Tokovinin, A. 2002, A&A, 382, 92

Shu, F. H., Adams, F. C., & Lizano, S. 1987, ARA&A, 25, 23

Silk, J. 1977, ApJ, 214, 152

Stamatellos, D., & Whitworth, A. P. 2009, MNRAS, 392, 413

Stamatellos, D., Hubber, D. A., & Whitworth, A. P. 2007, MNRAS, 382, L30

Stamatellos, D., Maury, A., Whitworth, A., & André, P. 2011, MNRAS, 413, 1787

Stauffer, J. R., Schultz, G., & Kirkpatrick, J. D. 1998, ApJ, 499, L199

Stauffer, J. R., et al. 1999, ApJ, 527, 219

Sylvester, R. J., Skinner, C. J., Barlow, M. J., & Mannings, V. 1996, MNRAS, 279, 915

Tabachnik, S., & Tremaine, S. 2002, MNRAS, 335, 151

Tanner, A. M., Gelino, C. R., & Law, N. M. 2010, PASP, 122, 1195

Tanner, A., White, R., Bailey, J., et al. 2012, ApJS, 203, 10

Tohline, J. E. 2002, ARA&A, 40, 349

Toomre, A. 1964, ApJ, 139, 1217

van der Veen, W. E. C. J., Habing, H. J., & Geballe, T. R. 1989, A&A, 226, 108

Vigan, A., Patience, J., Marois, C., et al. 2012, A&A, 544, A9

Whitworth, A., Bate, M. R., Nordlund, Å., Reipurth, B., & Zinnecker, H. 2007, Protostars and Planets V, 459

Woitas, J., Leinert, C., & Koehler, R. 2001, A&A, 376, 982

Wright, J. T., Gaudi, B. S. 2013, Planets, Stars and Stellar Systems, Volume III, 489-540

PUBLICATIONS

Brown dwarfs and giant planets as companions to solar-type stars: no gap but local minimum.
M. Reggiani et al.
A&A, *to be submitted*

Discovery of a protoplanet candidate in the HD 169142 transition disk.
M. Reggiani;
ApJ, *to be submitted*

Universality of the companion mass-ratio distribution.
M. Reggiani; M. R, Meyer
2013, A&A, *553, A124*

Quantitative evidence of an intrinsic luminosity spread in the Orion nebula cluster.
M. Reggiani; M. Robberto; N. Da Rio; M.R. Meyer; D. R. Soderblom;

L. Ricci
2011, A&A*, 534, A83.*

Binary Formation Mechanisms: Constraints from the Companion Mass Ratio Distribution.
M. Reggiani; M. R, Meyer
2011, ApJ*, 738, 60.*

The binary companion mass ratio distribution: an imprint of the star formation process?.
Parker, R. J.; Reggiani, M. M.
2013, MNRAS*, 432, 2378.*

The Hubble Space Telescope Treasury Program on the Orion Nebula Cluster
Robberto, M.; Soderblom, D. R.; Bergeron, E.; Kozhurina-Platais, V.; Makidon, R. B.; McCullough, P. R.; McMaster, M.; Panagia, N.; Reid, I. N.; Levay, Z.; Frattare, L.; Da Rio, N.; Andersen, M.; O'Dell, C. R.; Stassun, K. G.; Simon, M.; Feigelson, E. D.; Stauffer, J. R.; Meyer, M.; Reggiani, M.; Krist, J.; Manara, C. F.; Romaniello, M.; Hillenbrand, L. A.; Ricci, L.; Palla, F.; Najita, J. R.; Ananna, T. T.; Scandariato, G.; Smith, K.
2013, ApJS*, 207, 10.*

Direct imaging constraints on planet populations detected by microlensing.
Quanz, S. P.; Lafrenire, D.; Meyer, M. R.; M. Reggiani; Buenzli, E..
2012, A&A*, 541, A133*

CURRICULUM VITÆ

Contact information

Departement Physik
Institut für Astronomie
ETH Zürich, HIT J 33.2
Wolfgang-Pauli Str. 27
CH-8093 Zürich
Switzerland

Phone: +41 (0)44 632 09 56
Fax: +41 (0)44 633 12 38
E-mail: reggiani@phys.ethz.ch
Web: `http://www.astro.ethz.ch/people/mreggian`

Personal information

Date of Birth:	September 15th, 1984
Place of Birth:	Milano, Italy
Citizenship:	Italian
Marital Status:	Married
Mother Tongues:	Italian
Other Languages:	fluency and good written knowledge of English, basic knowledge of German

Education

Ph.D. candidate, ETH Zürich — Sept. 2009 - Jan. 2014
Title: The Companion Mass Function across the Stellar and Substellar Regime
Advisor: Prof. Dr. M.R. Meyer

M.Sc. in Physics, Università degli Studi, Milan, Italy — Sept. 2006- Apr. 2009
Title: A Study of the Star Formation History in the Orion Nebula Cluster
Advisor: Prof. Dr. G. Bertin
External Advisor: Dr. M. Robberto

B.Sc. in Physics, Università degli Studi, Milan, Italy — Sept. 2003- Dec. 2006
Title: CMB and cosmological parameters: forecasts from future experiments in polarization.
Advisor: Prof. Dr. D. Maino

Classical Languages High School "Daniele Crespi", Busto A., Italy — Sept. 1998- Jun. 2003

Research interests

Star and planet formation:
stellar and sub-stellar binary systems, orbital parameter distributions, binary, BD and planet formation mechanisms, direct imaging of planets.

Research experience

Ph.D. student, Institute of Astronomy, ETH Zürich	Sept. 2009 - Jan. 2014
Short-term Research Program at the STScI (Baltimore, MD)	Sept. 2008 - Jul. 2009

Teaching experience

Various duties including organising and composing exercises, and delivering lessons as teaching assistant for the following courses:

Anfängerpraktikum Beginners Lab for physics students	2009/2010
Astrophysics 1 for physics students	2010/2011
Vorgerckten-Praktikum Advanced Lab for physics students	2010
Astrophysics 1 for physics students	2011/2012
Vorgerckten-Praktikum Advanced Lab for physics students	2012
Astrophysics 1 for physics students	2013/2014

Public outreach

"*Scientifica*": Involvement in organizing an exhibition for the Scientifica event at the ETH Zürich	2011
"*Lo Spettacolo della Fisica*": Partecipation in a play about Physics for kids, Milan	2006-2008

Computer skills

Operating systems: Mac, Unix/Linux, MS Windows

Languages: IDL, Pyhton, LaTeX, Basic knowledge of C++, Fortran77

Hobbies/other interests

Various Sports, cooking, singing, playing the flute and reading